

Diss. ETH No. 20020

Vegetation-mediated impacts of trends in climate forcing on land hydrology

A dissertation submitted to
ETH ZURICH

for the degree of
DOCTOR OF SCIENCES

presented by

Paulo José da Silva Costa de Oliveira
M.Sc., University of San Francisco, USA
born on 23 April 1967
citizen of Portugal

accepted on the recommendation of

Prof. Dr. Sonia I. Seneviratne, examiner
Prof. Dr. Ulrike Lohmann, co-examiner
Dr. Edouard L. Davin, co-examiner
Dr. Christian H. Reick, co-examiner

Zurich 2012

Abstract

Human-induced changes to the climate system have brought about unprecedented impacts on the hydrologic cycle, which are expected to intensify in the coming future. External forcings act upon the various components of this complex system through non-linear interactions with the land surface at different spatio-temporal scales. The task of fully understanding these processes in order to better predict, and prepare for, the current and future development of the water cycle is challenging, given the constraints of a comprehensive assessment of its physical behaviour. Many advances have been made in the detection, characterization, and ability to predict the response of the water cycle as a result of changes to atmospheric forcings, but large uncertainties still remain. The study of land hydrology using current state-of-the-art land surface models can provide valuable insights toward the understanding of the involved biophysical processes, and help elucidate the ways in which forcing trends can affect the relevant components of the water cycle. This thesis uses land-surface modeling experiments and comparisons with observations to assess some of the effects of atmospheric forcing trends on land hydrologic processes, in addition to providing insights into the possible limitations of the datasets and simulation methodology.

Chapter 1 provides an overview of the current knowledge in the related fields in climate science that are relevant to, and provide the theoretical basis for, the research presented in this thesis. It includes a description of some recent findings with respect to the components of the global water and energy cycles and their interactions within the climate system. It also introduces the modeling tools and methodologies on which the subsequent chapters rely.

In Chapter 2, the sensitivity of the CLM land-surface model and of its output hydrologic variables to changes in global radiation is investigated in detail. Simulated trends in evapotranspiration and runoff in the second half of the 20th century are derived, and the potential direct and indirect effects of radiation trends, and their relative importance, are ascertained. Close attention is also paid to how changes to the partitioning of incoming solar radiation between its direct and diffuse fractions may affect the components of the water cycle. There, it is shown that the modeled hydrologic cycle response to the imposed radiation changes is relatively strong globally, and particularly in the tropics, but weak

in regions with soil moisture-limited evapotranspiration regime. In Europe and the Eastern U.S. the imposed solar dimming signal leads to an evapotranspiration reduction of 5% of the mean, and an enhancement of runoff by equal percentage, while the imposed brightening elicits a proportional response. The simulated impact of higher diffuse radiation fraction suggests mostly an increase of evapotranspiration in the tropics of 3% of mean due to increased photosynthesis from shaded leaves, but smaller opposite effects elsewhere due to the compensatory effect from lower ground evaporation. The runoff trend resulting from the imposed radiation/aerosols effect is of the same sign and approximate relative magnitude as those from other studies for other potential drivers of runoff change such as climate, CO₂, and land use.

In Chapter 3, recent hydrological variability and trends for annual time series of streamflow in Europe are investigated for several datasets: 1) near-natural small catchment streamflow observations integrated over large river basins; 2) river basin streamflow measurements at downmost stations from the GRDC dataset; 3) and simulations with the CLM land-surface model driven with state-of-the-art forcing datasets. In addition, the mean of a multi-model hydrologic study featuring the most commonly used latest-generation models is used for the evaluation of variability of runoff in the investigated basins. The CLM simulations agree with the observations reasonably well, especially in terms of runoff variability, although regional discrepancies exist mostly in the drier Southwestern European basins. Runoff from integrated near-natural catchments can be valuable for the validation of model-simulated runoff, as it is a good proxy for continental-scale basin behaviour and is sensitive to radiation forcing trends, especially in Western and East-central European river basins. The poorer performance of the simulations driven with one of the forcing datasets highlights the importance of atmospheric forcing to accurately simulate terrestrial hydrology. Despite the differences in scale and the large uncertainty expressed by an overall poor statistical significance level, near-natural streamflow trend behaviour and changes mostly show good agreement with GRDC observations and simulated data. The overall consistency between the integrated near-natural catchment and whole-basin GRDC data relativizes the possible impacts of scale, altitude or human water use on runoff in the investigated river basins.

Chapter 4 analyses the impacts of model resolution, atmospheric forcing, and the choice of land-surface model on the means, variability, and trends in land hydrology, globally and regionally. Offline land-surface model simulations with the CLM land-surface model are performed at two different resolutions

and driven with two different forcing datasets, including a recently developed product from the WATCH project. The results are compared to WATCH simulations computed with six different land-surface and global hydrologic models. The results reveal that the WATCH-driven CLM simulation generally lies within the WATCH multi-model spread and that the choice of forcing dataset can substantially affect the simulations, at least to the same order of magnitude as the model choice. Overall mean patterns in runoff and evapotranspiration reflect the distribution of precipitation from the forcing. Simulations driven with the same forcing exhibit similar trend patterns and magnitude, suggesting that the decadal variability of the water cycle components is more sensitive to differences in the forcing datasets than to differences in model parameterizations. For the inter-annual variability of the simulated processes, however, both the applied forcings and model parameterizations appear relevant. The means and trends in radiation forcing are well correlated with the multi-model ensemble runoff, but neither of the forcing datasets incorporate observed radiation brightening trends, and thus some of the simulated trends may be erroneous. Lastly, it is observed that in relative terms model resolution plays a modest role for simulation uncertainty, at least in the absence of higher forcing resolution.

Chapter 5 summarizes the main conclusions of this thesis, namely that land surface processes and their impacts on the water cycle are substantially affected by atmospheric forcing trends. Solar radiation impacts evapotranspiration and runoff in significant ways, and its partitioning between direct and diffuse fractions must also be taken into account. It is additionally identified that runoff observations from near-natural catchments can prove valuable for the validation of simulated runoff, as they are found to be good proxies for continental-scale basin behaviour and are sensitive to forcing trends. Lastly, the adequate simulation of land-surface hydrology depends on the choice of atmospheric forcing and land-surface model, which may bias the means, variability, and trends at the global and regional levels. Hence, this study shows both the potential and limitations of land surface models for assessing land hydrological trends, and especially highlights the necessity for the improvement of atmospheric forcing datasets to assess long-term changes in the land water cycle. It additionally shows the strong regional variations in the importance of respective atmospheric drivers, which can generally be related to variations in hydrological regime.

Résumé

Les activités humaines ont entraîné des impacts sans précédents sur le système climatique, et en particulier sur le cycle hydrologique, qui devraient s'intensifier à l'avenir. Les forçages externes agissent sur les différentes composantes de ce système complexe à travers d'interactions non-linéaires avec la surface du sol à différentes échelles spatio-temporelles. La tâche consistant à améliorer notre compréhension des processus dans le but de mieux prévoir et se préparer à l'évolution actuelle et future du cycle de l'eau est difficile, étant donné les contraintes d'une évaluation exhaustive de son comportement physique. De nombreux progrès ont été réalisés dans la détection, la caractérisation et la capacité à prédire la réponse du cycle de l'eau résultant de changements de forçages atmosphériques, mais de grandes incertitudes existent encore. L'étude de l'hydrologie terrestre à l'aide de modèles de surface les plus récents permet d'obtenir des indications précieuses pour la compréhension des processus biophysiques impliqués, et d'aider à élucider la manière dont les tendances dans le forçage peuvent affecter les composants principaux du cycle de l'eau. Cette thèse se base sur des expériences de modélisation de la surface terrestre et sur des comparaisons avec les observations pour évaluer certains effets des tendances dans les forçages atmosphériques sur les processus hydrologiques terrestres, à plus de donner des aperçus sur les limites possibles des ensembles de données et de la méthodologie des simulations.

Le chapitre 1 propose une vue d'ensemble des connaissances actuelles dans les domaines des sciences du climat pertinentes et qui fournissent la base théorique pour la recherche présentée dans cette thèse. Il comprend une description de résultats récents concernant les composants du cycle de l'eau et de l'énergie mondiale et leurs interactions au sein du système climatique. Les outils de modélisation et les méthodologies sur lesquelles reposent les chapitres suivants sont introduits.

Dans le chapitre 2, la sensibilité aux changements de rayonnement global du modèle de la surface terrestre CLM et de ses variables hydrologiques est étudiée en détail. Les tendances simulées de l'évapotranspiration et l'écoulement durant la seconde moitié du 20ème siècle sont calculées et les effets potentiels directs et indirects des tendances de rayonnement, ainsi que leur importance relative, sont évaluées. Une attention particulière est également accordée à la façon dont les modifications du

partitionnement du rayonnement solaire incident entre la fraction directe et la fraction diffuse peut affecter les composants du cycle de l'eau. Il est démontré que la réponse du cycle hydrologique modélisé suivant les changements de rayonnement solaire imposés est relativement forte au niveau global et en particulier dans les tropiques, mais faible dans les régions où le régime d'évapotranspiration du sol est limité par l'humidité. En Europe et dans l'Est des Etats-Unis, le signal d'atténuation solaire imposé conduit à une réduction de l'évapotranspiration de 5% de la moyenne et à une croissance de l'écoulement en pourcentage égal, tandis que l'éclaircissement imposé suscite une réponse proportionnelle au signal du forçage. L'impact de la simulation d'une fraction plus grande de rayonnement diffus suggère surtout une augmentation de l'évapotranspiration dans les tropiques de 3% de la moyenne en raison de la photosynthèse accrue provenant des feuilles ombragées, mais les effets opposés sont plus limités ailleurs à cause de l'effet compensatoire de l'évaporation du sol. La tendance de l'écoulement résultant de l'effet du rayonnement et des aérosols imposés est du même signe et de même magnitude relative approximativement que celle trouvée dans autres études sur d'autres facteurs potentiels de changement d'écoulement, comme le climat, le CO₂ et l'occupation des sols.

Dans le chapitre 3, les tendances et la variabilité hydrologique récentes des séries temporelles annuelles d'écoulement en Europe sont étudiées pour plusieurs ensembles de données: 1) des observations des bassins à petite échelle non-perturbés, intégrés à l'échelle des bassins continentaux; 2) des mesures d'écoulement au niveau des bassins continentaux des stations les plus en aval de l'ensemble de données de GRDC; 3) et des simulations avec le modèle de surface terrestre CLM forcées par des ensembles de données de forçage atmosphérique les plus récents. De plus, la moyenne d'une étude hydrologique multi-modèles avec les modèles de dernière génération les plus courants est utilisée pour l'évaluation de la variabilité de l'écoulement dans les bassins analysés. Les simulations avec CLM sont en raisonnablement bon accord avec les observations, en particulier en terme de variabilité de l'écoulement, même si des disparités régionales existent plutôt dans les bassins secs du sud-ouest européen. L'écoulement des petits bassins non-perturbés intégrés à l'échelle des bassins continentaux peut être précieux pour la validation de l'écoulement simulé par le modèle, car il est un bon indicateur du comportement du bassin à l'échelle continentale, et est sensible aux tendances du forçage radiatif, en particulier dans les bassins hydrographiques de l'Europe de l'ouest, ainsi que de l'Europe Centrale et de l'est. La performance plus faible des simulations forcées avec un des ensembles de données de forçage atmosphérique met en évidence l'importance du forçage atmosphérique pour la simulation des

processus hydrologiques terrestres. Malgré les différences d'échelle et la grande incertitude révélée par des faibles niveaux de signification statistique, le comportement et le changement des tendances de l'écoulement des petits bassins non-perturbés montrent pour la plupart un bon accord avec les observations de GRDC et les données simulées. La cohérence globale entre les observations des petits bassins non-perturbés intégrés et les données de GRDC à l'échelle des bassins continentaux relativise les effets possibles des variations d'échelle, d'altitude ou d'utilisation de l'eau dans les bassins étudiés.

Le chapitre 4 analyse les impacts de la résolution du modèle, du forçage atmosphérique, et du choix de modèle de surface terrestre sur les moyennes, la variabilité et les tendances en matière d'hydrologie terrestre, globalement et régionalement. Les simulations avec le modèle de surface terrestre Community Land Model (CLM) sont effectuées à deux résolutions différentes et conduites avec deux différents ensembles de données de forçage, y compris un produit développé récemment par le projet WATCH. Les résultats sont comparés aux simulations de WATCH calculées avec six modèles de surface terrestre et hydrologiques différents. Les résultats révèlent que la simulation de CLM forcée par WATCH se trouve en général dans la marge de fluctuation de ceux de l'ensemble multi-modèle WATCH et que le choix de forçage atmosphérique peut affecter significativement les simulations, au moins dans le même ordre de grandeur que le choix du modèle. En général, les comportements moyens de l'écoulement et de l'évapotranspiration reflètent la répartition des précipitations due au forçage. Les simulations conduites avec la même forçage manifestent les mêmes modes de comportement dans les tendances et l'ampleur, ce qui suggère que la variabilité décennale des composantes du cycle de l'eau est plus sensible aux différences dans les ensembles de données forçantes qu'aux différences dans les paramétrisations du modèle. Pour la variabilité inter-annuelle des processus simulés, toutefois, à la fois les forçages appliqués et les paramétrisations du modèle semblent importants. Les moyennes et les tendances de forçage radiatif sont bien corrélés avec l'écoulement de l'ensemble multi-modèles, mais aucun des ensembles de données incorpore les tendances d'éclaircissement de rayonnement observés, et donc quelques-unes des tendances simulées peuvent être potentiellement erronées. Enfin, il est observé qu'en termes relatifs, la résolution du modèle joue un rôle modeste dans l'incertitude des simulations, du moins en l'absence de résolutions de forçage plus hautes.

Le chapitre 5 résume les principales conclusions de cette thèse, à savoir que les processus de surface des terres et leurs impacts sur le cycle de l'eau sont sensiblement affectés par les tendances du forçage

atmosphérique. De plus, le rayonnement solaire affecte l'évapotranspiration et l'écoulement de façon significative et sa répartition entre les fractions directe et diffuse doit également être prise en compte. Les résultats montrent par ailleurs que les observations de l'écoulement provenant des bassins non-perturbés peuvent se révéler précieuses pour la validation de l'écoulement simulé, car elles se trouvent être de bons indicateurs pour le comportement du bassin à l'échelle continentale et sont sensibles aux tendances du forçage. Enfin, la simulation adéquate de l'hydrologie de la surface terrestre dépend du choix de forçage atmosphérique et du modèle de surface terrestre, ce qui peut biaiser les moyennes, la variabilité et les tendances aux niveaux global et régional. Ainsi, cette étude montre à la fois le potentiel et les limites des modèles de surface terrestre pour évaluer les tendances hydrologiques terrestres et souligne en particulier la nécessité pour l'amélioration des ensembles de données de forçage atmosphériques pour évaluer à long terme les changements dans le cycle de l'eau sur terre. Il est aussi démontré que les variations régionales dans l'importance des drivers atmosphériques respectifs, qui peuvent généralement être liées aux variations de régime hydrologique, sont fortes.

Table of contents

Abstract	iii
Résumé	vi
Table of contents	x
1 Introduction	1
1.1 The water and energy balances.....	4
1.2 The water cycle and climate change.....	5
1.3 Global dimming and global brightening.....	8
1.4 Land-surface modeling.....	10
1.5 The Community Land Model v3.5.....	11
1.6 Aims and outlines.....	15
2 Modeling radiation impacts on the water cycle	17
Abstract.....	19
2.1 Introduction.....	21
2.2 Methodology: Model and numerical experiment.....	23
2.3 Results.....	28
2.4 Discussion.....	35
2.5 Conclusions.....	40
2.6 Acknowledgements.....	41
3 Simulated and observed European runoff	43
Abstract.....	45
3.1 Introduction.....	47
3.2 Methodology: Observational datasets and model simulations.....	49
3.3 Results and discussion.....	55

3.4 Summary and conclusions.....	65
3.5 Acknowledgements.....	67
4 Model and forcing uncertainties: CLM vs. WATCH	69
Abstract.....	71
4.1 Introduction.....	73
4.2 Methodology: Models, forcing datasets and simulations.....	73
4.3 Results and discussion.....	76
4.4 Conclusions and outlook.....	84
4.5 Acknowledgements.....	86
5 Conclusions and outlook	87
5.1 Conclusions.....	89
5.2 Outlook.....	91
Bibliography	93
Acknowledgments	109
Curriculum Vitae	111

Chapter 1

Introduction

Introduction

“... il y a plusieurs petites ifles environnees & entourees d'eau de la mer, mefme quelques vnes qui ne contiennent pas vn arpent de terre ferme, esquelles il y à des puits d'eau douce; ce qui dōnne clairement à cōnoiftre que lefdites eaux douces ne prouiennent n'y de source ny de la mer; ains des efgouts des pluyes, trauerfant les terres iufques à ce qu'elles ayent trouué fond...”

(Bernard Palissy)¹

Securing reliable sources of freshwater has been a constant preoccupation of human societies. A vital element for subsistence, water has been since ancient times a main subject of people's interest, as they have struggled to better understand its cycles and the past, present and future trends in availability, in order to adapt to its changes. Yet, the scale of recent human-induced alterations to the climate system will pose perhaps one of humanity's greatest challenges, as we strive to adequately predict, and adapt to, likely unprecedented impacts on the water cycle. The climate system is a complex, non-linear entity influenced by external forcing, and interacts with the land surface at various spatio-temporal scales, whose workings are impossible to fully capture from observations alone. Modeling the water and energy cycles at the land-atmosphere interface can help understand these complex processes and interactions, separate the effects of the different forces at play, and ultimately improve society's ability to manage water resources. This thesis, based on land-surface modeling and comparisons with observations, aims at improving the understanding of the effects of observed trends in atmospheric forcing on the components of the terrestrial hydrologic cycle.

¹ Bernard Palissy (1580) is credited with the first clear formulation of the modern concept of the water cycle. In his “Admirable speeches on the nature of the waters and fountains...” he wrote: “... there are several small islands encircled and surrounded by sea water, even some which do not contain an acre of dry land, where one can find freshwater wells; this clearly lends itself to the understanding that the said fresh waters do not originate neither from spring nor from the sea; the same can be said for the runoff from the rains, traversing the lands until it finds a bottom...”

1.1 The water and energy balances

Climate on Earth is determined by the amount of incoming radiation from the sun. To achieve equilibrium, the outgoing longwave radiation has to balance the incoming shortwave radiation, a relationship coupled by a plethora of atmosphere and surface phenomena. Incoming radiation may be scattered and reflected by clouds and aerosols or absorbed in the atmosphere, and then further absorbed or reflected at the surface (Trenberth *et al.*, 2009). This radiation provides the energy necessary for the evaporation of water to form clouds, which in turn further dictate how much radiation is let through, reflected or absorbed, in an interaction that closely binds the water and energy cycles. The quantification of the global energy budget is challenging, and major improvements in its estimation were only possible after satellite observations which narrowed the theretofore large uncertainty in planetary albedo and outgoing longwave radiation became available (Kiehl and Trenberth, 1997). An estimation of the global energy flows is illustrated in Fig. 1.1 (Trenberth *et al.*, 2009). Satellite-derived estimates of precipitation also help in determining global surface latent heat fluxes, nonetheless large

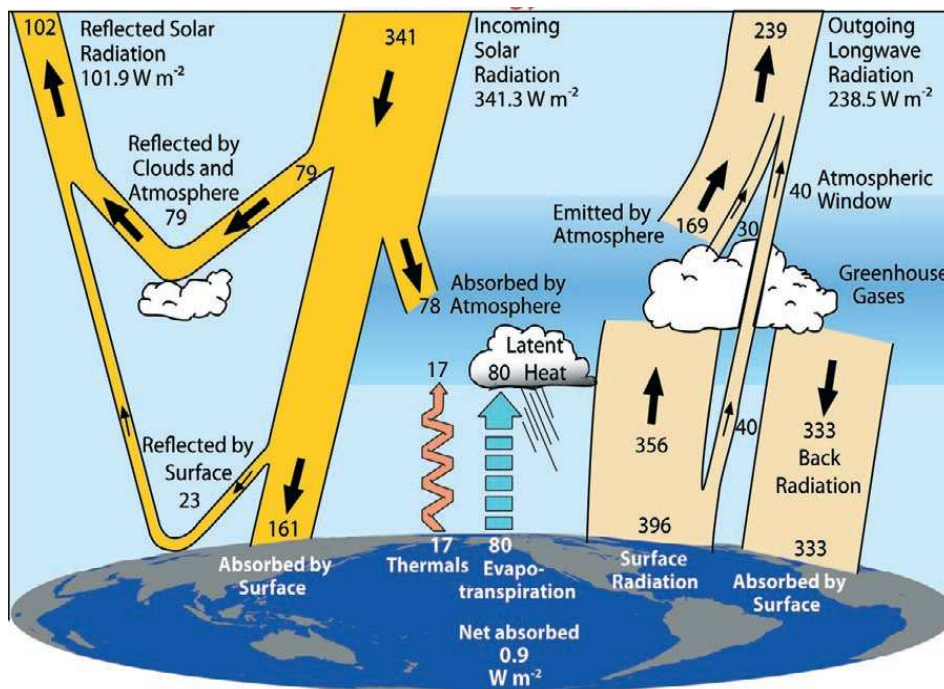


Figure 1.1: Earth's annual mean energy budget, in $W m^{-2}$, with broad arrows indicating the schematic flow of energy in proportion to their importance (from Trenberth *et al.*, 2009).

uncertainties in the energy and water budgets remain. Due to Earth's geometry causing differential heating, the atmosphere acts as a vehicle for the transport of energy from the tropics poleward, with variations to the top of atmosphere net radiation exhibiting an annual cycle due to fluctuations in Earth's albedo and solar irradiance (Fasullo and Trenberth, 2008). The top of atmosphere budgets are closed by the net upward surface energy flux consisting of shortwave and longwave radiative fluxes, and turbulent fluxes of latent and sensible heat (Mitchell, 1989). The global annual cycle of the net radiation has a range of about 8% of the net flow through the system, so a 5% error in the annual cycle is comparable to the climate change signal. The annual cycle in land energy storage on the order of 2% of the net flow is associated with moisture flows onto land, return river flows, and changes in solid and liquid water storage (Fasullo and Trenberth, 2008). It is thus important for models to be able to capture changes in land albedo, snow cover, vegetation, and hydrology.

1.2 The water cycle and climate change

Water vapour sensitivity to temperature suggests that the warming of the planet due to the greenhouse effect will impact the global water balance (Allen and Ingram, 2002). Multi-model analyses show that anthropogenic forcings would have already been responsible for increases in precipitation and changes to its latitudinal distribution (Zhang *et al.*, 2007), and combined satellite observations and model simulations reveal a link between rainfall extremes and temperature, additionally noting that the observed amplification of extremes is larger than predicted, implying that future change projections may be underestimated (Allan and Soden, 2008). Indeed, model-observation comparisons indicate that global land precipitation is controlled by external forcings (Fig. 1.2), but the quantification of possible future changes in the hydrologic cycle is difficult because observations are scarce and the physical constraints on this complex system are weak (Allen and Ingram, 2002). It is thus important to investigate trends in measurable hydrological variables such as evapotranspiration (hereafter referred to as "ET") and runoff, and study how climate change affects related surface processes and exchanges. Although available ET observations are insufficient to detect robust, long-term trends (e.g. Seneviratne *et al.*, 2010), studies of pan evaporation observations (e.g. Roderick and Farquhar, 2002), modeling of land-atmosphere interactions (e.g. Seneviratne *et al.*, 2006), and combined modeling and observation studies (e.g. Teuling *et al.*, 2009) concur that external drivers impact the land water cycle through changes in ET. In addition, runoff, the difference between precipitation and ET on long time scales,

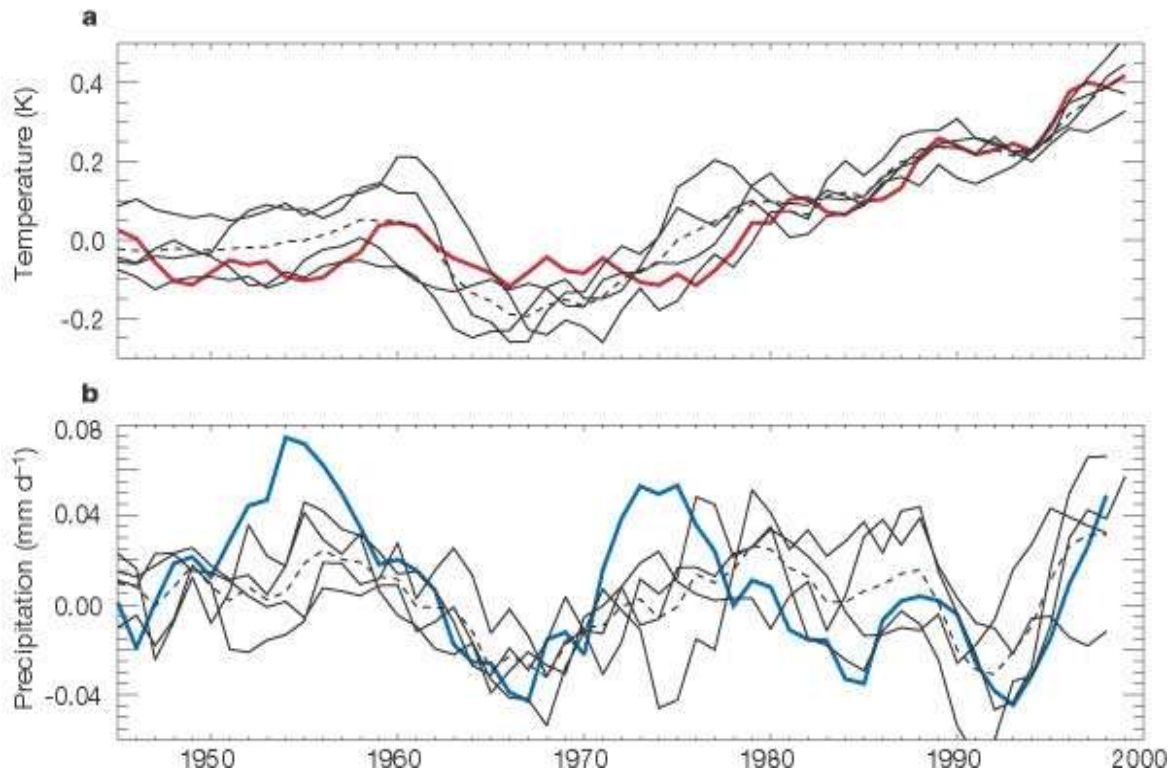


Figure 1.2: Changes in observed global-mean temperature (a, in red) and land precipitation (b, in blue) over the past 55 years compared with HadCM3 climate model run from a four-member initial-condition ensemble with estimates of anthropogenic, solar and volcanic forcing. Dashed line shows ensemble mean (from Allen and Ingram, 2002).

plays a key role in the water cycle as it returns the net fluxes from land-atmosphere interactions to the oceans, also affecting soil moisture and ET. An estimation of the global water storage reservoirs and fluxes is illustrated in Fig. 1.3 (Trenberth *et al.*, 2007). A measure of water availability so critical for human health, economic activity and ecosystem function, runoff has also been changing in the 20th century, but large-scale runoff studies have often reached conflicting outcomes regarding the magnitude and even sign of modeled and observed trends (e.g. Labat *et al.*, 2004, Legates *et al.*, 2005; Milly *et al.*, 2005; Krakauer and Fung, 2008; Dai *et al.*, 2009). In fact, the study of trends in runoff is marred with obstacles, as long-term measurements are scarce and expensive to maintain, methodological issues and errors in measurements and data processing are not uncommon, and data are often not made available (Hannah *et al.*, 2010). Nonetheless, runoff observations agree that changes have occurred, some as a

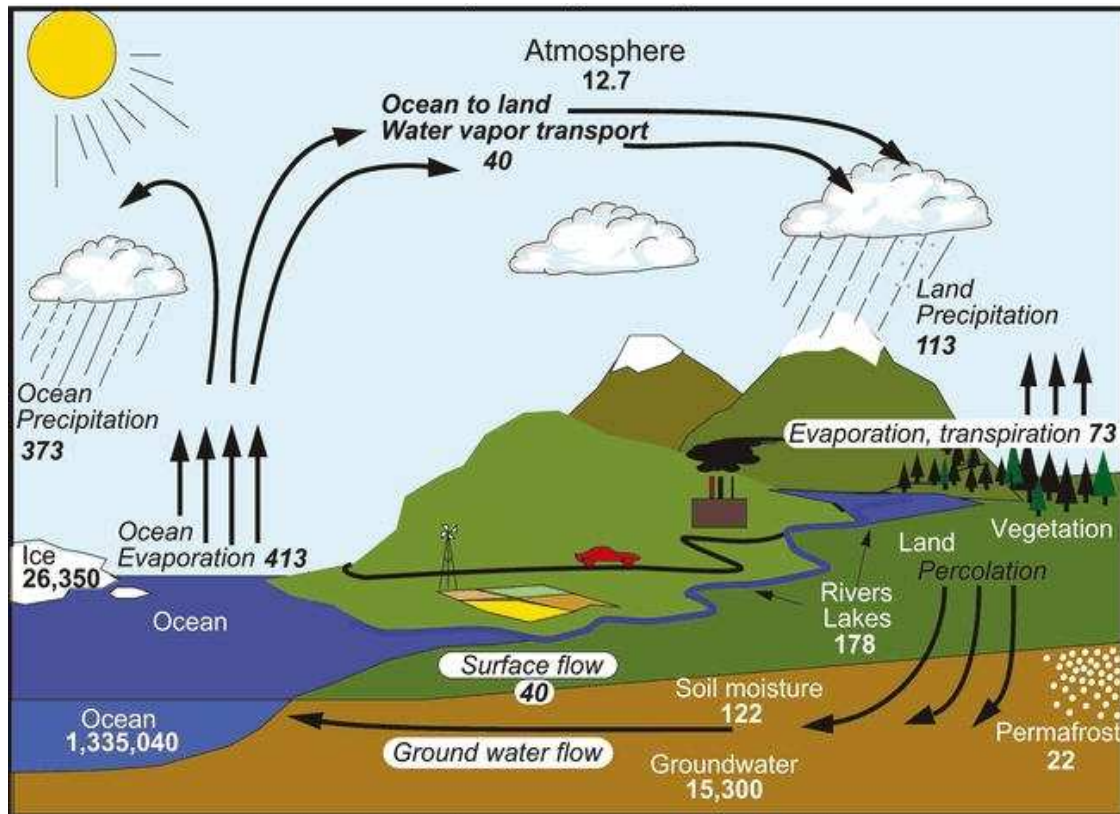


Figure 1.3: The hydrological cycle, with estimates of the main water reservoirs given in plain font in 10^3 km^3 , and the moisture flows in italic font in $10^3 \text{ km}^3 \text{ yr}^{-1}$ (from Trenberth *et al.*, 2007).

result of such human-induced, non-climate effects as land cover alteration (Vörösmarty and Sahagian, 2000) or water diversion for human use (Döll *et al.*, 2009), while much has also been attributed to external forcings in the form of precipitation and temperature trends (McCabe and Wolock, 2002; Peterson *et al.*, 2002; Milliman *et al.*, 2008). Runoff is also influenced by vegetation, itself sensitive to atmospheric CO_2 -induced climate change: this includes alterations to land-use/land-cover (Piao *et al.*, 2007; Gerten *et al.*, 2008) and the effects of increased atmospheric CO_2 through plant transpiration (Gedney *et al.*, 2006; Betts *et al.*, 2007; Gerten *et al.*, 2008) and plant fertilization (Piao *et al.*, 2007; Alkama *et al.*, 2010), or changes to radiation from different aerosol load or direct/diffuse radiation partitioning (Gedney *et al.*, 2006; Oliveira *et al.*, 2011) affecting photosynthesis. Table 1.1 gives an overview from land-surface modeling studies of the magnitude of some drivers of runoff change with respect to the climate impact (Oliveira *et al.*, 2011). Model simulations for the elaboration of

CHAPTER 1: INTRODUCTION

Table 1. Comparison of modeled runoff trends from climate [mm/yr²] and other drivers [as % of climate trend] from various studies.

Land-surface model	Forcing data	Publication	Time period	Domain	Climate ^a	Other drivers			
						Radiation / Aerosols	Diffuse radiation	CO ₂	Land use
CLM3.5	NCEP/NCAR Reanalysis	[Oliveira et al., 2011]	1960-1990	Europe	-1.82	-23%	5%	–	–
				Global	-0.40	-108%	18%	–	–
			1951-2002	Europe	-0.30	–	–	–	–
				Global	-0.30	–	–	–	–
ORCHIDEE	[IPSL CM4 output]	[Alkama et al., 2010]	1900-1999	Global	+0.18	–	–	6%	–
LPJml	CRU TS 2.1	[Gerten et al., 2008]	1951-2002	Global	-0.12	–	–	-23%	-14%
			1901-2002	Global	+0.16	–	–	21%	28%
ORCHIDEE	CRU TS 2.1	[Piao et al., 2007]	1901-1999	Global	+0.15	–	–	-27%	53%
				Europe	+0.19	–	–	-5%	53%
HadCM3	CRU05	[Gedney et al., 2006]	1960-1994	Europe	-0.19	-21%	–	-132%	11%
				Global	-0.14	-93%	–	-179%	0%

^a Includes trends intrinsic to atmospheric forcing datasets: precipitation, temperature, humidity, wind.

projections into the 21st century suggest that larger changes to mean and extreme runoff conditions are expected (e.g. Milly *et al.*, 2005; Hirabayashi *et al.*, 2008), although there are still large uncertainties regarding flood projections, because the involved processes are complex (IPCC, 2012). A substantial portion of 20th century hydrologic change was externally forced, making models essential to helping characterize future changes to the components of the water cycle.

1.3 Global dimming and global brightening

Volcanic signals have been detected in changes to global precipitation in the second half of the 20th century, confirming that shortwave forcings may exert a large influence on the water cycle (Gilett *et al.*, 2004). Similarly, incident solar radiation at the surface has changed in the last half-century, as an initial dimming trend from approximately 1960 to 1990 preceded an ongoing period of widespread brightening (Wild *et al.*, 2005; Streets *et al.*, 2006). Observations reveal a large, widespread “dimming” of incoming radiation amounting to a global period average of 9 W m⁻² (Stanhill and Moreshet, 1992), observable from ground stations (Stanhill and Cohen, 2001) and satellites (Pinker *et al.*, 2005). Dimming likely has anthropogenic causes due to an increase in atmospheric aerosol loading from fossil fuel emissions and associated increase in cloud formation (e.g. Lohmann and Feichter 2005). Since

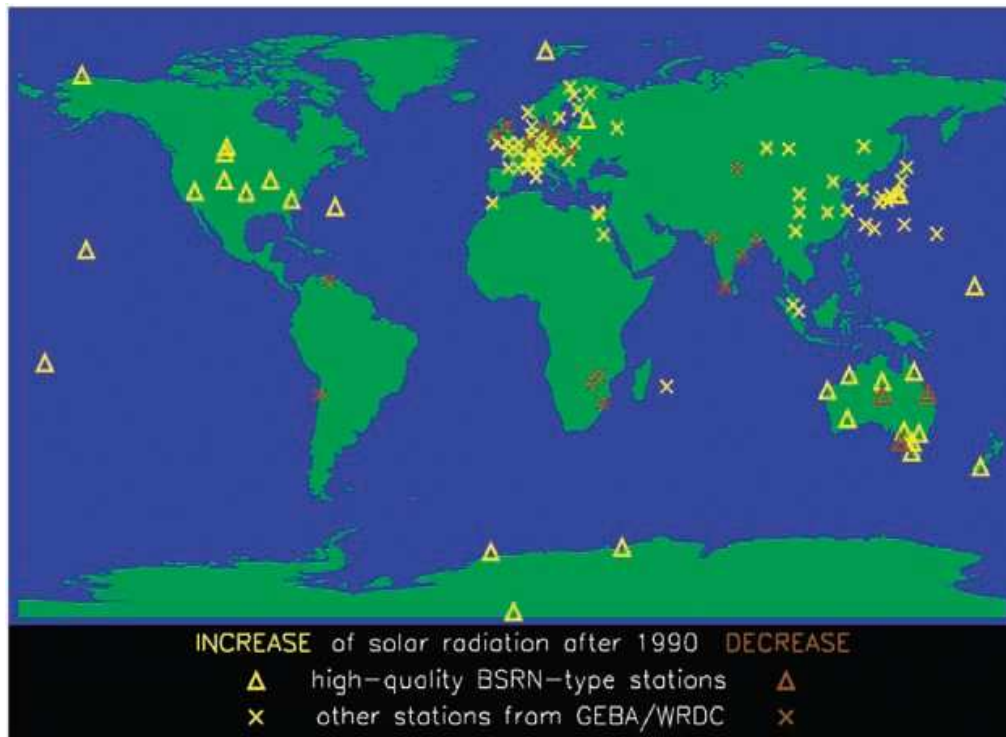


Figure 1.4: Distribution of solar radiation observations: sites measuring an increase in surface radiation after 1990 are marked in yellow; sites measuring a decrease are shown in brown. High-quality observations are triangles, other sites are crosses (from Wild *et al.*, 2005).

approximately 1990, more effective clean-air regulations, added to the decline in heavy-polluting eastern European economies, have probably led to a reversal from dimming to brightening, as noted in global-wide observations (Wild *et al.*, 2005). A map of the stations measuring this recent increase in solar radiation is included in Fig. 1.4 (Wild *et al.*, 2005). Some of this radiative energy surplus (in the case of the brightening) at the surface is consumed by evaporation and moist convection, and later released in the atmosphere through condensation (Richter and Xie, 2008), implying that any alterations in the available energy will induce changes in the water fluxes (Wild and Liepert, 2010). However, the current generation of climate models does not capture most of the 20th century variability in the hydrologic cycle, likely due to the inadequate representation of surface solar dimming and brightening (Wild and Liepert, 2010). Changes in shortwave downward radiation have been shown to impact land hydrology, from regional observational studies, e.g., based on soil moisture measurements and surface

flux and runoff observations (Robock and Li, 2006; Teuling *et al.*, 2009), but global analyses cannot be conducted solely based on observations. An improved knowledge of variations of the surface radiation balance and their forcing factors are key to our understanding of past, present and future changes in the hydrological cycle, and their use in a modeling framework should allow for more realistic simulations and predictions of the hydrological cycle in the future.

1.4 Land-surface modeling

Land-surface modeling applies numerical models that integrate complex hydrologic and physical processes occurring at the land surface, between the surface and the atmosphere, and within the soil column (Liang, 2005). There is strong evidence that land-surface perturbations cause changes in climate, and climate models are sensitive to the land surface as these changes affect the water and energy cycles at different spatial and temporal scales (Pitman, 2003). A land-surface model includes physical processes related to the energy and water budgets, and operates over large spatial domains with short temporal scales. Processes are interconnected and limited by the available water and energy (e.g., ET links the energy and water cycles; soil moisture connects different physical and hydrological aspects). Land-surface models can be coupled to atmospheric models to study the interconnections between the atmosphere and the land surface, which can improve the accuracy of numerical weather forecasts and climate predictions that play a dominant role in hydrologic forecasting (Liang, 2005). They require as input meteorological, soil, and vegetation data of increasing quality and resolution. The recent representation of the vegetation as dynamic is changing our understanding of the interactions between vegetation and a changing climate (Tang and Bartlein, 2008). Manabe's "Bucket" model was the first to represent land-surface impacts within the context of climate simulations, and included simplified hydrologic processes, a simple energy balance equation, and no vegetation (Manabe, 1969). A second generation of such models, or "biophysical" models such as the Biosphere-Atmosphere Transfer Scheme (BATS) and the Simple Biosphere (SiB) model, already represented plant stomatal conductance, although they calculated it only empirically (Dickinson *et al.*, 1986; Sellers *et al.*, 1986). These models also included a more complex energy budget to realistically represent energy exchanges between the land surface and the atmosphere, and ET was related to soil moisture through a simple linear "beta" factor. Additionally, they also incorporated a soil resistance component to soil evaporation

(Jarvis, 1976). The third and current generation, or “physiological” land-surface models, has stomatal conductance explicitly related to photosynthetic assimilation (Ball *et al.*, 1987). Despite the complexity of current land-surface schemes, there are large discrepancies among models in the magnitude, regional and land type-specific behaviour, with respect to such important issues as the dependency of ET on soil moisture, often resulting in divergent outcomes for similar scenarios (Seneviratne *et al.*, 2010). Therefore, relevant biophysical processes related to soil moisture-vegetation interactions, and their impacts on hydrology, need to be further ameliorated and complemented with adequate validation.

1.5 The Community Land Model v3.5

The Community Land Model version 3.5 (hereafter referred to as “CLM”) is a numerical model that simulates land-surface processes within the context of global climate simulations (Oleson *et al.*, 2004, 2008; Stöckli *et al.*, 2008). Among the various biophysical processes represented in the model, the most relevant to this thesis include:

- solar and longwave radiation interactions with vegetation and soil;
- latent heat (ground evaporation, canopy transpiration, and canopy interception) and sensible heat (ground and canopy) fluxes;
- stomatal control on transpiration and plant photosynthesis;
- soil hydrology, including surface and sub-surface runoff, infiltration, and groundwater;
- vertical profiles of water and temperature calculated for 10 soil layers and up to five snow layers;
- a river routing scheme.

Spatial heterogeneity is represented as a nested sub-grid hierarchy in which each grid cell is composed of various land units (glacier, wetland, vegetated, lake and urban), and the vegetated land unit features up to 17 plant functional types (hereafter referred to as "PFTs"). These PFTs differ by their radiative properties, root distribution, aerodynamic parameters and physiological properties. Biophysical processes are simulated for each sub-grid unit, and grid-scale surface variables and fluxes are derived by aggregating the sub-grid fluxes. CLM divides the canopy into sunlit (receiving both direct and diffuse light) and shaded (receiving only diffuse light) fractions (Oleson *et al.*, 2004; Thornton &

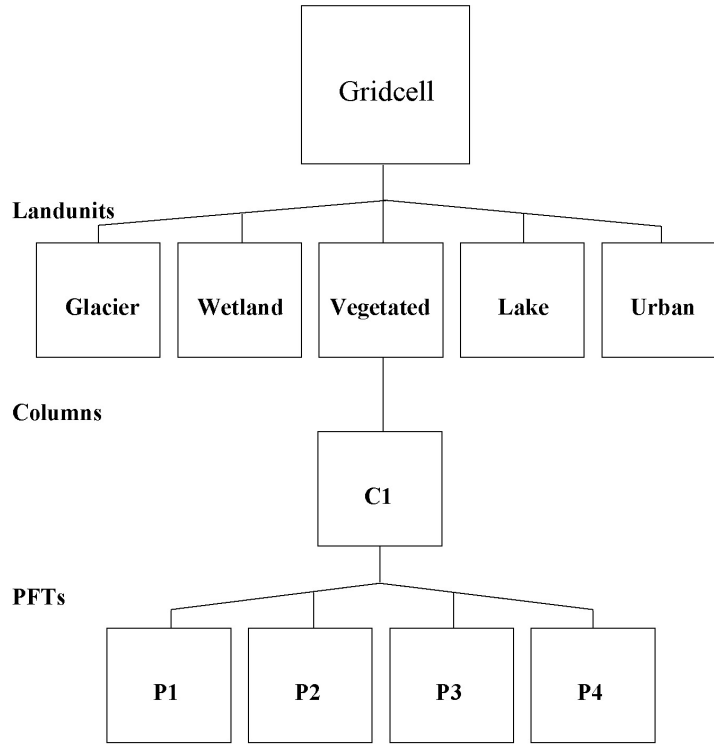


Figure 1.5: Configuration of the CLM subgrid hierarchy (from Oleson *et al.*, 2004).

Zimmermann, 2007), taking into account the connection between stomatal conductance and photosynthesis. The direct (I_{dir}) and diffuse (I_{dif}) radiation fluxes absorbed by the vegetation are computed using a two-stream canopy radiative scheme, respectively:

$$I_{\text{dir}} = 1 - I_{\text{dir}\uparrow} - (1 - \alpha_{\text{g dif}}) I_{\text{dir}\downarrow} - (1 - \alpha_{\text{g dir}}) e^{-K(L+S)} \quad (1)$$

$$I_{\text{dif}} = 1 - I_{\text{dif}\uparrow} - (1 - \alpha_{\text{g dif}}) I_{\text{dif}\downarrow} \quad (2)$$

where $I_{\text{dir}\uparrow}$ and $I_{\text{dif}\uparrow}$ are the upward diffuse fluxes per unit incident direct and diffuse flux, respectively. $I_{\text{dir}\downarrow}$ and $I_{\text{dif}\downarrow}$ are the downward diffuse fluxes below the vegetation per unit incident direct and diffuse radiation, and $\alpha_{\text{g dir}}$ and $\alpha_{\text{g dif}}$ the direct and diffuse ground albedos, while L and S are the exposed leaf area index and stem area index, and K the optical depth of the direct beam (Oleson *et al.*, 2004). The stomatal conductance and photosynthesis are calculated separately for sunlit and shaded leaves, as

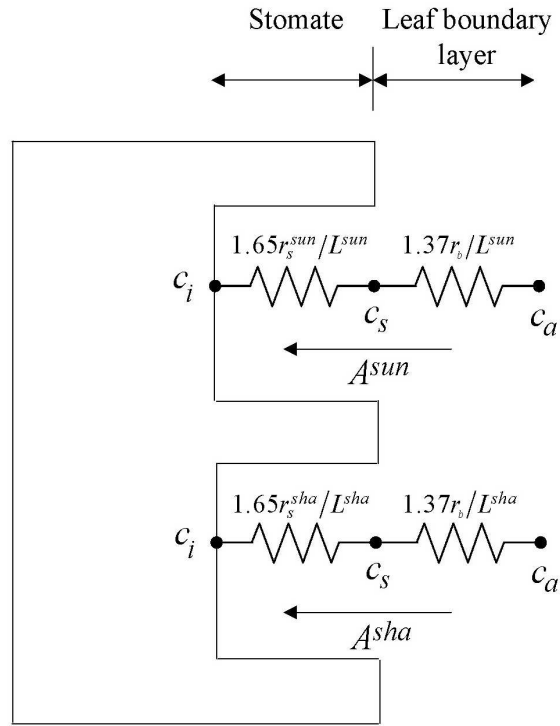


Figure 1.6: Schematic diagram of photosynthesis (from Oleson et al., 2004).

illustrated in Fig. 1.6. Photosynthesis varies non-linearly with solar radiation depending on the light response from stomata, which also depend on air humidity, CO₂ concentration, leaf temperature, and soil moisture stress (Collatz et al., 1991; Oleson et al., 2004), taking into account the CO₂ concentration of the atmosphere, c_a , at the leaf surface, c_s , and inside the leaf, c_i , as well as the leaf boundary layer resistance, r_b . Leaf stomatal resistance, r_s , and photosynthesis, A , both for the sunlit and shaded portions (A_{sun} and A_{sha} , respectively), are then integrated at the canopy level scaled by their respective leaf area indices, L_{sun} and L_{sha} , yielding the following relationships for total canopy photosynthesis, A_{can} (equation 3) and canopy conductance $G_{s\ can}$ (equation 4):

$$A_{can} = A_{sun} L_{sun} + A_{sha} L_{sha} \quad (3)$$

$$G_{s\ can} = (1/r_{s\ sun}) L_{sun} + (1/r_{s\ sha}) L_{sha} \quad (4)$$

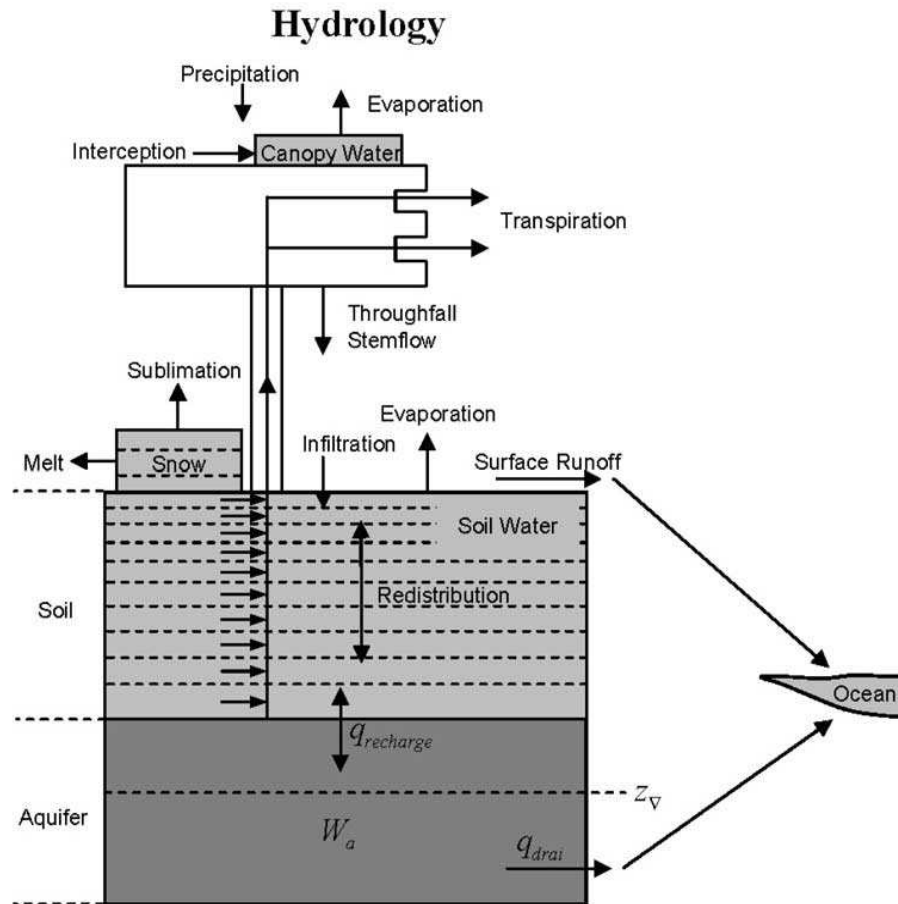


Figure 1.7: Hydrologic processes simulated by CLM (from Oleson *et al.*, 2004).

The CLM hydrology represents such processes as interception, throughfall, canopy drip, snow accumulation, infiltration, surface and subsurface runoff, soil moisture, and the partitioning of ET between canopy evaporation, plant transpiration, and bare soil evaporation (Oleson *et al.*, 2004, 2008). The soil hydrology is based on a TOPMODEL runoff model, which parametrizes surface runoff as consisting of overland flow and infiltration excess, and includes an unconfined aquifer added to the bottom of the soil column (see illustration in Fig. 1.7). CLM has been thoroughly tested and compared with FLUXNET and GRDC data for the simulation of hydrology and other fluxes of energy and nutrients, and performs well for a wide range of land biomes (Oleson *et al.*, 2008; Stöckli *et al.*, 2008).

1.6 Aims and outlines

The following main objectives are addressed in this thesis:

- Verify the sensitivity of CLM and its output hydrologic variables to changes in global radiation
- Investigate modeled ET and runoff trends in the second half of the 20th century, the potential direct and indirect effects of radiation trends, and their relative importance
- Study how changes to the partitioning of solar radiation between its direct and diffuse fractions can have a detectable effect on the water cycle
- Analyse variability and trends in observed runoff from small-scale, undisturbed European catchments, and compare them to other observations and model-derived runoff at the continental basin level
- Investigate the effects of solar radiation and precipitation as potential causes for the identified streamflow trend differences
- Analyse, through an inter-model comparison, the impacts of the chosen land-surface model, model resolution, and atmospheric forcing on the means, inter-annual variability, and trends in total evapotranspiration and surface runoff, at the global and regional levels

This thesis is sub-divided into five chapters with the following contents:

Chapter 1: Introduction and motivation

Chapter 2: Vegetation-mediated impacts of trends in global radiation on land hydrology: a global sensitivity study (Oliveira *et al.*, 2011)

Chapter 3: Simulated and observed inter-annual variability and trends in European runoff (Oliveira *et al.*, submitted to *J. Hydrol.*)

Chapter 4: Model and forcing uncertainties affecting the simulation of terrestrial hydrology: an analysis based on CLM3.5 and WATCH simulated data

Chapter 5: Conclusions and outlook

Chapter 2

Modeling radiation impacts on the water cycle

Modeling radiation impacts on the water cycle

Vegetation-mediated impacts of trends in global radiation on land hydrology: A global sensitivity study

Paulo J. C. Oliveira¹, Edouard L. Davin¹, Samuel Levis² and Sonia I. Seneviratne¹

¹ Institute for Atmospheric and Climate Science, ETH Zurich, 8092 Zurich, Switzerland

² National Center for Atmospheric Research, Boulder, Colorado, U.S.A.

(published online in Glob. Chang. Biol., doi: 10.1111/j.1365-2486.2011.02506.x., 2011)

Abstract

Incident solar radiation has changed in the last 50 years, as an initial dimming trend from 1960 to approximately 1990 was followed by an ongoing brightening period, with concomitant changes in the partitioning between direct and diffuse fractions. Such radiation changes are expected to affect the global water cycle. In this study, we use the Community Land Model (CLM) to perform global offline simulations for the 1948-2004 period and study the effects of solar forcing changes on trends in evapotranspiration and runoff.

The modeled components of the hydrologic cycle respond strongly to the imposed radiation changes in several regions, especially in the tropics. Exceptions are regions with soil moisture-limited evapotranspiration regime, such as the U.S. Great Plains. In Europe and the Eastern U.S. the imposed 7 W/m² solar dimming for 1960-1990 leads to an evapotranspiration reduction of 1.5 W/m² or approximately

5% of the mean, and an enhancement of runoff by equal percentage. In these regions the imposed 6 W/m^2 solar brightening leads to a 3 W/m^2 increase of evapotranspiration in 1990-2004, and a runoff reduction of between 7 and 10% of the mean. Additional simulations investigating the impact of higher diffuse radiation fraction during 1960-1990 suggest mostly an increase of evapotranspiration in the tropics of 2.5 W/m^2 (3% of mean) due to increased photosynthesis from shaded leaves, but with smaller opposite effects elsewhere due to lower ground evaporation.

The runoff trend resulting from the imposed radiation/aerosols effect is of the same sign and approximate relative magnitude as those calculated, in various studies, for other potential drivers of runoff change such as climate, CO_2 or land use, thus strengthening the claim that radiation effects on runoff are not to be neglected. Understanding the impacts of radiation on the water cycle will affect projections of river flow and freshwater availability for human consumption.

2.1 Introduction

Incident global solar radiation (i.e. shortwave downward radiation, hereafter also referred to as “SWdown”) at the land surface has changed in the last 50 years, as an initial dimming trend approximately from 1960 to 1990 was followed by an ongoing period of widespread brightening (Wild *et al.*, 2005; Streets *et al.*, 2006; Wild, 2009). Indeed, observations since 1958 have revealed large, significant widespread reductions in incoming radiation, which, despite considerable spatial variation, amount to a global average of 9 W/m^2 by 1985 (Stanhill and Moreshet, 1992). This phenomenon has been suggested to be limited to sites in urban areas and associated with human population density (Alpert and Kishcha, 2008), but other studies claim it is widespread throughout the northern hemisphere (e.g. Liepert, 2002). Nonetheless, this pre-1990 dimming was identified in observation records from ground stations (Stanhill and Cohen, 2001) as well as satellite measurements (Pinker *et al.*, 2005). In theory, causes for this dimming could include changes to orbital parameters or solar output, but these occur at geological time scales and have been estimated at an order of magnitude smaller than the observed values (Wild, 2009). Likely, dimming has anthropogenic causes due to an increase in atmospheric aerosol loading from fossil fuel emissions and associated increase in cloud formation, and is well correlated with pollution sources and vehicle traffic at latitudes of higher industrialization and population (Alpert and Kishcha, 2008; Wild, 2009). Since approximately 1990, more effective clean-air regulations, added to the decline in heavy-polluting Eastern European economies, have likely contributed to a reversal from dimming to brightening, as noted in most global-wide observations (Wild *et al.*, 2005). This has been duly recognized by the research community and summarized in the latest IPCC report (2007), whose accepted global average radiation change values we adopt in this study. Additionally, observations in recent decades from several locations across Europe, North America and China have hinted also at changes in the partitioning of global solar radiation into its direct and diffuse components (Abakumova *et al.*, 1996; Li *et al.*, 1998; Liepert, 2002; Che *et al.*, 2005). Although aerosol loading trends and radiation partitioning have been noted to vary regionally and temporally in some of the above-mentioned regions during the dimming period (Liepert and Tegel, 2002), increased aerosol loadings can generally be assumed to contribute to a higher fraction of scattered light enhancing plant photosynthesis (e.g. Gu *et al.*, 2003), a mechanism possibly responsible for a quarter of the accumulated land carbon sink over the 20th century (Mercado *et al.*, 2009). Such effects are important in the context

of volcanic eruptions (e.g. Gu *et al.*, 2003) as well as proposed geoengineering options (e.g. Crutzen, 2006).

The reported changes in the amount and partitioning of SWdown in past decades are likely to have had important implications for trends in evapotranspiration (hereafter referred to as “ET”) and associated water cycle components in many regions, since net radiation is one of the factors limiting ET (e.g. Roderick and Farquhar, 2002; Teuling *et al.*, 2009; Pieruschka *et al.*, 2010; Seneviratne *et al.*, 2010), and the impact of the direct/diffuse partitioning on plant photosynthesis may be linked with impacts on ET. Terrestrial ET is a key component of the climate system, linking the hydrologic, energy and carbon cycles, amounting to up to 60% of the total land precipitation (Oki and Kanae, 2006), and using up over half of the net radiation on land in the process (Trenberth *et al.*, 2009), but observations are lacking at the global scale (Jung *et al.*, 2010, Seneviratne *et al.*, 2010). Runoff, a measure of water availability so important for human health, economic activity, ecosystem function and geophysical processes, has also been found to be significantly impacted by external forcing in the 20th century, and larger changes are expected in the coming decades (Milly *et al.*, 2005).

Regarding the impact of changes in absolute SWdown on land hydrology, regional observational studies, e.g., based on soil moisture measurements in Russia and Ukraine (Robock and Li, 2006) or water-balance budgets and lysimeter data in Europe (Teuling *et al.*, 2009), have indeed suggested some effects. However, global analyses cannot be conducted based on observations alone. Indeed, available ET observations are insufficient to detect robust, long-term, regional to continental trends given the short record length at most sites from the FLUXNET network (Baldocchi *et al.*, 2001) and the limited number of sites with long-term lysimeter measurements (Seneviratne *et al.*, 2010). Furthermore, linking information from pan evaporation measurements with actual ET trends is not less difficult or uncertain (e.g. Teuling *et al.*, 2009). Also runoff observations are often lacking or affected by human water use in many areas, and disagreements regarding the magnitude and even sign of trends in runoff on the continental scale persist (Labat *et al.*, 2004; Legates *et al.*, 2005; Dai *et al.*, 2009). Additionally, the drivers for observed hydrologic changes cannot be easily attributed, as they are influenced by a large number of physical and biological processes at the land surface.

Ultimately, the temporal and spatial coverage characteristics of hydrologic observations limit the ability to adequately represent the biophysical environment and land-surface hydrology fluxes in global-wide,

multi-decadal studies. More importantly, observations incorporate all potential driving effects, making it more difficult to study specific mechanisms and separate causes. Thus, despite its documented shortcomings and oversimplifications, land surface modeling is a suitable tool to investigate the sensitivity of land hydrology to forcing variables, and in particular to the reported changes in global radiation. Here, we use the Community Land Model version 3.5 (CLM) to perform global offline simulations of land-surface processes, to study the effects of changes in amount and partitioning of global solar radiation on the hydrologic cycle. Specifically, we set out to ascertain whether and how the model and its output hydrological variables are sensitive to changes in global radiation. Additionally, we investigate modeled trends for regions of the northern hemisphere in the second half of the 20th century, the potential direct and indirect effects of radiation trends and their relative importance. Lastly, we ask whether changes in the partitioning of solar radiation between direct and diffuse fractions can have a detectable effect on the water cycle.

2.2 Methodology: Model and numerical experiment

2.2.1 The Community Land Model (CLM)

CLM is a numerical model that represents land surface processes within the scope of global climate simulations (Oleson *et al.*, 2008; Stöckli *et al.*, 2008; Oleson *et al.*, 2004). Biophysical processes simulated by CLM include: solar radiation interactions with vegetation and soil; energy and mass fluxes between plant canopy, soil, and snow; plant photosynthesis; soil hydrology, including surface runoff, infiltration, and groundwater discharge; and a river routing scheme. Spatial heterogeneity is represented as a nested sub-grid hierarchy in which each grid cell is composed of various land units and multiple plant functional types. Furthermore, vertical profiles of water and energy are calculated for ten soil layers and up to five snow layers. Biophysical processes are simulated for each sub-grid unit independently, and surface variables and fluxes are then averaged by area.

Photosynthesis varies non-linearly with solar radiation depending on the light response from stomata, which also depend on air humidity, CO₂ concentration, leaf temperature, and soil moisture stress (Collatz *et al.*, 1991; Oleson *et al.*, 2004). Leaf optical properties determine reflection and absorption of radiation, so sunlit leaves at the top of the canopy are easily light-saturated while those in lower, shaded

areas are usually unsaturated (Sellers *et al.*, 1992). Thus, CLM3.5 divides the canopy into sunlit (receiving both direct and diffuse light) and shaded (receiving only diffuse light) fractions (Oleson *et al.*, 2004; Thornton and Zimmermann, 2007), taking into account the link between stomatal conductance and photosynthetic activity through a formulation adapted from Collatz *et al.*, (1991). Photosynthetic assimilation is calculated after Farquhar *et al.*, (1980) and Collatz *et al.*, (1991) for C3 plants, and Collatz *et al.*, (1992) and Dougherty *et al.*, (1994) for C4 plants. As clouds and other atmospheric particles can enhance the diffuse fraction of solar radiation, making photosynthetically active radiation more accessible throughout the canopy and rendering it more efficient (Roderick *et al.*, 2001), CLM3.5 computes, at each step, the direct and diffuse radiation fluxes absorbed by the vegetation using a two-stream canopy radiative transfer scheme that takes into account the optical depth and zenith angle of the direct beam, and scattering (Oleson *et al.*, 2004). The default configuration of the model, used in particular for all the control simulation, features a model standard 70% / 30 % global partitioning of SWdown radiation into its respective direct and diffuse fractions.

CLM3.5 has been thoroughly tested and compared to FLUXNET and GRDC data with respect to its simulation of hydrology and other fluxes of energy and nutrients, and was found to perform well for a wide variety of land biomes (Oleson *et al.*, 2008; Stöckli *et al.*, 2008). Known simulation limitations include low runoff in the Amazon as well as overall low amplitude of the annual cycle in terrestrial water storage throughout most tropical river basins (Oleson *et al.*, 2008).

2.2.2 Forcing data and experimental setup

2.2.2.1 Forcing trends

The conducted simulations are performed at a resolution of 2.5° longitude by approximately 1.9° latitude (except runoff at 0.5° by 0.5°) driven by a 57-year (1948-2004) atmospheric forcing dataset composed of 6-hourly fields of meteorological data combining reanalysis and observational datasets (Qian *et al.*, 2006), after a previously spun equilibrium state and a subsequent run through a forcing data period of no less than five years to ensure negligible initialization drift. Atmospheric CO₂ concentration is kept constant at the 280 ppm level. Additional land surface data for soil texture are derived from the FAO/UNESCO dataset, and vegetation cover parameters for the 17 chosen plant functional types are

based on MODIS satellite measurements and other sources (Lawrence and Chase, 2007). All land surface data are kept constant.

The Qian *et al.* (2006) forcing has been used in numerous applications (e.g. Qian *et al.*, (2007); Dai *et al.*, (2009); Randerson *et al.*, (2009)), and shown to perform well with respect to the various components of the water cycle (Oleson *et al.*, 2008; Dai *et al.*, 2009). The NCEP/NCAR reanalysis product, on which the Qian *et al.* (2006) forcing is based, has been shown to match SWdown radiation observations poorly, especially in higher latitude regions such as northern Eurasia (Troy and Wood, 2009). After adjustment with observation datasets, in particular with cloud data, the used SWdown forcing showed reasonable performance (Qian *et al.*, 2006), at least on a par with other forcing datasets with similar temporal characteristics available at the time of the simulations.

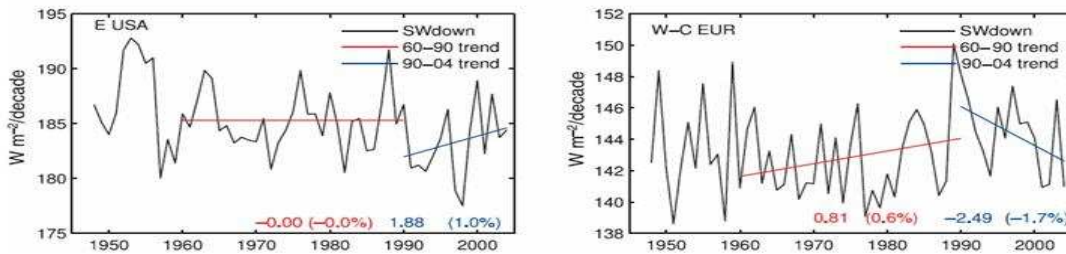


Fig. 1: Time series of shortwave downward radiation from the Qian *et al.* (2006) forcing dataset, averaged for two regions: eastern US (left) and West-Central Europe (right). Decadal trends are shown for the dimming and brightening periods, both in absolute value and as the percentage of the mean.

However, SWdown is still overestimated especially during the observed dimming period, as seen from the absence of a dimming signal in either of the two regional averages shown for the control simulation in Figure 1. Hence it is necessary to impose additional forcing signals to simulate realistic SWdown radiation in Experiment 2 below. SWdown, as well as the other five forcing variables (precipitation, surface air temperature, specific humidity, wind speed, and surface pressure), have been tested and noted to perform reasonably well, in particular the components of the water cycle (Qian *et al.* 2006). However, known issues such as daily precipitation frequency and intensity remain, leading to possible

erroneous trends in ET and runoff. To minimize this problem, analyses performed on all experiments focus only on anomalies after the subtraction of control.

2.2.2.2 Experimental setup

An overview of the conducted numerical experiments is provided hereafter and summarized in Table 1. Three sets of experiments were performed:

Table 1. Summary of CLM global simulations.

Simulation	Period					
	1948	1950	1960	1970	1990	2004
1. Control (CTL)	Qian forcing *					
2. Extreme sensitivity (XDim / XBri)		Extreme dimming / Extreme brightening **				
3. Realistic sensitivity (RealRad)			Realistic dimming ***		Realistic brightening ***	
4. Real direct / diffuse (DirDif)			Increased diffuse ****			

* 1948-2004 forcing from Qian et al. [2006] dataset.

** Qian et al. [2006] forcing except SWdown: 1%/year is subtracted (added) globally to a repeated sequence of the 1948-2004 climatology in annual steps.

*** Qian et al. [2006] forcing except SWdown: 7 W/m² dimming followed by 6 W/m² brightening signals are imposed to equal published estimations [IPCC 2007]: globally, 0.23 (W/m²)/year are subtracted for dimming 1960-1990 (0.43 (W/m²)/year added for brightening 1990-2004).

**** Qian et al. [2006] forcing except SWdown: 1960-1990 diffuse fraction increased to match reports from former Soviet Union 1955-1993 [Abakumova et al., 1996]: diffuse fraction added by 1.5%/decade starting from 70% direct/30% diffuse default reaching 65.5% direct/34.5% diffuse at end of 30 years, globally.

1) Experiment 1 (“Extreme sensitivity”): Idealized “extreme” experiment over the 1950-1970 time period investigating the impact of imposed extreme anomalies in incident global radiation

a) CTL: control simulation using Qian *et al.* (2006) forcing dataset for 1948-2004

b) XDim: “extreme dimming” simulation, using Qian *et al.* (2006) forcing for 1950-1970, except for SWdown which includes an imposed (unrealistically large) decreasing trend of 1% per year

c) XBri: “extreme brightening” simulation, using Qian *et al.* (2006) forcing for 1950-1970, except for SWdown which includes an imposed (unrealistically large) increasing trend of 1% per year

Note that the trends imposed in XDim and XBri are two to five times larger than some of the highest estimates regarding trends in global radiation during the dimming and/or brightening phases (IPCC, 2007), amounting to a total global mean change of 32 W/m² over the 20 years. The purpose of this first

experiment is to provide an estimate of the absolute sensitivity of CLM to imposed extreme changes in global radiation.

2) Experiment 2 (“Realistic sensitivity”): Experiments for the 1948-2004 time period investigating the impact of imposed realistic forcing perturbations in incident global radiation

a) CTL: control simulation using Qian *et al.* (2006) forcing for 1948-2004

b) RealRad: “realistic radiation” simulation, using Qian *et al.* (2006) forcing for 1948-2004 for all other variables except SWdown, which is modified to include “realistic” perturbations over the dimming and brightening periods (superimposed on the Qian *et al.* (2006) 1948-2004 time series): Decrease of 7 W/m^2 in total, i.e. $0.23 \text{ (W/m}^2\text{)/yr}$, over the time period 1960-1990 globally (dimming period), followed by an increase of 6 W/m^2 in total, i.e. $0.43 \text{ (W/m}^2\text{)/yr}$, over time period 1990-2004 globally (brightening period).

The imposed trends in the RealRad simulation are chosen to match published estimates (IPCC, 2007). However, it should be noted that trends in global radiation likely have not been globally uniform, contrary to what is assumed in the RealRad experiment (in particular because the aerosol loading has varied between regions). Due to lack of corresponding radiation observations in many regions (Wild *et al.*, 2005), exact trends cannot be inferred everywhere. Hence, in those regions without SWdown observations, the RealRad experiment simply provides a sensitivity analysis of the potential impact of global radiation trends.

3) Experiment 3 (Real direct/diffuse partitioning): Experiments for the 1960-1990 time period investigating the impact of imposed forcing perturbations in direct/diffuse global radiation partitioning

a) CTL: control simulation using Qian *et al.* (2006) forcing for 1948-2004

b) DirDif: increased diffuse fraction simulation, using Qian *et al.* (2006) forcing for 1960-1990 except for SWdown, with modified SWdown partitioning changed globally at a rate of increased diffuse of 1.5% of total global radiation per decade, reaching 65.5% direct / 34.5% diffuse at the end

of the 30-year period (instead of model standard fixed 70% / 30% partitioning as in all previous simulations).

DirDif simulates an extreme increase in the diffuse fraction of total radiation similar to that reported for the Soviet Union and China in recent decades (Abakumova *et al.*, 1996; Che *et al.*, 2005).

This particular experimental setup, where we impose changes only to radiation keeping other factors (atmospheric forcing fields including CO₂, and land cover) constant, and then analyse the anomalies after subtraction of the control values, allows for a better separation between possible concurring effects of existing forcing trends, while maintaining the temporal variability as close to reality as possible.

2.3 Results

2.3.1 Experiment 1: Extreme global radiation experiments

Analysis of the results of the CTL simulation (not shown) used in all three experiments shows some differences in noted trends in hydrologic variables. In Europe and eastern U.S.A. the ET trend compared to the half-century mean is either zero or slightly positive ($\sim 1\%$ /decade) during the dimming phase, and $\sim 2\text{-}3\%$ /decade during the brightening period. Runoff results show considerably larger regional and temporal variation, as Europe sees a shift from a negative $\sim 2\text{-}4\%$ /decade during the dimming period to a positive $\sim 7\text{-}15\%$ /decade, while in the eastern U.S.A. they go from a positive 7% /decade to a negative 18% /decade in the same periods.

We first present the results of the extreme global radiation experiments, i.e. extreme dimming (XDim) and extreme brightening (XBri) compared with CTL. The analysis focuses on differences in simulated ET (including transpiration and ground evaporation components) and runoff between the sensitivity and control experiments.

Figure 2 reveals that Experiment 1 exhibits a strong simulated response of the analysed water cycle components to the imposed solar radiation anomalies in large parts of the globe. Overall, trends are regionally consistent, and dimming is shown to decrease ET and increase runoff, with the opposite behaviour observed for brightening. ET change is largest in tropical forests, where the imposed decadal trend (hereby defined as ten times the annual trend obtained from the slope of the linear regression line)

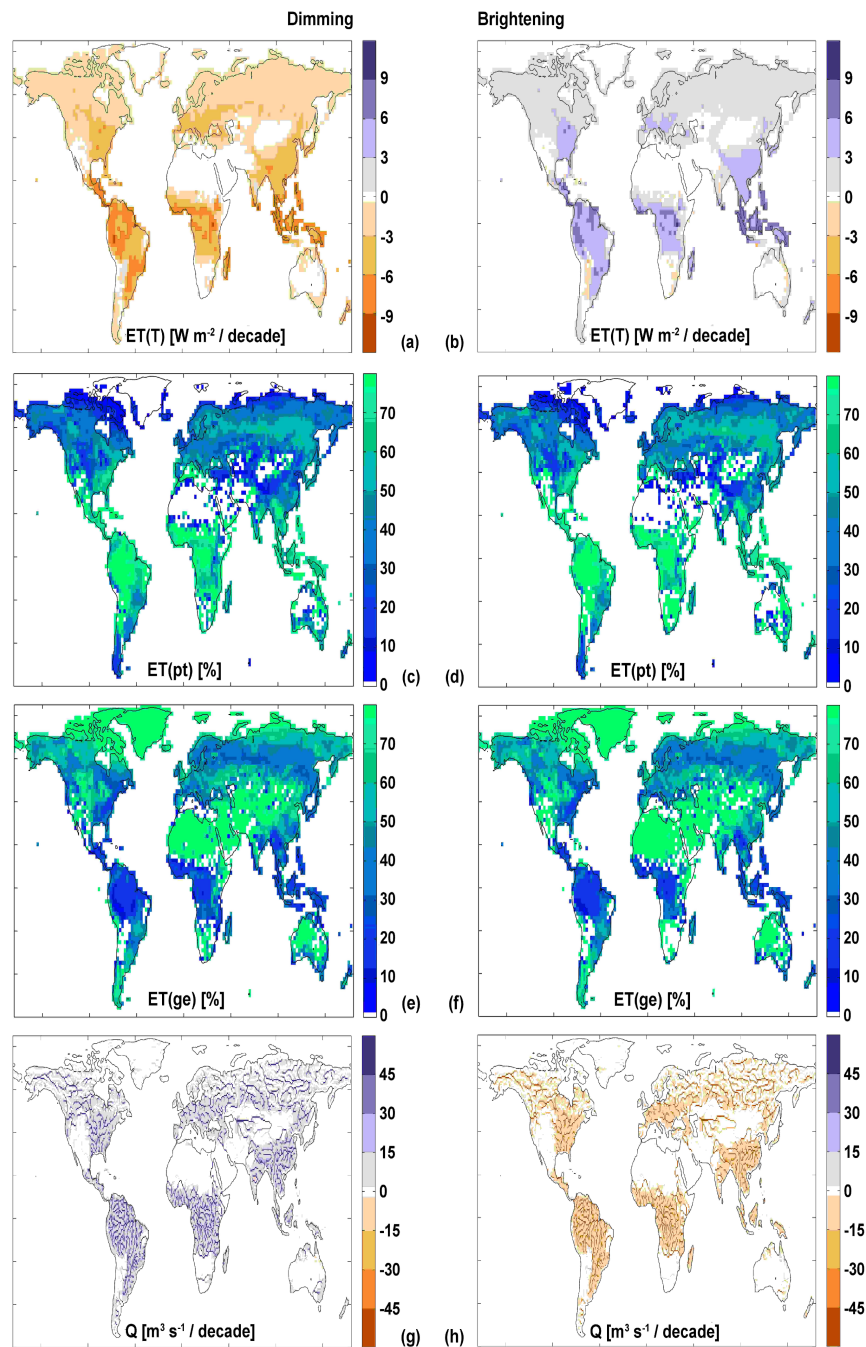


Fig. 2: Experiment 1: sensitivity to extreme dimming (brightening) signals, with global maps of the difference between decadal trends of XDim, left column (XBri, right), and CTL simulations for: (a, b) total evapotranspiration ($W m^{-2}$); (c, d) plant transpiration, and (e, f) ground evaporation (% of change in total evapotranspiration); and (g, h) river runoff ($m^3 s^{-1}$).

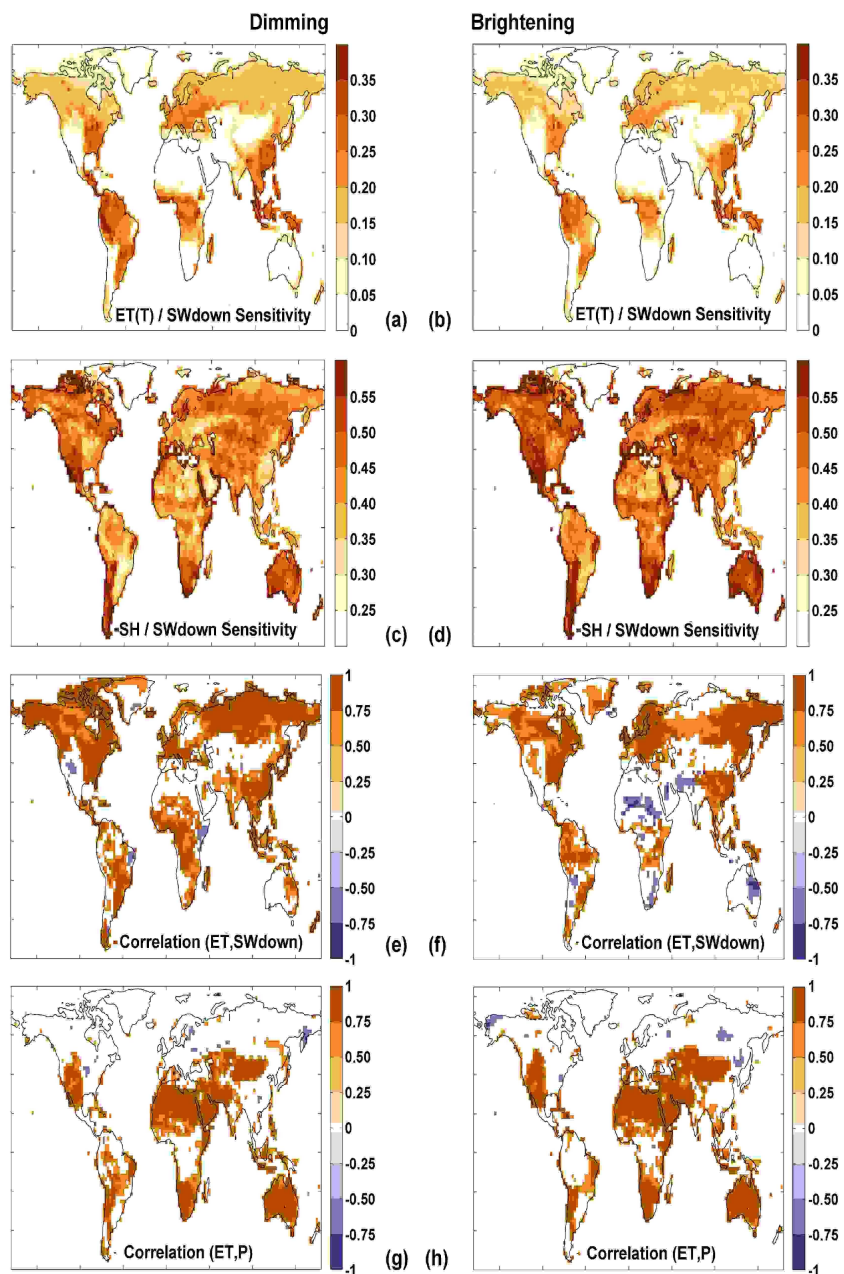


Fig. 3: Sensitivity of decadal trends of total evapotranspiration (a, b) and sensible heat (c, d) for each $W m^{-2}$ of shortwave downward radiation increase for XDim (left) and XBri (right), subtracted by CTL; (e–h): analysis of evapotranspiration drivers in CLM3.5, i.e. correlation ET/SWdown and corr ET/P on yearly time scales (only grid cells significant at 5% level are shown).

is often in excess of 6 W/m^2 , as the annually imposed 1%-change impacts radiation more strongly in absolute terms in regions with already high SWdown (Fig. 2a-b). In these regions, most of the signal in total ET comes from the impact of the imposed radiation changes on plant transpiration, responsible for more than 70% of the total ET trend (Fig. 2c-d). Elsewhere, however, ground evaporation is found to play an equally important role (Fig. 2e-f). Note that changes to canopy interception evaporation have a negligible contribution to overall ET changes in all regions (not shown). Runoff is affected in similar regions as ET, with decadal changes of approximately 10% of the half-century mean in the Amazon basin trend, and other strong response areas throughout the tropics and extending to southeast South America, southeast Asia and eastern U.S.A. (Fig. 2g-h). Further we assess the simulated sensitivity of ET and sensible heat flux to radiation changes, expressed in W/m^2 for each W/m^2 of imposed SWdown radiation. The sensitivity of total ET to radiation changes in the model is found to be higher in Europe, Eastern U.S.A., Eastern China and in the tropics (Fig. 3a,b). These regions are expected to have a radiation or energy-limited ET regime according to several analyses of observational and modeling data (Seneviratne *et al.*, 2006; Teuling *et al.*, 2009; Seneviratne *et al.*, 2010), which is consistent with this outcome. Indeed, a wet regime characterized by high correlation with radiation but low correlation with precipitation should show increased sensitivity to the imposed SWdown changes, as opposed to what would be expected in arid, water-limited regions. Sensible heat flux appears to be particularly sensitive to the imposition of extreme radiation trends (Fig. 3c-d), which is likely caused by limitations of this offline setup, as radiation is made to change while surface temperature is unrealistically kept unaltered. An analysis of the yearly correlation of simulated ET with the imposed SWdown and precipitation (P) forcing in the XDim and XBri runs (Fig. 3e-h) reveals similar patterns of ET regimes as those identified in previous studies (see above), indicating that regions most sensitive to the imposed radiation anomalies are indeed characterized by humid climate regimes, while more arid regions are instead better correlated with precipitation. It is noteworthy that the CLM ET regime distribution assessed from these correlation analyses matches multi-model analyses and eddy-covariance observation results well (Teuling *et al.*, 2009), and thus appears to be realistic.

2.3.2 Experiment 2: *Realistic* global radiation experiments

Figure 4 displays the CLM response to the imposed “realistic” dimming and brightening signals in Ex-

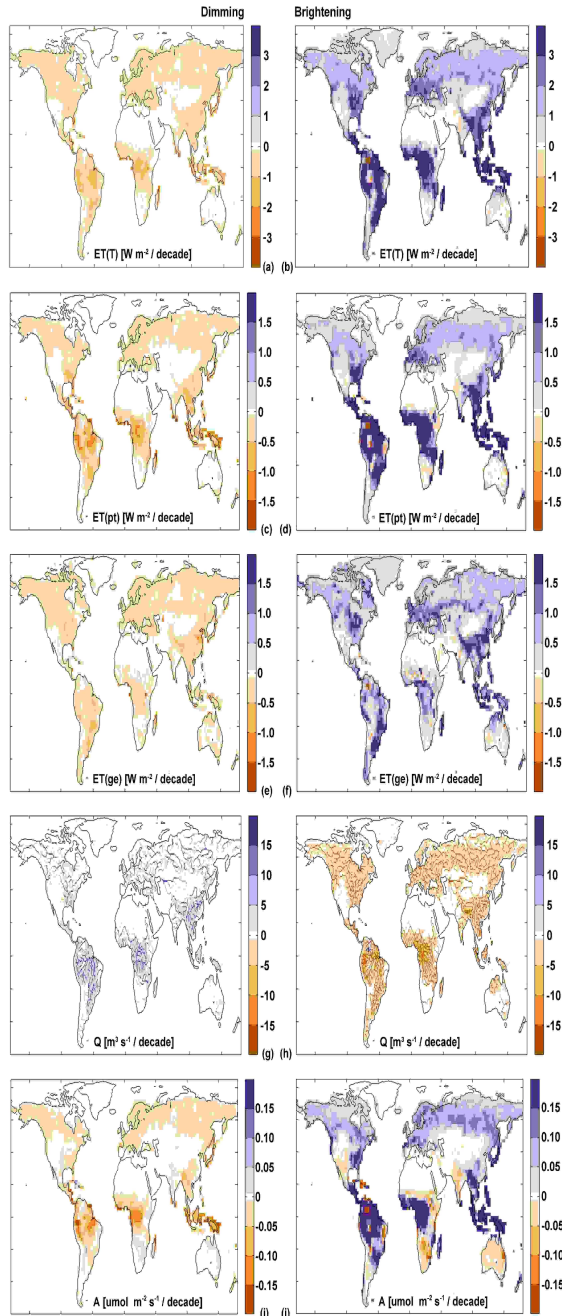


Fig. 4: Experiment 2: impact of 1960–1990 solar dimming, left column (1990–2004 solar brightening, right) on the water cycle: global maps of difference between decadal trends of RealRad and control (CTL) simulations for: total evapotranspiration (a, b), plant transpiration (c, d), ground evaporation (e, f), and river runoff (g, h); similarly for photosynthesis (i, j).

experiment 2 (for time period 1948–2004). The net impact on the water cycle components is smaller than that produced by the extreme radiation experiment but is nonetheless non-negligible, especially in several areas of the northern hemisphere where solar radiation changes have been observed. Anomalies in West-central Europe ($35^{\circ} - 55^{\circ}$ N latitude, 10° W – 10° E longitude), in particular, show a decadal ET reduction in excess of 0.5 W/m^2 during the dimming period and an increase of over 2 W/m^2 per decade during the brightening (Fig. 4a-b). Conversely, runoff rises in this region during the dimming period by approximately $3 \text{ m}^3/\text{s}$ per decade, or 1.4% of the half-century mean, while the brightening causes a decadal drop equivalent to 7% of the mean (Fig. 4g-h).

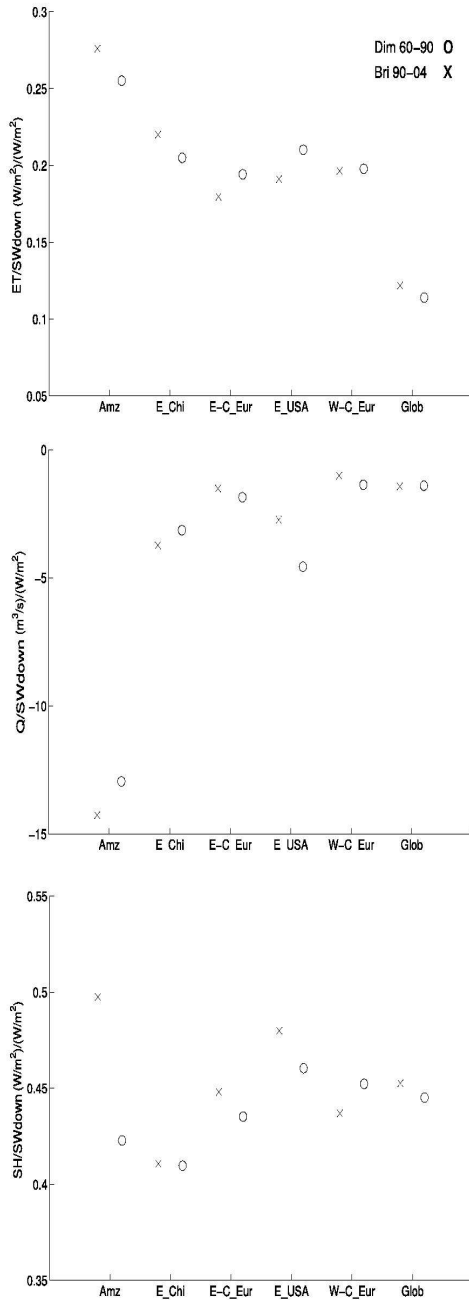


Fig. 5: Sensitivity of decadal trends of total evapotranspiration (a), runoff (b), and sensible heat (c) to each $W m^{-2}$ of shortwave downward radiation increase, for the dimming and brightening periods.

Results of similar magnitude and relative proportion are found for ET in East-central Europe ($45^{\circ} - 65^{\circ}$ N latitude, 10° E – 45° E longitude), where decadal runoff decreases by $18 m^3/s$ during the brightening period. For the Eastern U.S. ($25^{\circ} - 50^{\circ}$ N latitude, $90^{\circ} - 60^{\circ}$ W longitude), the “realistic” simulation shows a decadal ET decrease of $0.5 W/m^2$ during the dimming phase, or 1% of the half-century mean value, and an increase in excess of $2 W/m^2$, or 4% of the mean, during the brightening phase. ET changes in all above regions for either period come mostly from equal contributions from plant transpiration and ground evaporation (Fig. 4c-f). Similarly to Exp. 1, tropical forests exhibit a strong response of the water cycle to the imposed radiation signals, coming mostly from plant transpiration changes that match photosynthesis activity well, both

spatially and quantitatively (Fig. 4i-j). The relative magnitudes of runoff decadal trends in RealRad with respect to control are approximately the same, for either time period, as those for the above European regions. Photosynthesis decadal trend behaviour follows that of plant transpiration for both time periods in all regions, but its magnitude relative to its half-century mean was only approximately 1/3 the percentage of the latter. The sensitivity of the components of the hydrologic cycle to each W/m^2 of radiation changes shows regional variations, but differs only slightly between dimming and brightening periods (Fig. 5). ET sensitivity to radiation change is higher in the Amazon, at almost three times the global average, with mid-latitude regions falling somewhere around $0.2 (W/m^2)/(W/m^2)$. With the exception of the tropical Amazon basin, where vegetation mediated processes exert a substantial impact on all components of the water cycle, river runoff sensitivity to radiation is modest everywhere else. Sensible heat, however, shows a consistent $0.4-0.5 (W/m^2)/(W/m^2)$ sensitivity to radiation in all regions, for both periods.

2.3.3 Experiment 3: Impact of direct / diffuse partitioning

Figures 6 and 7 display the impact of changes in direct / diffuse radiation partitioning in Experiment 3, compared to CTL. These show significant effects on land hydrology. A relative increase in the diffuse fraction, with total radiation remaining constant, produces increases in ET that reach $0.5 W/m^2$ per decade in some tropical regions (Figs. 6, 7). Smaller increases are also noted in other tropical regions, in northern and eastern North America, and across northern Eurasia (Fig. 7). With the exception of the latter region, ET rises almost exclusively due to plant transpiration, which more than offsets a faint contrary signal from ground evaporation. Overall, ET changes coincide with increased photosynthesis and decreased stomatal resistance from shaded leaves, both in terms of spatial distribution and relative intensity. Reductions to river runoff are largely negligible.

2.3.4 Radiation effect comparison: dimming vs direct / diffuse partitioning

As radiation changes simulated in subchapters 3.2 and 3.3 above were both observed during the period 1960-1990, we set out to compare regional patterns of the relative contribution and magnitude of their effects on biophysical and hydrologic variables. Thus, increased diffuse radiation fraction was found to cause a rise in total ET in all regions, an effect of opposite sign but smaller absolute value than that resulting from global dimming (Fig. 6). Decadal trend anomalies for increased diffuse radiation range

from an approximate 0.2 W/m^2 rise in eastern U.S.A. and the Amazon basin ($10.5^\circ \text{ S} - 3^\circ \text{ N}$ latitude, $72.5^\circ - 50^\circ \text{ W}$ longitude), or about 25-30% the absolute magnitude of that from the dimming, to less than 0.1 W/m^2 in Europe and eastern China ($21.5^\circ - 40.5^\circ \text{ N}$ latitude, $100^\circ - 120^\circ \text{ E}$ longitude), equivalent to an effect four to eight times smaller than that from dimming. The drop in runoff as a result of increased diffuse radiation is very modest compared to the increase from solar dimming, with the only noticeable exception found in the Amazon region.

To investigate the potential role of soil moisture in the noted changes to the water cycle during the dimming phase we calculate its anomalies for both the “realistic” dimming and the increased diffuse fraction experiments. Results (not shown) indicate that decadal trends in soil moisture, both at the surface (top 6 cm) and deeper (top 104 cm) soil columns, rarely reach 0.5% of the mean for non-arid regions, and are therefore assumed to play a minor part in the noted radiation-induced hydrologic changes.

2.4 Discussion

The CLM land-surface model responds to incoming solar radiation rise with increased ET and decreased runoff in regions with energy-limited ET regime, and the opposite behaviour is found when radiation decreases. In the case of extreme radiation change the water cycle response is strong, especially in regions where the heat and water fluxes are higher, such as tropical forests. Areas where ET is mostly water limited (Fig. 3g,h) show it is insignificantly or weakly correlated with SWdown, as radiation-induced evaporation changes depend on moisture availability. While a coupled system may also experience concomitant changes in atmospheric water availability and air temperature as a result of ET variation, the offline nature of these experiments limits our ability to capture the behaviour of the entire system in a more realistic fashion, in what constitutes one of the caveats of the study. Nonetheless, with extreme brightening plant transpiration is enhanced to a point where it may return as much as half the additional energy in the form of latent heat, leaving less water on the surface to flow into rivers, with the opposite is true for extreme dimming. However, extreme radiation signals imposed offline on the global scale are physically unrealistic and the response is only an indication of general model behaviour. Indeed, they are in particular large artificial radiation changes uncoupled from a possible response of atmospheric temperature.

CHAPTER 2: MODELING RADIATION IMPACTS ON THE WATER CYCLE

The implementation of “realistic” solar radiation signals, observed in recent decades in regions such as Europe and the eastern U.S.A. but missing in forcing datasets, produces substantial impacts on ET and runoff. There, for the dimming period of 1960-1990 the modeled response is a decadal decrease in ET of about 0.5 W/m^2 (mostly due to changes to its plant transpiration and ground evaporation components in approximately equal proportions) and a concurrent decadal increase in runoff of nearly 1.5% of the half-century mean. The runoff annual trends as a result of the radiation/aerosols effect (-23% and -108% relative to the magnitude of the climate-induced trends for Europe and globally, respectively) are similar to those from Gedney *et al.* (2006) obtained for an analogous experiment (-21% and -93%),

Table 2. Comparison of modeled runoff trends [mm/yr^2] from various studies.

Land-surface model	Forcing data	Publication	Time period	Domain	Climate ^a (P+T+Hu+Wi)	Other drivers ^b			
						Radiation / Aerosols	Diffuse radiation	CO ₂	Land use
CLM3.5	NCEP/NCAR Reanalysis	<i>This study</i> ^c	1960-1990	Europe	- 1.82	+ 0.41 ^d [- 23%]	- 0.09 ^e [5%]	-	-
				Global	- 0.40	+ 0.43 ^d [- 108%]	- 0.07 ^e [18%]	-	-
			1951-2002	Europe	- 0.30	-	-	-	-
				Global	- 0.30	-	-	-	-
ORCHIDEE	[IPSL CM4 output]	[Alkama <i>et al.</i> , 2010]	1900-1999	Global	+ 0.18	-	-	+ 0.01 [6%]	-
LPJml	CRU TS 2.1	[Gerten <i>et al.</i> , 2008]	1951-2002	Global	- 0.12	-	-	+ 0.03 [- 23%]	+ 0.02 [- 14%]
			1901-2002	Global	+ 0.16	-	-	+ 0.03 [21%]	+ 0.04 [28%]
ORCHIDEE	CRU TS 2.1	[Piao <i>et al.</i> , 2007]	1901-1999	Global	+ 0.15	-	-	- 0.04 [- 27%]	+ 0.08 [53%]
				Europe	+ 0.19	-	-	- 0.01 [- 5%]	+ 0.10 [53%]
HadCM3	CRU05	[Gedney <i>et al.</i> , 2006]	1960-1994	Europe	- 0.19	+ 0.04 [- 21%]	-	+ 0.25 ^f [- 132%]	- 0.02 [11%]
				Global	- 0.14	+ 0.13 [- 93%]	-	+ 0.25 ^f [- 179%]	0.00 [0%]

^a Includes trends intrinsic to atmospheric forcing datasets: precipitation, temperature, humidity, wind.

^b Values in brackets show percentage relative to climate trend.

^c Domains: Europe latitude 37N-72N, longitude 11W-30E; Global latitude 60S-90N.

^d 1960-1990 runoff trend only from imposed additional shortwave radiation forcing trend equivalent to -2.94 mm/yr^2 .

^e 1960-1990 runoff trend only from increased diffuse fraction by 1.5%/decade starting from the 70%/30% direct/diffuse model default, reaching 65.5%/34.5% at end of 30 years, globally.

^f Unlike other studies investigating sensitivity to CO₂, Gedney *et al.* (2006) does not take into account the CO₂ fertilization (LAI) effect.

and are approximately of the same order of magnitude as those calculated, in various studies, for other potential drivers of runoff change such as climate, CO₂ or land use (Table 2), thus strengthening the claim that radiation effects on runoff trends are not to be neglected. Similarly, the 0.6% decrease in ET

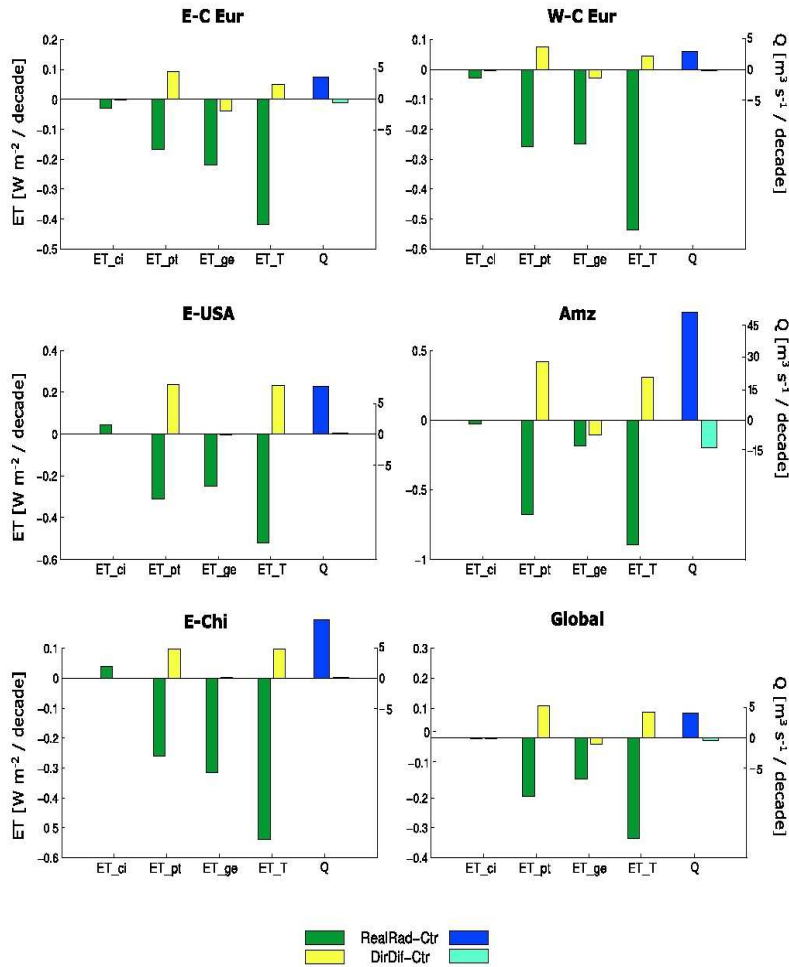


Fig. 6: Comparison of decadal trends of RealRad (dimming) and DirDif simulations are subtracted by control trend, for runoff (Q), total evapotranspiration [ET(T)], and its three components [canopy interception (ET_{ci}), plant transpiration (ET_{pt}), and ground evaporation (ET_{ge})], at the global and various regional scales (East-Central Europe, West-Central Europe, eastern US, Amazon, and eastern China).

obtained as a result of dimming radiation is of exactly the same magnitude as the effect of climate forcing alone (not shown), and larger than the 0.2% drop from a double-CO₂ effect on plant physiology from a 50-year coupled simulation (Cao *et al.*, 2009).

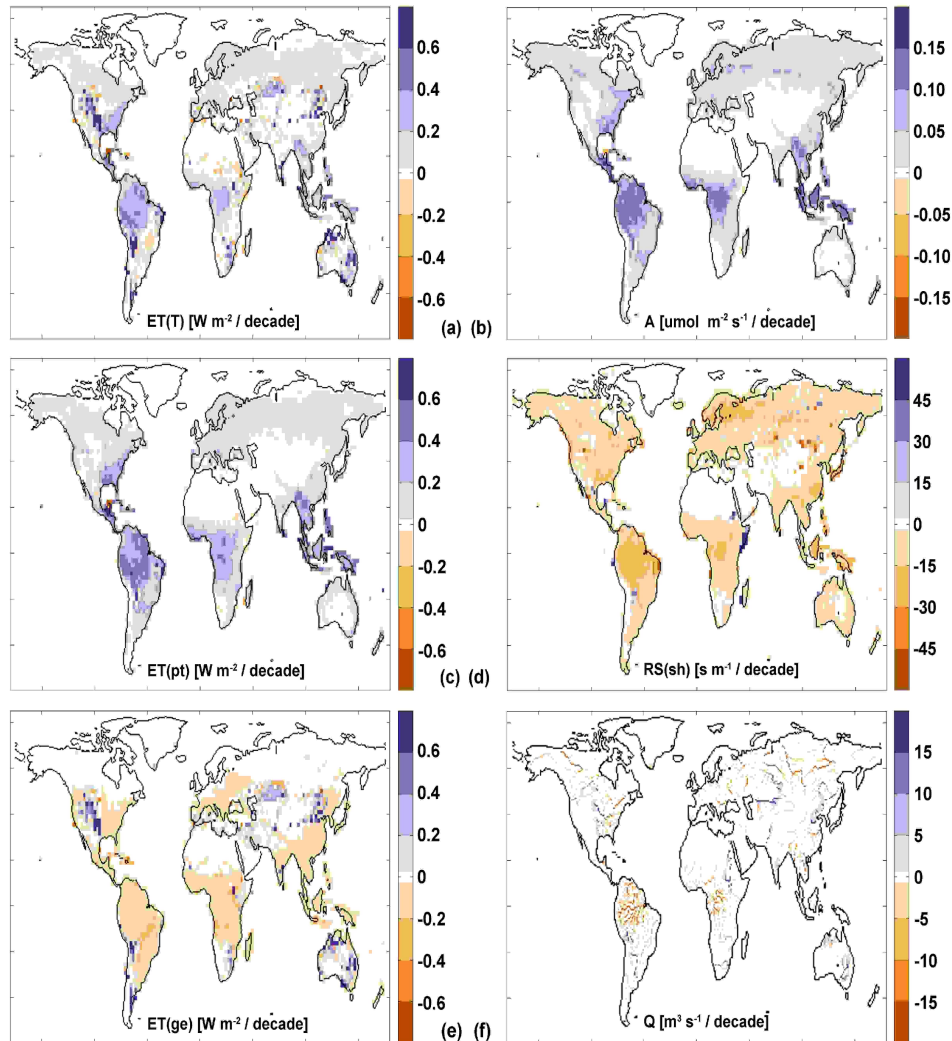


Fig. 7: Experiment 3: sensitivity of land-surface processes to direct/diffuse radiation partitioning, with global maps of difference between decadal trends of DirDif and CTL simulations for total evapotranspiration and its plant transpiration and ground evaporation components (a, c, e); photosynthesis (b); shaded leaf stomatal resistance (d); and runoff (f).

The application of a reverse signal of similar magnitude to a period twice as small such as the 1990-2004 solar brightening elicits a qualitatively similar but proportionally stronger response, as ET rises by 2 W/m^2 per decade while runoff has a decadal drop of almost 7% of its mean value. Some noted discrepancies between models in trends for the global domain shown in Table 2 are likely a result of documented differences in model performance forcing datasets and time periods used. Indeed, Gerten *et al.* (2008) found a high decadal variability of simulated runoff trends with the LPJ model, suggesting that assessed trends strongly depend on the considered period (with variations of up to one order of magnitude on the global scale for 30-year periods), thus making relative effects of the investigated drivers (indicated in percent in Table 2) more relevant than the absolute trends for the comparisons across studies.

Some of the analysed variables of the climate system behave differently with respect to sensitivity to each W/m^2 of radiation change. In mid-latitude regions vegetation mediated processes respond more strongly to radiation, while river runoff is less sensitive, both for dimming and brightening. Sensible heat, however, shows a consistently high sensitivity to radiation changes, which may question some beliefs from previous accounts that stated the opposite (Wild *et al.*, 2008). Part of this behaviour may nonetheless be due to the uncoupled nature of the experiments (see above).

One caveat to this simulation might be that the observed dimming and brightening signals were limited to locations of observation sites in developed regions in the northern hemisphere, while the “realistic” signals were imposed globally. However, the fact that the experiment is offline ensures the removal of teleconnection effects. In addition, the selection of 1990 as the break point between periods of inverse radiation signal, although generally acceptable globally, might be inadequate for some regions, which may impact the results. Also, changes in aerosol loadings affect variables other than radiation, such as precipitation (Ramanathan *et al.*, 2001) and temperature, which may also play important roles for resulting hydrological trends. Some regions, in particular, are still undergoing significant aerosol loading presently, e.g. India (Padma Kumari and Goswami, 2010). This problem is partly accounted for, since most of the analysis is done based on the anomalies resulting from subtracting the control simulation results. Nonetheless, further studies should attempt to validate the modeled runoff output with observed data from anthropogenically-intact watersheds, in which case the break point selection issue should be further addressed. Lastly, despite the model standard interpolation function, the employed 6-hourly for-

cing data does not fully capture the daily and annual cycles for such important fields as incoming solar radiation, which might lead to an underestimation of the variability. Future investigations should attempt to quantify the effect of the temporal resolution of the forcing on similar simulation results.

The reported increase in the diffuse fraction of total radiation also impacts the hydrologic cycle by increasing ET – over 0.5 W/m^2 per decade in tropical regions due to plant transpiration. A concomitant increase in photosynthesis, mostly due to a rise in shaded leaf stomatal conductance, was noted, which is consistent with the notion that as sunlit leaves are often light saturated, more incoming diffuse radiation will have a positive net effect on shaded leaf photosynthesis (Mercado *et al.*, 2009). Conversely, the opposite, albeit smaller, effect on ground evaporation is a result from less total radiation reaching the ground in vegetated areas, since a greater direct and diffuse total is now captured by the canopy. Comparing the effects on ET of an increase in diffuse fraction to those resulting from global dimming shows that, while the former tend to be almost one order of magnitude smaller and of opposite sign, they can play relevant roles in the energy and water balances in such regions as the Eastern U.S. or the tropics. Outside of arid regions, the effect of soil moisture does not seem to play a significant role in either radiation-induced water cycle changes during the dimming period.

2.5 Conclusions

Observed changes into solar radiation in recent decades have been shown to affect photosynthesis and the carbon balance, and should also impact key components of the hydrologic cycle such as ET and runoff. To clearly understand the mechanisms driving global, multi-decadal hydrologic changes by relying solely on hydrologic observation data is a challenging task, as such datasets often have large associated uncertainties and inadequate spatio-temporal coverage, and typically incorporate possible confounding effects. This makes land-surface modeling a useful tool to study the effects of modifications in the solar forcing on land hydrology. Modeled components of the water cycle respond strongly to extreme radiation change, especially in the tropics. A more realistic 1960-1990 solar dimming may have caused, in regions of Europe and the Eastern U.S.A., a decadal decrease in ET of about 0.5 W/m^2 , mostly as a result of equal changes to plant transpiration and ground evaporation, and a concurrent decadal increase in runoff of nearly 1.5% of the half-century mean. Conversely, an imposed 1990-2004 solar brightening signal for those regions may have risen ET in 2 W/m^2 per decade, lowering decadal

runoff by about 7% of its mean. Reported increases in the diffuse fraction of solar radiation may have also impacted ET, raising it up to 1 W/m² per decade in the tropics. Higher plant transpiration, which accompanies increases in photosynthesis from more shaded leaf stomatal conductance, appears to be the responsible mechanism. Conversely, less direct radiation reduced ground evaporation, responsible for a drop in ET of similar magnitude in some marginally arid regions. Additional studies should seek to validate the modeled runoff output with observed streamflow data from non-impacted watersheds, and further analyse the hydrologic impacts of direct / diffuse radiation by implementing better radiation partitioning. Furthermore, global, two-dimensional data on the partitioning of solar radiation between its direct and diffuse fractions is scarce, and further studies are necessary to implement appropriate radiation forcing and analyse the impacts on the various components of the water cycle. Ultimately, a more complete understanding of the mechanisms and processes driving the impacts of solar radiation on the hydrologic system is fundamental for the development and parameterization of land-surface schemes and the improvement of predictions of climate and water resources.

2.6 Acknowledgements

We thank Martin Wild for useful discussions, and two anonymous reviewers for their helpful comments. We are also thankful to Nicola Gedney for providing the relevant numbers of the Gedney *et al.* (2006) study for Table 2. We acknowledge partial financial support from the EC FP7 Project CARBO-Extreme (FP7-ENV-2008-1-226701) and the CCES MAIOLICA project.

Chapter 3

Simulated and observed European runoff

Simulated and observed European runoff

Simulated and observed inter-annual variability and trends in European runoff

Paulo J. C. Oliveira¹, Edouard L. Davin¹, Boris Orłowsky¹, Kerstin Stahl^{2,3}, Lena M. Tallaksen³
and Sonia I. Seneviratne¹

¹ Institute for Atmospheric and Climate Science, ETH Zurich, 8092 Zurich, Switzerland

² Institute of Hydrology, University of Freiburg, Freiburg, Germany

³ Department of Geosciences, University of Oslo, Norway

(submitted to Journal of Hydrology)

Abstract

This study analyses decadal variability and changes in streamflow in Europe for the period 1960-2004 based on a network of measurements from near-natural small catchments, and compares these results with analyses of large-basin observations from the Global Runoff Data Center (GRDC) and offline land-surface model simulations driven by state-of-the-art forcing datasets. In nearly all basins, inter-annual variability of streamflow is large and long-term trends are therefore difficult to detect, although decadal variations in the trends are found in some basins. We find that the decadal streamflow trends and inter-annual variability from the near-natural catchments exhibit good overall agreement with the GRDC observations despite the scale discrepancy. Southwestern European basins exhibit the poorest correlation between simulated and observed runoff on the inter-annual time scale, but for these basins

all observed and simulated datasets display a significantly negative 1960-1985 trend behaviour, which is not present in the following decades. This is contrary to the generally expected effect of the dimming and brightening radiation signals on runoff, and is likely due to a competing effect from trends in precipitation, which show opposite tendencies. On the other hand, no clear decadal trends are found in the Western and East-central European river basins, with the exception of the Seine. Overall, the model simulations display a reasonable agreement with the observations with respect to inter-annual variability, but exhibit a (non-significant) tendency for positive trends in the Rhone, Garonne and Loire river basins after 1986, which is not identified in the observational datasets. This appears to be mostly due to deficiencies in the forcing datasets, and highlights the critical role of atmospheric forcing for hydrological products of land surface model simulations.

3.1 Introduction

Climate change has already impacted runoff in the 20th century, and more changes are projected for the coming decades despite large uncertainties in these projections (e.g. Milly *et al.*, 2005; IPCC, 2012). River runoff, a measure of water resource availability, is essential to support many ecosystems and for the well-being of human societies. Therefore, a thorough understanding of the mechanisms underlying these changes is necessary to accurately forecast and prepare for future climate conditions. However, climate and the water cycle are complex systems in which confounding signals are often simultaneously at play.

Modeling and observational analyses of changes to climate system components have suggested different potential direct and indirect impacts on the generation of surface runoff or river flow from various climate factors, including the effects of precipitation on streamflow (e.g. McCabe and Wolock, 2002), of temperature on snow melt (e.g. Brown, 2000), as well as of aerosols/radiation (e.g. Liepert *et al.*, 2004; Oliveira *et al.*, 2011) or atmospheric CO₂ concentrations (e.g. Gedney *et al.*, 2006; Piao *et al.*, 2007; Morgan *et al.*, 2011) on surface evapotranspiration (hereafter referred to as "ET"). Also, direct human-induced, non-climate causes can be relevant, for instance land-cover change (Vörösmarty and Sahagian, 2000) or water withdrawals and reservoirs (Döll *et al.*, 2009). Comparative analyses across river basins can be challenging due to the large heterogeneity in hydrologic characteristics (McMahon *et al.*, 2007), and impacts of a given climate variable on basin runoff may vary between regions and between time periods for the same regions due to several factors such as climate regime (Milly and Dunne, 2002), changes to land cover (Piao *et al.*, 2007) or soil phase (Serreze *et al.*, 2002), basin size (Laudon *et al.*, 2007) or elevation (Viviroli and Weingartner, 2004), among others. In addition, long-term measurement networks are scarce, expensive and difficult to maintain, methodological issues and errors in measurements and data processing are not uncommon, and data are often missing or simply not available on administrative or technical grounds (Hannah *et al.*, 2010). Unsurprisingly, large-scale runoff studies yield different and conflicting outcomes regarding the magnitude and even the sign of modeled and observed trends (e.g. Probst and Tardy, 1987; Labat *et al.*, 2004, Legates *et al.*, 2005; Milly *et al.*, 2005; Krakauer and Fung, 2008; Dai *et al.*, 2009; Haddeland *et al.*, 2011), as well as with respect to the attribution of causes for these trends (e.g. Gedney *et al.*, 2006; Piao *et al.*, 2007; Gerten *et al.*, 2008; Alkama *et al.*, 2010; Oliveira *et al.*, 2011).

Incident solar radiation observations at the earth surface display changes in the last 50 years, as an initial dimming trend (-7 W/m^2 for the total period) from 1960 to 1990, or to approximately 1985 in Europe, was followed by an on-going brightening period (6 W/m^2 total) as a result of a decrease in atmospheric aerosol loads (IPCC, 2007; Wild *et al.*, 2005; Wild, 2009). Such changes are expected to affect the global water cycle, as solar radiation plays a potentially relevant role in land hydrology with implications for trends in ET and associated components such as runoff, net radiation being one of the factors limiting ET (e.g. Roderick & Farquhar, 2002; Teuling *et al.*, 2009; Seneviratne *et al.*, 2010). Indeed, the radiation/aerosol effect has been estimated to affect runoff trends in Europe, leading to a possible attenuation, for the period from 1960 to approximately 1990, of more than 20% of the magnitude of the negative runoff trend calculated from climate alone (Gedney *et al.*, 2006; Oliveira *et al.*, 2011).

Basin-scale runoff observations such as those provided by the Global Runoff Data Centre (hereafter referred to as “GRDC”) are essential to adequately investigate continental-scale patterns of hydrologic change (e.g. Milly *et al.*, 2005). However, because of their size, they are impacted by anthropogenic disturbances such as withdrawals for human use, which can be of substantial magnitude (Döll *et al.*, 2009). Thus, observations from near-natural catchments, despite their often small size and consequent less integrative properties, can help elucidate patterns of hydrological changes in the absence of such confounding effects (e.g. Stahl *et al.*, 2010). As an additional source of information, land-surface modeling can also complement analyses based on small-scale or large-scale observational datasets, as it provides improved geographical coverage of corresponding analyses, further allowing for the disentanglement of concurring effects in the investigation of runoff trends and their causes (e.g. Seneviratne *et al.*, 2010; Oliveira *et al.*, 2011; Stahl *et al.*, 2012).

Here we use a European network of streamflow records from near-natural small catchments to analyse streamflow changes integrated at the river basin scale for the period 1960-2004. We compare them to the downstream discharge of large basins from the GRDC dataset, and to model output from two offline simulations using the Community Land Model version 3.5 (hereafter referred to as “CLM”) forced both with the WATCH Forcing Data (Weedon *et al.*, 2010) and the NCEP-derived Qian *et al.* (2006) atmospheric forcing datasets (hereafter referred to as “WFD” and “q06”, respectively). In addition, the observations are compared to the mean of six model simulations from the WaterMIP project (see Section 2.5), which are also driven by the WFD for the period 1985-1999 (Weedon *et al.*, 2010;

Haddeland *et al.*, 2011). The 10 selected European river basins are: Danube (Western portion), Douro, Ebro, Elbe, Garonne, Loire, Rhein, Rhone, Seine, and Weser. An observation dataset for precipitation from E-OBS (Haylock *et al.*, 2008) is also used to investigate the effect of atmospheric forcing on land hydrology. The integration of streamflow from small catchments and their comparison to discharge from large river basins or model-simulated runoff are challenging, as the two types of data series are subject to different processes taking place at different spatial and temporal scales. The main focus of this study is to analyse the decadal variability and trends in observed runoff from small-scale, near-natural European catchments, to compare them with observations and model-derived runoff at the continental basin level, and to investigate the effects of solar radiation and atmospheric forcing as potential causes for the identified differences.

3.2 Methodology: Observational datasets and model simulations

3.2.1 Near-natural catchment streamflow dataset

The dataset of European near-natural streamflow records from small catchments is available from the combined dataset of the European Water Archive of the UNESCO IHP FRIEND programme (<http://www.unesco.org/new/en/natural-sciences/environment/water/ihp/ihp-programmes>) and the WATCH project, and is currently hosted at GRDC. It is a homogeneous, quality-controlled dataset of daily discharge from over 400 small catchments with no substantial anthropogenic impact (Stahl *et al.*, 2010). Catchment areas are generally smaller than 1000 km² (on average 413 km²) and cover the period 1960-2004. The dataset also includes information on the measurement coordinates, mean catchment elevation, and drainage basin area. Time-series of mean annual discharge from sub-catchments within each of the 10 considered larger continental basins are area-weighted according to catchment area into a basin-integrated time-series (hereafter referred to as "integrated catchments"). Analyses reported here are performed at the basin-integrated level (Fig. 1). Catchments with more than 10% of missing data are excluded from the basin-integration analysis.

3.2.2 GRDC global river discharge dataset

GRDC is a global database of daily and monthly time-series of river discharge, with data access and use condition information available from Grabs (1997). It also contains information on gauging station

elevation, coordinates, and associated river basin area. Monthly streamflow data from the downmost gauging station for 10 selected European basins (Danube, Douro, Ebro, Elbe, Garonne, Loire, Rhine, Rhone, Seine, and Weser) for the period 1960-2004, whenever available in continuous time-series, are averaged to annual values for all analyses (Table 1 and Fig. 1). The longest available gauge data from a further upstream station are used for the Douro basin, so the considered study area portion for this basin excludes regions located further downstream from any analyses for all datasets. A similar approach is used for the Danube basin, with the GRDC data coming from the Bratislava gauge station in order for it to be better comparable to the near-natural catchment data located upstream from this station, approximately two thousand kilometres from the river mouth which is subject to a different climate regime. The GRDC data have been used in several applications, such as for the derivation of estimates of changes in terrestrial water storage (e.g. Mueller *et al.*, 2011a), and the evaluation of long-term trends in annual evapotranspiration (e.g. Teuling *et al.*, 2009).

3.2.3 E-OBS precipitation gridded dataset

The E-OBS gridded precipitation data was derived through interpolation of the ECA&D station dataset featuring a European network of 2316 stations (Haylock *et al.*, 2008), and has been widely used in modeling and observation comparison studies. For high-resolution regional data in regions with a high density of stations, E-OBS shows excellent correlation despite a slight negative bias and some known errors in mountainous areas and outside winter months, mostly due to interpolation error (Hofstra *et al.*, 2009).

3.2.4 Community Land Model simulations

The Community Land Model is a numerical model that represents land-surface processes within the context of global climate simulations (Oleson *et al.*, 2004, 2008; Stöckli *et al.*, 2008). Biophysical processes simulated by CLM include: solar radiation interactions with vegetation and soil; energy and mass fluxes through the plant canopy; photosynthesis; soil and snow hydrology including surface runoff, infiltration, groundwater discharge; and a river routing scheme. Spatial heterogeneity is represented by a sub-grid hierarchy of various land units and multiple plant functional types, and vertical profiles of water and energy are calculated for 10 soil layers and up to five snow layers. The currently used version (3.5) as well as previous versions of CLM have been thoroughly tested and compared with observational

datasets such as Fluxnet and GRDC with respect to their simulation of land hydrology and other fluxes of energy and nutrients, and were found to perform well for a wide variety of land biomes (Oleson *et al.*, 2008; Stöckli *et al.*, 2008; Dai *et al.*, 2009). CLM has also been shown to perform well when coupled to a regional climate model over Europe (Davin *et al.*, 2011; Davin and Seneviratne, 2012).

In this study CLM simulations are performed with the version 3.5 in offline mode, at resolutions of either $0.5^\circ \times 0.5^\circ$ (WFD) or approximately $1.9^\circ \times 2.5^\circ$ (q06), depending on the resolution of the forcing data. The atmospheric CO_2 concentration of 280 ppm and all land-surface ancillary data and characteristics are kept constant throughout the experiment. As driver for the CLM simulations, we use the WFD and q06 forcing datasets, and the two-dimensional runoff output from each of these two simulations (hereafter referred to as "CLMwatch" and "CLMq06", respectively) is analysed after being routed along the river network using a river transport model. To minimize model initialization drift, CLM simulations start from a pre-spun equilibrium state.

The q06 dataset is composed of 6-hourly fields of meteorological data at a resolution of approximately $1.9^\circ \times 2.5^\circ$ combining NCEP-derived reanalysis and observational data for the 57-year period of 1948–2004. It has been used in various studies and compared to observational land hydrology datasets, and has been suggested to be of satisfactory quality regarding water cycle components, especially outside the tropics (Qian *et al.*, 2006; Oleson *et al.*, 2008; Dai *et al.*, 2009).

The WFD, which consists of 3-hourly atmospheric forcing fields, is derived from ERA-40 reanalysis via interpolation to half-degree resolution and elevation correction based on CRU and GPCC observations for the 44-year period 1958-2001 (Weedon *et al.*, 2010). Its shortwave downward radiation field is adjusted to CRU data with respect to cloud cover, and also corrected for the direct and indirect aerosol effects using the HadGEM2-A global climate model. It includes a bias correction of temperature and precipitation, but not of other fields including radiation, humidity and wind (Weedon *et al.*, 2010) which may still lead to substantial errors in simulated ET and runoff fluxes (Haddeland *et al.*, 2012). However, this dataset is already extensively used within the hydrologic modeling community and has shown good performance with respect to runoff from large basins (Weedon *et al.*, 2010; Haddeland *et al.*, 2011), as well as for percentiles from the flow duration curve (Gudmundsson *et al.*, in press). In addition, Stahl *et al.* (2012) have recently compared the WFD-driven model output at 0.5° resolution to runoff at the catchment scale, and overall found good qualitative agreement for long-term annual tendencies but without evaluation of their statistical significance.

3.2.5 WATCH ensemble simulations

The WaterMIP model intercomparison within the WATCH project features 11 latest generation land-surface and global hydrologic models that, despite the different range in model time steps, forcing variables, energy balance approaches, runoff, snow and ET schemes used among them, have each been shown to perform adequately in the representation of land hydrology for the period 1985-1999 (Haddeland *et al.*, 2011). That study shows that models are consistent with respect to some of the relevant components of the water cycle, although notable differences in runoff exist, especially in drier regions of the world. Here, 6 out of these 11 models (hereafter referred to as "the WaterMIP6 models", namely: HTESSEL, JULES, LPJml, MPI-HM, ORCHIDEE, and VIC) are selected, and their ensemble mean calculated for comparison to other simulated and observed data. This model subset is the same as the one used for the creation of the total runoff ensemble field in the WATCH 20th Century Ensemble product (Weedon, 2011). Each model uses its own elevation, soil, and vegetation maps, and their basic descriptions and detailed inter-comparisons are provided in Haddeland *et al.* (2011). The 15-year simulation period for analysis is preceded by a spin-up over a period of 5 years, to ensure negligible initialization drift. The WaterMIP6 simulations use a common interpolator to adapt the temporal resolution of the WFD to the needs of each individual model, and two-dimensional runoff output is further routed to the river mouth for analysis, using a common routing network. Runoff output from these models is aggregated into a multi-model mean for comparison with observations and CLM simulations.

3.2.6 Data handling and intercomparison of datasets

The analyses are performed on the annual time scale, as water withdrawals and regulation have been reported to mostly affect seasonal values in the discharge of large river basins (Döll *et al.*, 2009). Only GRDC basins containing a minimum of three sub-catchments with no missing values are used to derive the integrated near-natural catchment dataset. Model analyses for the Danube river basin are limited to the portion west of 18° E (Fig. 1), due to the lack of near-natural catchment data in the eastern half of this basin. Time-series of streamflow from the integrated catchments, GRDC, and CLMwatch, as well as WFD time-series for precipitation and shortwave downward radiation and E-OBS precipitation observations are separately analysed for two sub-periods according to the radiation period, i.e. 1960-1985 ("radiation dimming") and 1986-2004 ("radiation brightening"), to investigate the potential effects

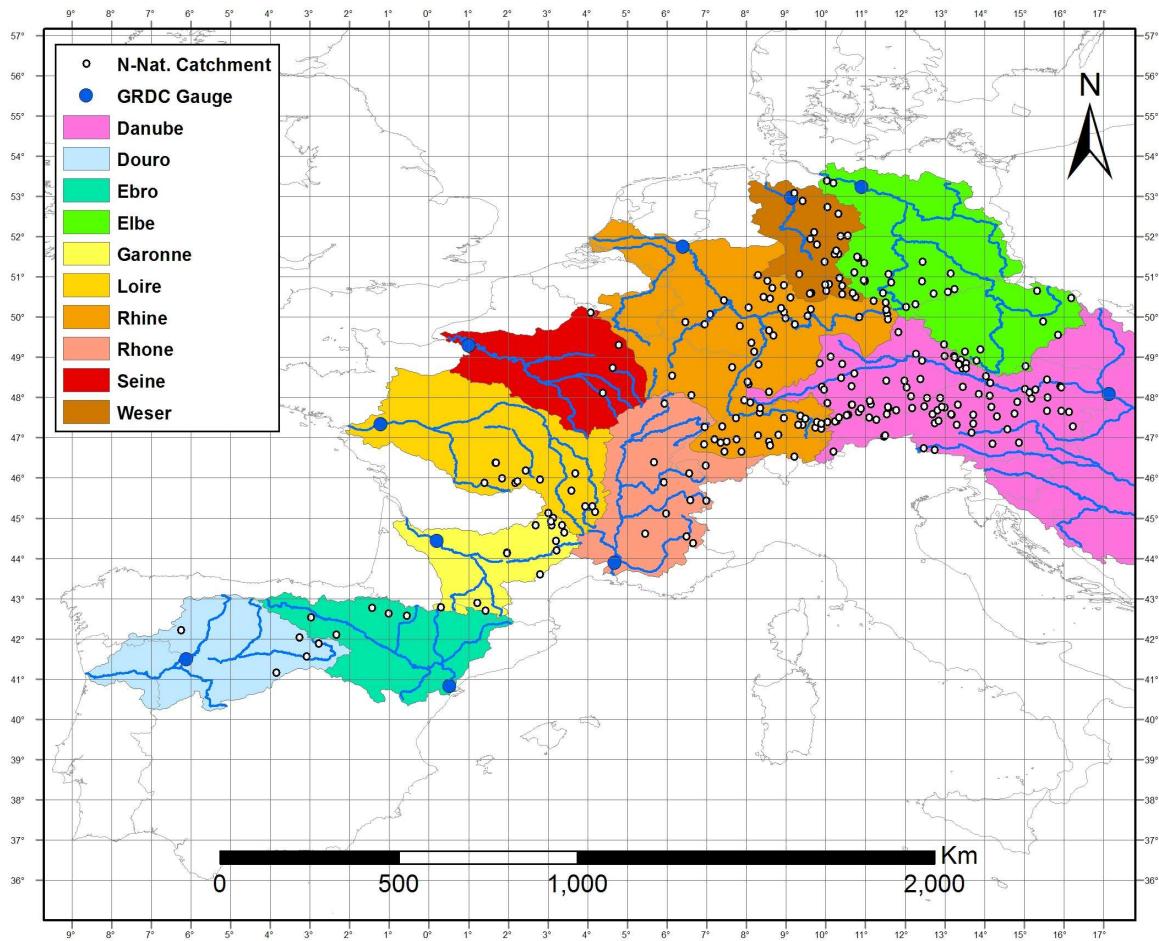


Fig. 1: Map of Europe with the study area and location of the large-scale river basins, main river channels, near-natural catchment stations (small white dots) and GRDC gauge stations (large blue dots).

of changes in shortwave downward radiation on runoff (see Introduction). Note that these periods are chosen as being approximately indicative of the respective dimming and brightening periods, although the definition of the two time frames is not exact (Wild 2009). The length of the available data series varies according to dataset and basin (see Table 1).

3.2.7 Analysis of decadal changes and trends

Results from runoff trend analyses for each basin including both observed and simulated datasets are calculated, with annual trends given in mm/yr and in percentage of total period mean, and the latter

CHAPTER 3: SIMULATED AND OBSERVED EUROPEAN RUNOFF

Table 1. Length of available time series of observed and forcing/simulated data used in this study, by river basin.

Dataset*	DANUBE	ELBE	RHINE	WESER	DOURO	EBRO	GARONNE	LOIRE	RHONE	SEINE
<i>OBSnecat (Q)</i>	1960-2004	1960-2004	1960-2004	1960-2004	1960-2004	1960-2004	1960-2004	1960-2004	1960-2004	1960-2004
<i>OBSgrdc (Q)</i>	1960-2004	1960-2004	1960-2004	1960-2001	1960-1991	1960-1999	1960-1999	1960-1999	1960-1999	1971-2004
<i>OBSseobs (P)</i>	1960-2004	1960-2004	1960-2004	1960-2004	1960-2004	1960-2004	1960-2004	1960-2004	1960-2004	1960-2004
<i>CLMqian06</i>	1960-2004	1960-2004	1960-2004	1960-2004	1960-2004	1960-2004	1960-2004	1960-2004	1960-2004	1960-2004
<i>CLMwatch</i>	1960-2001	1960-2001	1960-2001	1960-2001	1960-2001	1960-2001	1960-2001	1960-2001	1960-2001	1960-2001
<i>WMIPwatch</i>	1985-1999	1985-1999	1985-1999	1985-1999	1985-1999	1985-1999	1985-1999	1985-1999	1985-1999	1985-1999

* Datasets: *OBSnecat (Q)* - integrated near-natural catchments streamflow; *OBSgrdc (Q)* - GRDC discharge; *OBSseobs (P)* - E-OBS precipitation; *CLMq06 - q06*-driven CLMrunoff; *CLMwatch* - WFD-driven CLMrunoff; and *WMIPwatch* – considered WFD-driven WaterMIP models' mean runoff (see Table 2).

value is additionally displayed as decadal trend. Further, correlation analyses are performed for each basin, for selected pairs of datasets, upon subtraction in both datasets of the few non-mutually-existing pairs of values possibly existing at the beginning and end of each time-series (Table 1).

Trend assessment in hydrological records has been a challenging task for some time, as no uniform practice has been established. Known issues include non-normality of the data, auto-correlation in the time series and further external influences (Chen and Grasby, 2009). Robust estimation methods for trend magnitude and existence of trends are therefore employed in this study. Here we estimate the trend magnitude by the slope estimate of a classic linear regression analysis. While in most cases within our datasets of annual data auto-correlation is small and negligible, the non-normality of the runoff data and the regression residuals prevent a strict evaluation of the trend estimate in terms of uncertainty from the regression framework alone. For each integrated catchment and in the two analysed time periods we therefore assess the significance of the trend estimate being different from zero by comparing it to the quantiles of the empirical distribution of trend estimates from a 10000 member bootstrap ensemble. This ensemble is generated through randomly drawing with replacement from the original runoff values of a given integrated catchment and period. Since on average these reshuffled series are trend-free, the bootstrap ensemble represents the null hypothesis of no-trend. If, e.g., the original trend estimate lies outside of the central 95% of this bootstrap distribution, then the null of no trend can be rejected at the 5% level. The standard error of the slope is used in the display of the trends as a visual measure of uncertainty. However, given the non-normality of the data from which it is derived, any significance interpretation of the trend estimate based on the standard error is potentially misleading.

For the trend analyses, the basin data are further aggregated into regions of similar climatic regime for

ease of interpretation of the results. Thus, basin data are area-averaged into the following regions: east-central (E-C) Europe for the Danube, Elbe, Rhine, and Weser basins; southwest (SW) Europe for the Ebro and Douro basins; and western (W) Europe for the Garonne, Loire, Seine, and Rhone basins. The results are presented in three additional barplots added to the right of the individual basin data.

Despite the differences between “streamflow”, or the flow of water in streams and rivers, “discharge”, a measure of flow at a gauging station, and grid-cell level “runoff”, for this study integrating the flow of surface water at different spatial and temporal scales all river discharge is converted into runoff per unit area for ease of comparison, upon performing the unit and domain conversions deemed appropriate.

3.3 Results and discussion

3.3.1 Runoff variability and cross-correlations of analysed datasets

3.3.1.1 Overall comparison

As illustrated in Figures 2 and 3 (see also Table 2), there is good overall agreement among the time-series of observed and simulated streamflow datasets for all basins. Fig. 2 particularly illustrates a reasonably good match in inter-annual variability and occurrence of wet and dry years. Such extreme years generally occur in different years for different basins and usually stay within two standard deviations from the mean. These differences are probably a result of the markedly different climate regimes along the latitudinal gradient, to which the various basins are subjected. The correlation between standardized time-series shows that the highest values (typically $R \sim 0.9$) are found within the pair of observational datasets, as well as the pair of CLM simulations, for almost all basins (Table 2). However, in the Douro the WFD-driven simulated streamflow is better correlated with the GRDC observations than with the integrated catchments. Despite the shorter time-series (15 years), the WaterMIP6 model mean is generally well correlated with other datasets except in SW European basins. All correlations between dataset pairs are significant to the 0.5 % level (not shown).

3.3.1.2 Integrated catchments vs. GRDC

One objective of this study is to assess the extent to which regional signals extracted from near-natural catchment datasets over large spatial domains can be related to large-scale signals associated with

CHAPTER 3: SIMULATED AND OBSERVED EUROPEAN RUNOFF

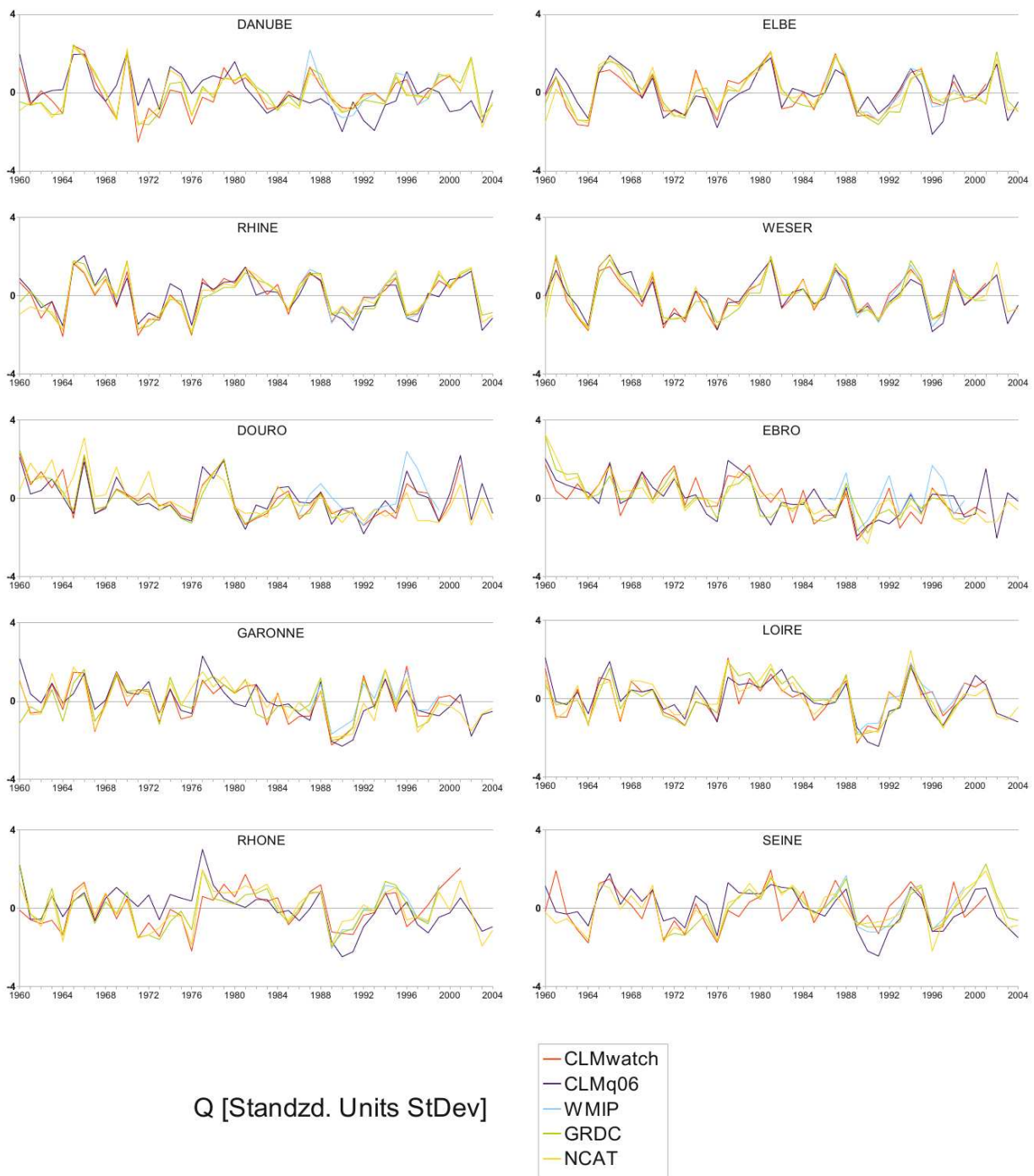


Fig. 2: Comparison of standardized anomalies (in units of standard deviation) of 1960-2004 time-series of river runoff from: CLM-modeled output (red line from WATCH-driven forcing, purple line from q06-driven forcing); WaterMIP6 model ensemble mean ("WMIP", light blue), mean GRDC downmost basin gauge observations (green); and integrated near-natural catchment observations ("NCAT", yellow).

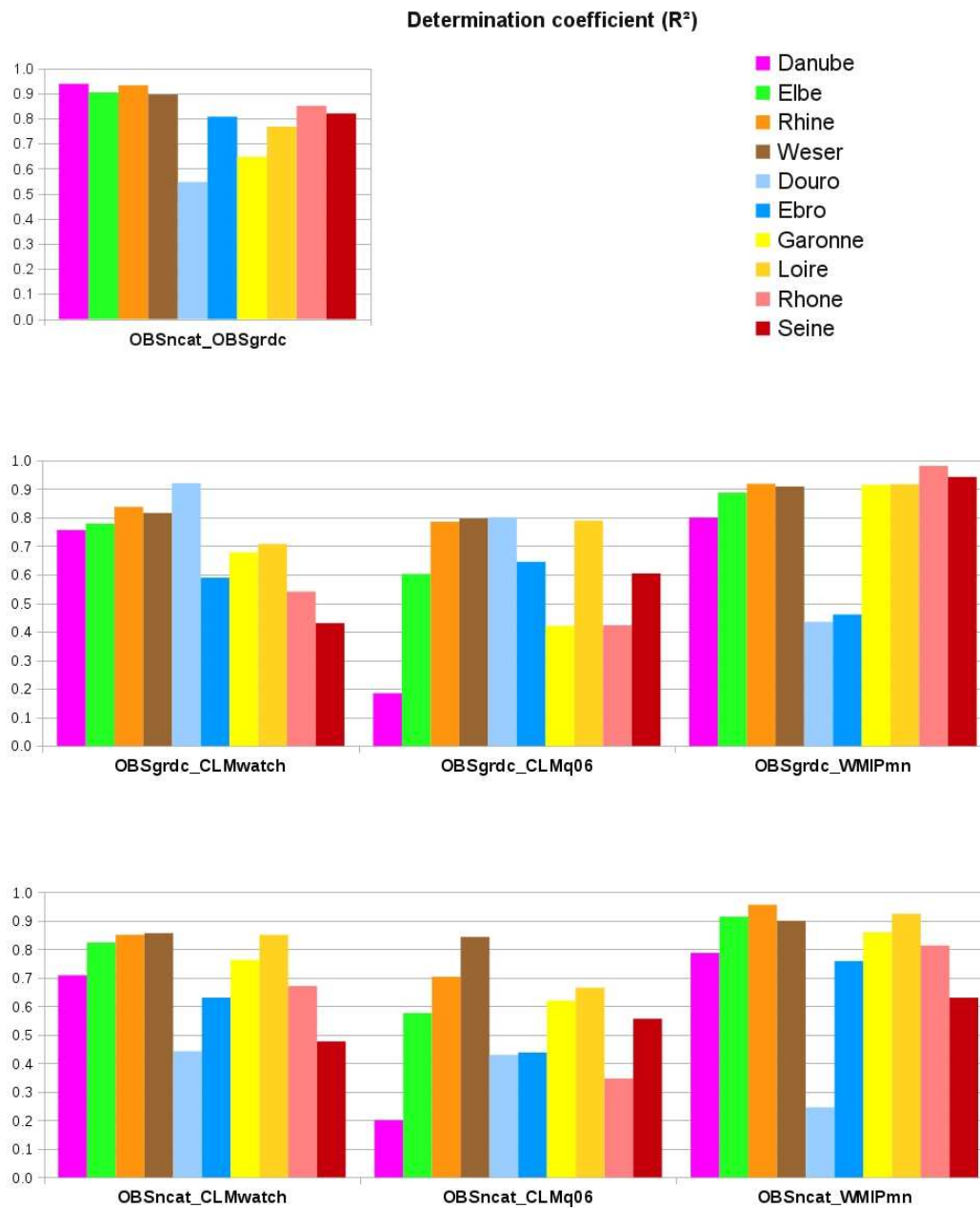


Fig. 3: Correlation (determination coefficient, or R^2) between entire coinciding contiguous length of the following data pairs: the integrated near-natural catchment ("OBSncat") and GRDC ("OBSgrdc") observation datasets (top); the GRDC observations and the CLMwatch, CLMq06 and WaterMIP6 ensemble mean ("WMIPmn") simulated runoff data (middle); and between the integrated catchments and the simulated runoff from CLMwatch, CLMq06 and WaterMIP6 (bottom).

regional climate regimes or climate change. Indeed, the R^2 value between the integrated catchment and the GRDC observational datasets is generally very high, showing that they are consistent despite their scale discrepancy, the limited number of near-natural catchments in some basins, and the fact that the GRDC does not exclude the effects from human water use and land use changes (Fig. 3, top panel).

3.3.1.3 GRDC vs. model simulations

Overall, the GRDC observations agree well with the three simulated runoff datasets (Fig. 3, middle panel). Results show that the WaterMIP6 ensemble model mean almost always correlates better with the GRDC dataset than the CLMwatch simulation, which confirms the often obtained result that an ensemble mean is generally better than any single model (e.g. Guo *et al.*, 2007; Gudmundsson *et al.*, in press). These results are generally consistent across Europe except in the southwest basins of the Douro and Ebro. The shorter duration of the available GRDC data series in the Douro basin may be responsible for some of the differences observed. The poorest overall performance of the CLMq06 simulation is not surprising, as this difference is likely due in part to the spatial resolution of the q06-driven simulation being 19 times coarser than that of the WFD-driven simulations. It is also a consequence of the known better quality of some of the atmospheric forcing fields for Europe in the WFD dataset (Haddeland *et al.*, 2011).

Table 2. Summary of correlations (R)* between pairs of standardized time-series of simulated and observed runoff datasets for 1960-2004 period**, by river basin.

Dataset*** pair	DANUBE	ELBE	RHINE	WESER	DOURO	EBRO	GARONNE	LOIRE	RHONE	SEINE
<i>OBSncat_OBSgrdc</i>	0.97	0.95	0.97	0.95	0.74	0.90	0.80	0.88	0.92	0.91
<i>OBSncat_CLMwatch</i>	0.84	0.91	0.92	0.93	0.67	0.79	0.87	0.92	0.82	0.69
<i>OBSncat_CLMq06</i>	0.45	0.76	0.84	0.92	0.66	0.66	0.79	0.82	0.59	0.75
<i>OBSncat_WMIPwatch</i>	0.89	0.96	0.98	0.95	0.50	0.87	0.93	0.96	0.90	0.79
<i>OBSgrdc_CLMwatch</i>	0.87	0.88	0.92	0.90	0.96	0.77	0.82	0.84	0.74	0.66
<i>OBSgrdc_CLMq06</i>	0.43	0.78	0.89	0.89	0.89	0.80	0.65	0.89	0.65	0.78
<i>OBSgrdc_WMIPwatch</i>	0.89	0.94	0.96	0.95	0.66	0.68	0.96	0.96	0.99	0.97
<i>CLMwatch_CLMq06</i>	0.92	0.95	0.94	0.93	0.95	0.88	0.77	0.87	0.78	0.87
<i>CLMwatch_WMIPwatch</i>	0.43	0.70	0.95	0.96	0.94	0.75	0.95	0.93	0.94	0.95

* All correlations are significant to the 0.5% level (not shown).

** Data series length varies according to dataset and basin (see Table 1).

*** Datasets: OBSncat - integrated near-natural catchments streamflow; OBSgrdc - GRDC discharge; CLMwatch - WFD-driven CLM runoff; CLMq06 - q06-driven CLM runoff; and WMIPwatch - WFD-driven WaterMIP models' mean runoff.

3.3.1.4 Integrated catchments vs. model simulations

The model simulated runoff mostly correlates equally well with the integrated catchment observations as it does with GRDC, again with the exception of the two SW European basins. This regional peculiarity is further illustrated in Fig. 4, where we see that only 30-40% of the runoff variability can be explained by precipitation, unlike in the rest of Europe where this value usually approaches 70%.

Note that in the following analyses featuring the CLM model, we focus only on the CLMwatch simulation, given the poorer performance of CLMq06 identified in this section.

3.3.2 Decadal variability and trends in observed and simulated runoff

Here we present the analysis of runoff trends for three time periods, 1960-1985, 1986-2004/2001, and 1960-2004/2001, with trends significant at the 5% level indicated in bold face, while non-significant trends at this level are italicized (see Table 1 for time-series lengths, and Table 3 for trends). For the

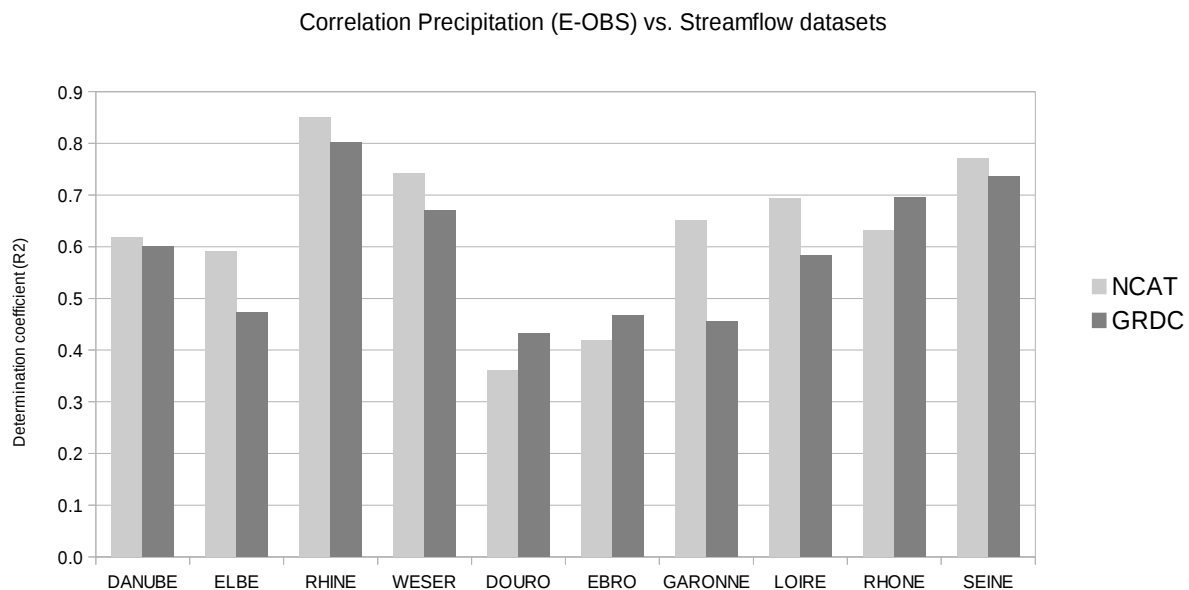


Fig. 4: Correlation (determination coefficient, or R^2) between E-OBS precipitation and observed streamflow from the integrated near-natural catchment ("NCAT") and GRDC datasets, for the selected European basins in the period 1986-2004. All correlations are significant to the 1% level. GRDC data year availability varies with the basin and does not always span the entire period (See Table 1).

CHAPTER 3: SIMULATED AND OBSERVED EUROPEAN RUNOFF

Table 3. Comparison of trends* in runoff for simulated and observed runoff datasets for periods** 1960-1985, 1986-2004, and 1960-2004, by river basin.

Dataset*** 1960-1985		DANUBE	ELBE	RHINE	WESER	DOURO	EBRO	GARONNE	LOIRE	RHONE	SEINE
CLMwatch	Annual [mm/yr]	-0.76	0.88	2.98	-0.79	-10.60	-2.17	-3.58	0.65	5.76	-2.66
	Annual [% mean]	-0.30	0.35	0.31	-0.12	-2.69	-0.79	-0.28	0.18	0.93	-0.12
OBSgrdc	Annual [mm/yr]	0.55	0.18	0.93	-1.19	-3.86	-4.73	0.92	2.91	0.34	14.21
	Annual [% mean]	0.11	0.11	0.20	-0.43	-2.79	-3.04	0.24	1.12	0.06	5.57
OBSncat	Annual [mm/yr]	0.56	1.77	4.10	0.66	-8.40	-12.80	0.20	2.44	4.01	4.89
	Annual [% mean]	0.07	0.60	0.72	0.18	-2.52	-2.72	0.04	0.55	0.44	1.41
Dataset*** 1986-2004		DANUBE	ELBE	RHINE	WESER	DOURO	EBRO	GARONNE	LOIRE	RHONE	SEINE
CLMwatch	Annual [mm/yr]	0.84	-1.22	3.17	-0.16	15.13	1.68	20.54	6.21	16.30	-0.54
	Annual [% mean]	0.33	-0.49	0.33	-0.02	3.83	0.61	1.63	1.70	2.64	-0.02
OBSgrdc	Annual [mm/yr]	1.39	-0.26	0.26	-2.11	NaN	0.69	2.32	1.30	4.78	2.24
	Annual [% mean]	0.28	-0.15	0.05	-0.77	NaN	0.44	0.62	0.50	0.84	0.88
OBSncat	Annual [mm/yr]	1.11	-1.75	-1.36	-1.89	-1.11	-0.35	-0.09	-0.09	-4.94	1.75
	Annual [% mean]	0.15	-0.59	-0.24	-0.53	-0.33	-0.08	-0.02	-0.02	-0.55	0.50
Dataset*** 1960-2004		DANUBE	ELBE	RHINE	WESER	DOURO	EBRO	GARONNE	LOIRE	RHONE	SEINE
CLMwatch	Annual [mm/yr]	-0.15	0.08	3.05	-0.55	-0.80	-0.70	5.61	2.77	9.78	-1.85
	Annual [% mean]	-0.06	0.03	0.31	-0.09	-0.20	-0.26	0.45	0.76	1.58	-0.09
OBSgrdc	Annual [mm/yr]	0.90	0.00	0.64	-1.54	-3.21	-2.84	1.41	2.35	1.89	7.52
	Annual [% mean]	0.18	0.00	0.14	-0.56	-2.33	-1.82	0.37	0.90	0.33	2.95
OBSncat	Annual [mm/yr]	0.79	0.28	1.79	-0.42	-5.32	-7.55	0.08	1.37	0.23	3.57
	Annual [% mean]	0.11	0.10	0.31	-0.12	-1.60	-1.61	0.01	0.31	0.03	1.03

* Values in bold type indicate trends significant to the 5% level, and values in italics indicate non-significant trends (see Section 2.6 for discussion of statistical significance of trends). Trends for datasets for which less than 14 years of data is available are indicated by "NaN".

** Or longest portions thereof - see Table 1 for time series lengths.

*** Datasets: CLMwatch - WFD-driven CLM runoff; OBSgrdc - GRDC discharge; and OBSncat - integrated near-natural catchments streamflow.

overall time period and for the two observational datasets, the analysis reveals that nearly all basins show non-significant trends, with the exception of the large negative GRDC trend in the Douro basin. However, a tendency for positive trends in the W and E-C European basins (except the Weser in the GRDC data) and negative trends in the SW basins are found. The lack of significance of the trends is partly due to the large inter-annual variability of the data (Fig. 2), as also highlighted in Gerten *et al.* (2008). Pronounced negative trends, some of them statistically significant, dominate in simulated and observed runoff from SW European basins for the 1960-1985 time period, while modest, non-significant negative and mostly positive trends are found elsewhere in both time periods (Table 3, and Fig. 5). This is consistent with the main findings of a recent study analysing individual station trend behaviour of the same catchments (but without analyses of significance; Stahl *et al.*, 2010), and other regional and global runoff studies with similar scope (e.g. Milliman *et al.*, 2008; Dai *et al.*, 2009; Lorenzo-Lacruz *et al.*, 2011). These contrasting trends between the SW and other European basins can be partly related to the

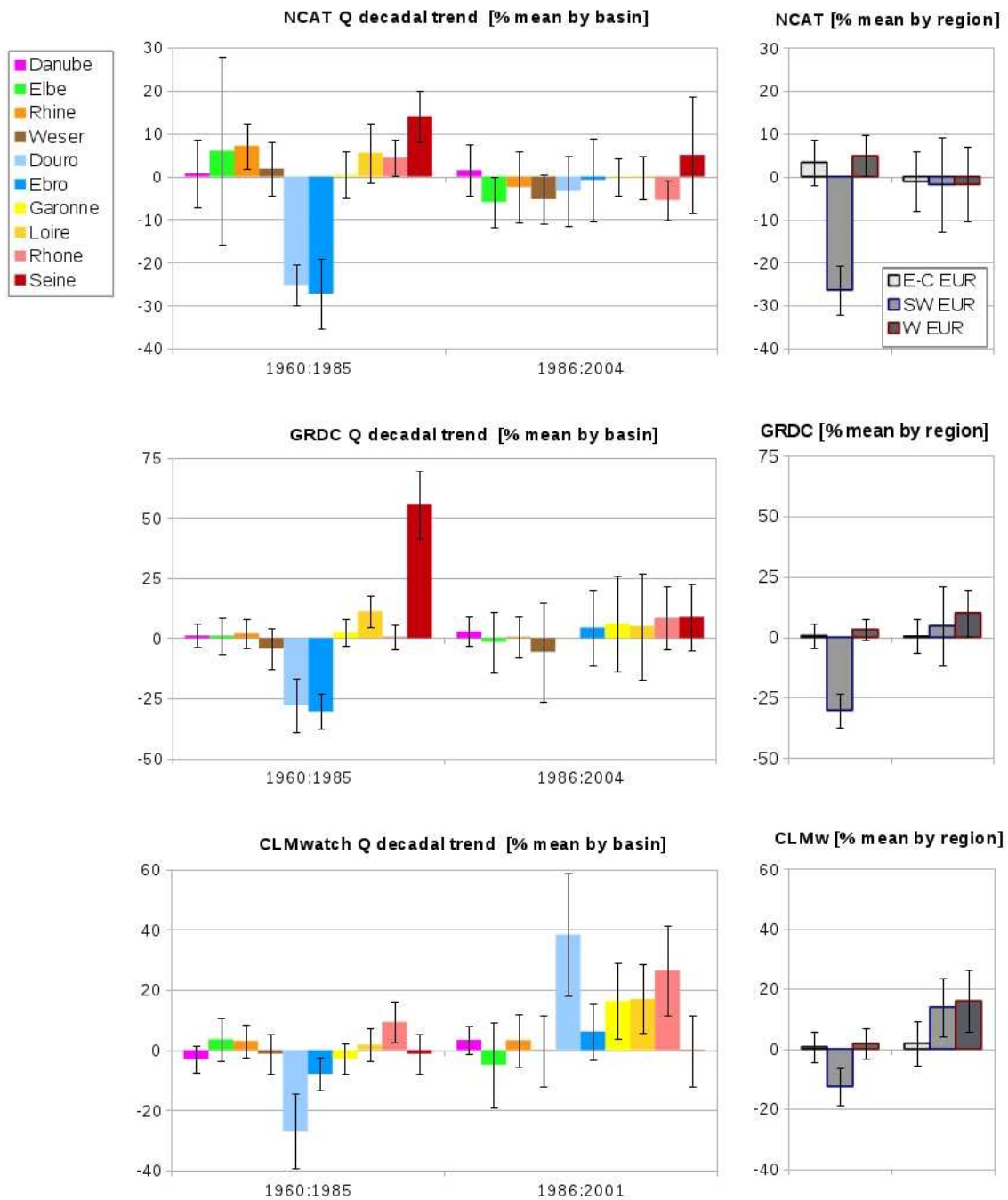


Fig. 5: Decadal trends (as % of mean) in integrated near-natural catchment streamflow, GRDC basin discharge, and CLM-WATCH model simulated runoff in periods 1960-1985 and 1986-2004/2001 for area-integrated basins (left) and regional averages (right). Error bars indicate standard error of the slope (see Section 2.6 for the interpretation of trend uncertainty). Length of available time series varies with dataset and basin (See Table 1). Only data series with at least 14 years of consecutive data are represented.

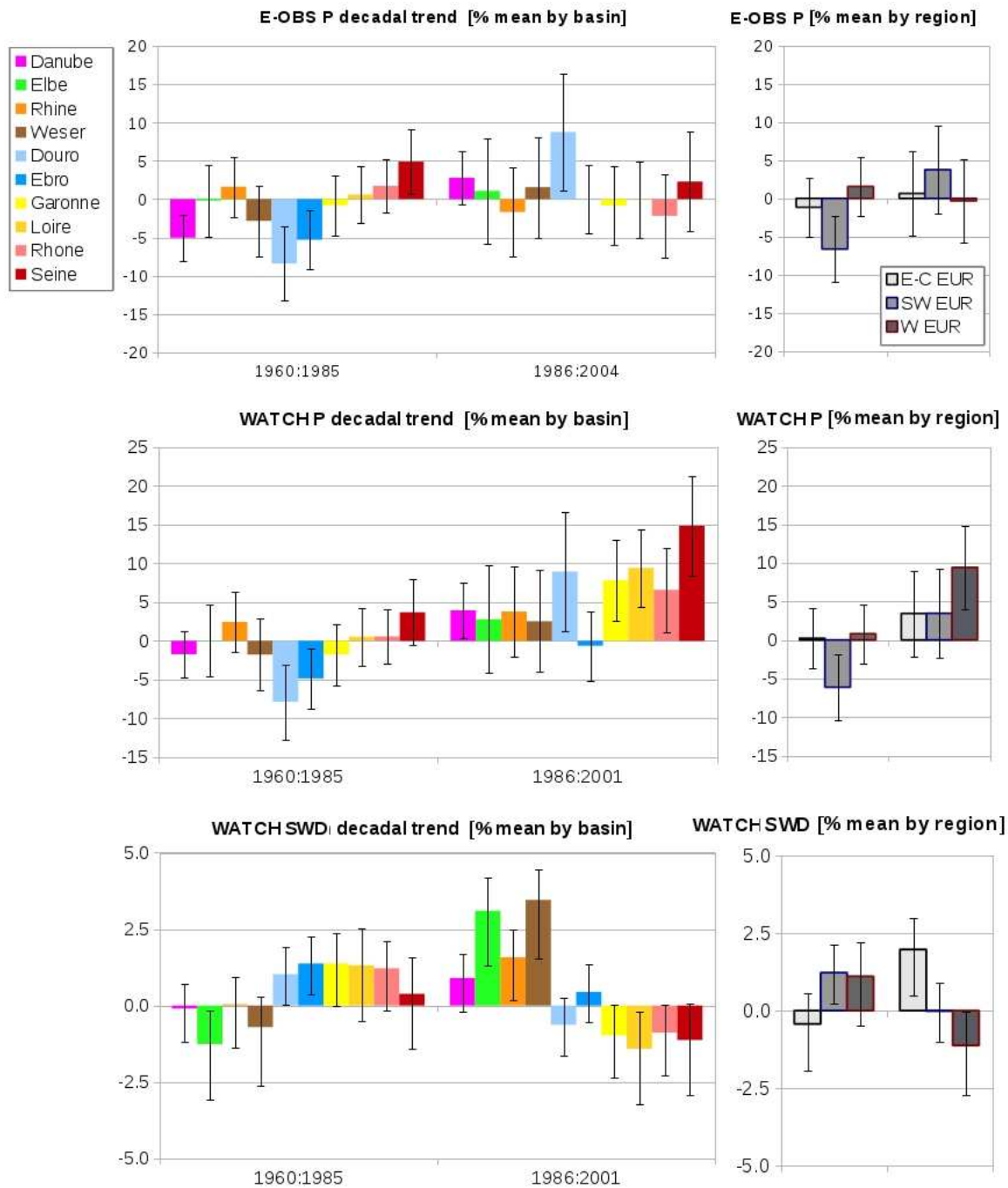


Fig. 6: Decadal trends (as % of mean) of precipitation from E-OBS (top) and WFD (middle), and of WATCH Forcing Data shortwave downward radiation (bottom) in periods 1960-1985 and 1986-2004/2001, for selected European basins (left) and regional averages (right). Error bars indicate standard error of the slope (see Section 2.6).

respective trends in precipitation forcing (Fig. 6), although other causes such as increases in water consumption or in ET from land cover changes may also play a role (López-Moreno *et al.*, 2011; Lorenzo-Lacruz *et al.*, 2011). Reductions in precipitation and runoff in SW Europe have also been suggested to be linked with changes in North Atlantic Oscillation patterns (Trigo *et al.*, 2004).

Regarding the differences in trends between the two periods (dimming and brightening phases in 1960-1985 and 1986-2004, respectively), the two SW European basins exhibit a streamflow increase in excess of 20% of the mean per decade, going from a very negative earlier period to a substantially reduced or almost no-trend later on. Conversely, many of the other European basins, the Seine most notably amongst them, exhibit the opposite tendency for the corresponding periods, with a generally positive earlier-period trend changing to a much reduced or even negative signal over time (although it should be noted that most of these trends are non-significant in both periods, see Table 3). This is consistent with a possible impact of shortwave radiation trends (dimming and brightening) on runoff in these basins, which is also expected since ET is mostly radiation-limited in Europe with the exception of the Mediterranean region (Teuling *et al.*, 2009, Seneviratne *et al.*, 2010). The critical role of the climate and ET regime is highlighted by the fact that the differences between the two periods are overall opposite in the SW vs. other European basins. The somewhat more extreme behaviour found in the Seine is possibly a consequence of the small number of stations (4) and of their location at a very low average elevation of 255 m compared to most other basins, although the fact that the GRDC dataset also displays a marked extreme behaviour in this basin (see Table 3) may be indicative of an actual signal. This may be explained by the stronger trends in observed precipitation for this basin when compared with its regional neighbours (Fig. 6, top).

To evaluate the realism of the WFD and the WFD-driven simulations, and the extent to which observed and simulated runoff is sensitive to atmospheric forcing, we assess the consistency of the identified runoff trends in the integrated catchment dataset with those from the GRDC dataset and the CLM simulation (Fig. 5). The identified streamflow trend patterns over both periods are overall consistent between datasets for most basins and basin-aggregated regions, although the model simulations exhibit a (non-significant) tendency for positive trends in the Rhone, Garonne and Loire river basins after 1986, which is not identified in the observational datasets (Fig. 5 and Table 3). Furthermore, the CLMwatch simulation displays a large positive trend in the Douro after 1986, which is not seen in the observational datasets, and it does not capture the marked positive trends in the Seine river basins over the time period

1961-1985. On the other hand, the CLMwatch simulation agrees with the observations regarding the presence of a strong negative trend in the SW European basins, as well as qualitatively regarding the attenuation (or in the case of the model a the reversal) of this trend after 1985.

The overall geographical patterns of the trends, which indicates a strong tendency for runoff decrease in SW Europe, and an overall tendency for a slight increase in Western and East-Central Europe, are also consistent with previous findings regarding global and regional precipitation trends, which note a general precipitation increase in northern mid- to high latitudes, and no trend or slight reduction in southern European regions (Trenberth *et al.*, 2007; Zhang *et al.*, 2007). This is largely supported by the analysis of the E-OBS trends (Fig. 6), which reveal a strong negative precipitation tendency over the Iberian Peninsula during the dimming period.

Regarding the tendency of the model for positive trends in the Rhone, Garonne and Loire river basins after 1986, which are not found in the observational datasets, analysis of the WFD forcing fields (Fig. 6, middle and lower) reveals that the reason may lie in erroneous precipitation and radiation forcing. Indeed in these basins, the WFD display large increases in precipitation after 1985, which are not found in the E-OBS dataset. In addition, in these and other basins, the radiation forcing trends have signals opposite to those expected from observational studies, with a noted brightening during the earlier dimming phase and vice-versa for the later period in regions other than E-C Europe (Wild *et al.*, 2005). Similar issues were identified in the commonly used q06 forcing (Oliveira *et al.*, 2011), which highlight the key importance of accurate forcing datasets for inferring hydrological trends from offline land surface model simulations.

In addition to climate-induced changes, human impacts on trends in streamflow have been shown to be non-negligible, with the drier regions across the globe among the most affected areas mostly as a result of increases in water withdrawals for human consumption in domestic, industrial and agricultural use, most notably irrigation (Döll *et al.*, 2009). In dry regions, including SW Europe, anthropogenic annual flow reduction amounts to an average 35% of the natural value. In SW Europe, in particular, other hydrologic changes due to dam regulation and water management are noted, but these affect mostly seasonal flow patterns (Lorenzo-Lacruz *et al.*, 2011). However, changes to land management and landscape structure have been proposed as the most plausible explanation for a decrease in headwater runoff in the Ebro, as natural vegetation re-growth from land abandonment induces an increase in ET (López-Moreno *et al.*, 2011).

Despite using some of the best available models, forcing and observation data, an apt comparison of catchment streamflow with simulated runoff can still be marred by issues related to the scale and characteristics of the compared areas, which may substantially impact flow and trends. The $0.5^\circ \times 0.5^\circ$ resolution WFD is interpolated from the $1^\circ \times 1^\circ$ ERA-40 reanalysis, and in spite of the elevation correction and adjustments to CRU for some fields, there is an inevitable spatial averaging effect that is expected to potentially misrepresent individual gridcell fluxes at higher elevations. Landscapes with unaltered hydrology tend to exist in the least accessible regions of complex topography, and this is indeed the case with the near-natural catchment dataset used here, where lowland areas are underrepresented (Stahl *et al.*, 2011). However, the overall good agreement between the GRDC and integrated near-natural catchment data suggests that effects of resolution, altitude and human water use may not be as acute as often assumed, at least for the considered river basins.

3.4 Summary and conclusions

This study investigates recent hydrological variability and trends for the annual time series of streamflow covering the time period 1960-2004 in Europe from several datasets: 1) Near-natural small-catchment streamflow observations integrated over large river basins; 2) river-basin streamflow measurements at downmost stations from the GRDC dataset; 3) and simulations with the CLM land surface model driven with state-of the art forcing datasets. In addition, the ensemble mean of a multi-model hydrologic study featuring the most commonly used latest-generation hydrologic and land-surface models is used for the evaluation of the interannual variability of runoff in the investigated river basins.

The CLM simulations reasonably agree with the observations, especially in terms of the interannual runoff variability. Regional discrepancies with respect to the inter-annual variability occur mostly in the two SW European basins, which are subject to a drier climate regime where runoff is poorly correlated with precipitation. However, these basins are also characterized by a poor density of the near-natural catchment data, and the Douro has shorter time series, which could affect the results as well. The poorer performance of the simulation driven with the q06 dataset reinforces the notion that reliable atmospheric forcing datasets are essential to accurately simulate terrestrial hydrology (see also Mueller *et al.*, 2011b). In addition, it is noted that for the most part simulated runoff from the WaterMIP6 ensemble

model mean matches observations better than that from single-model CLM simulations.

Despite the large uncertainty expressed by the overall poor statistical significance level, indications of basin-integrated, near-natural streamflow trend behaviour and trend changes show good agreement with GRDC observations and simulated data for most basins. In W and E-C European basins the positive trend during the earlier radiation dimming period, and the later greatly diminished or even reversed trend during the radiation brightening period, appear consistent with results from previous modeling and observation studies. In SW basins this is not noted, possibly because of competing trends in precipitation. However, it must be re-emphasized that all but a few trends in SW European basins and the Seine during the dimming period are statistically non-significant.

Many of the underlying catchments are located in mountainous regions, which contribute a disproportionately high amount of runoff—from 20-50% in humid areas to as much as 50-90% in arid regions (Viviroli & Weingartner, 2004)—, are subject to fewer losses through evaporation, and have a regulatory effect on basin-wide streamflow through snow dynamics. With rising temperature and precipitation reported for alpine regions in recent decades (Stewart, 2009), and greater snow pack at very high altitudes but decreased snow at lower elevations (Beniston et al., 2002), understanding the dynamics of near-natural catchments may help predict the changes to the hydrologic balance of the more populated downstream regions. However, the overall consistency between the near-natural catchment and whole-basin GRDC data relativizes the possible impacts of scale, altitude or human water use in the investigated river basins.

Further model-observation comparison studies are necessary to advance the understanding of long-term decadal variability and trends of runoff in Europe. This is essential to produce better water resource predictions, despite the limitations imposed by the lack of long-term near-natural catchment observations in many regions and the insufficient information on human interference on large continental basin discharge. Nonetheless, our results also suggest that improved atmospheric forcing datasets and model resolution would be greatly beneficial to produce more reliable hydrological datasets. The reasonable overall agreement in trends and variability between simulated and observational datasets for most basins is an indication that efforts to improve the understanding of physical processes and measurement networks can eventually lead to a better characterization of system behaviour, which bodes well for a long-term improvement of simulations and projections of hydrologic changes.

3.5 Acknowledgements

We thank Sam Levis (NCAR) and Christian Reick (MPI - Hamburg) for helpful discussions and comments. Streamflow data are provided by national hydrometric services through the Global Runoff Data Centre, Koblenz, Germany. The study is also a contribution to UNESCO IHP-VII and the Euro-FRIEND project. The authors thank all data providers: national authorities for the observed streamflow records, the creators

of the WATCH Forcing Data and the hydrological multi-model output. We acknowledge partial financial support from the EU FP7 CARBO-Extreme (FP7-ENV-2008-1-226701), CCES MAIOLICA, and EU FP7 DROUGHT-R&SPI (No. 282769) projects. We also acknowledge the E-OBS dataset from the EU FP6 project ENSEMBLES (<http://ensembles-eu.metoffice.com>), the multi-model dataset from the European Union EC-FP6 funded Integrated Project WATCH (No. 036946, <http://www.eu-watch.org>) and the data providers in the ECA&D project (<http://eca.knmi.nl>).

Chapter 4

Model and forcing uncertainties: CLM vs. WATCH

Model and forcing uncertainties: CLM vs. WATCH

Model and forcing uncertainties affecting the simulation of terrestrial hydrology: An analysis based on CLM3.5 and WATCH model simulated data

Paulo J. C. Oliveira, Edouard L. Davin, and Sonia I. Seneviratne

Institute for Atmospheric and Climate Science, ETH Zurich, 8092 Zurich, Switzerland

Abstract

This chapter analyses the impacts of model resolution, atmospheric forcing, and model choice on the means, inter-annual variability, and trends in total evapotranspiration and surface runoff from land surface model simulations. We perform offline simulations for the period 1985-1999 using the Community Land Model version 3.5 at two different resolutions (but with same forcing resolution) and driven with two different forcing datasets including a recently developed product from the WATCH project. The results are compared to model simulations computed with six selected WATCH land-surface and global hydrologic models. The results reveal that the WATCH Forcing Data-driven CLM simulation generally lies within the WaterMIP multi-model spread and that the choice of forcing dataset can significantly affect the simulations, at least to the same order of magnitude as the model choice. Overall mean patterns in runoff and evapotranspiration are found to generally reflect the distribution of precipitation from the forcing. Moreover, the various WATCH Forcing Data-driven simulations exhibit

similar trend patterns and magnitude, suggesting that the decadal variability of the components of the water cycle is more sensitive to differences in forcing datasets than in parameterization choices. For its part, inter-annual variability is affected both by the forcing and parameterization choices, with the mean of the six WATCH models displaying the highest values for evapotranspiration. It is found that neither of the forcing datasets incorporate observed radiation brightening trends, which may thus be a significant source of error in the simulations. Lastly, the conducted simulations suggest that model resolution plays a comparably smaller role in simulation uncertainty, at least in the absence of corresponding increase in forcing resolution.

4.1 Introduction

Previous model intercomparison studies have shown large variations among Land Surface Models (LSMs) mostly related to uncertainties in soil moisture, land cover and vegetation (PILPS: Henderson-Sellers *et al.*, 1993; GSWP-2: Dirmeyer *et al.*, 2006; LUCID: Pitman *et al.*, 2009). Here, offline simulations with the Community Land Model (hereafter referred to as "CLM") version 3.5 are compared to six model simulations from the WaterMIP project (hereafter referred to as the "WaterMIP6 models"), which are driven by the WATCH Forcing Data ("hereafter referred to as "WFD") 0.5° x 0.5° resolution atmospheric forcing dataset for the period 1985-1999 (Weedon *et al.*, 2010; Haddeland *et al.*, 2011), all part of the WATER and global CHange (WATCH) project (Haddeland *et al.*, 2011). The WFD is also used to drive a simulation with CLM3.5. To assess the role of atmospheric forcing, simulations are additionally performed using the standard NCEP-based forcing for CLM3.5 (Qian *et al.*, 2006, hereafter referred to as "q06"). Simulations with this forcing are done at two different resolutions (half-degree versus T62, but without changes in forcing resolution), thus enabling to quantify the role of model resolution.

In the following, the impacts of the chosen land-surface model, model resolution, and atmospheric forcing on the means, inter-annual variability, and trends in total evapotranspiration (hereafter referred to as "ET") and surface runoff are assessed. A trend analysis is done at the global scale and for 11 regional domains encompassing the most relevant large climate regions. Two main purposes of these analyses are: 1) To assess the performance of CLM3.5 compared to other state-of-the-art land surface and land hydrological models; 2) to evaluate the accuracy of the q06 forcing dataset compared to a more recently developed forcing dataset. This is particularly relevant, since the q06 dataset has been used in a number of land hydrological applications (e.g. Qian *et al.*, 2007, Dai *et al.*, 2009, Oliveira *et al.*, 2011).

4.2 Methodology: Models, forcing datasets and simulations

4.2.1 Land-surface models

4.2.1.1 The Community Land Model

CLM is a land-surface model that simulates biophysical processes such as radiation interactions with vegetation and soil; energy and mass fluxes between plant canopy, soil, and snow; photosynthesis; soil

hydrology featuring surface runoff and infiltration (Oleson *et al.*, 2004, 2008; Stöckli *et al.*, 2008). Land-surface data for soil texture are derived from the FAO/UNESCO dataset, and vegetation cover parameters for the 17 chosen plant functional types are mostly based on MODIS satellite measurements (Lawrence & Chase, 2007). The simulation of hydrologic fluxes by the currently used (3.5) and previous versions has been tested and compared with FLUXNET and GRDC data, showing good performance for a wide range of land cover types (Oleson *et al.*, 2008; Stöckli *et al.*, 2008).

4.2.1.2 The WATCH multi-model ensemble

The model intercomparison within the WATCH project features 11 latest generation land-surface and global hydrologic models that, despite the differences in time steps, forcing variables, energy balance approaches, runoff, snow and ET schemes, have each been shown to perform adequately in the representation of land hydrology (Haddeland *et al.*, 2011). Here, six out of these 11 models are selected, namely: HTESSEL, JULES, LPJml, MPI-HM, ORCHIDEE, and VIC. Their ensemble mean is calculated for comparison to other simulated data. This six-model subset is the same used for the creation of the total runoff ensemble field in the WATCH 20th Century Ensemble product (Weedon, 2011), and present the advantage of being standard schemes coupled to climate models, like CLM (Haddeland *et al.*, 2011). Their basic descriptions and detailed inter-comparisons are provided in Table 1. While generally models are found to behave consistently with respect to some of the relevant components of the water cycle, the study by Haddeland *et al.* (2011), focusing only on the mean state of hydrologic variables for the study period, finds notable differences in runoff, especially in drier regions across the globe, which is possibly caused by differences in the used ET schemes. It is suggested that inter-model discrepancy may be an important source of uncertainty.

4.2.2 Atmospheric forcing datasets

4.2.2.1 The WATCH Forcing Data

The WFD contains data for temperature, wind, humidity, pressure and longwave downward radiation in daily, 6-hourly or 3-hourly time steps, as well as shortwave downward radiation, rain and snow at 3-hourly time steps (Weedon *et al.*, 2010). The WFD fields are provided at a spatial resolution of $0.5^\circ \times 0.5^\circ$ and are based on the ERA-40 reanalysis of the European Centre for Medium Range Weather Forecasting (Uppala *et al.*, 2005). This dataset is widely regarded within the land hydrology modeling community as one of the best available atmospheric forcings (Haddeland *et al.*, 2011).

CHAPTER 4: MODEL AND FORCING UNCERTAINTIES: CLM VS. WATCH

Table 1. Selected models, including their characteristics (adapted from Haddeland et al., 2011)

Model name ¹	Model time step	Meteorological forcing variables ²	Energy balance	Evapotranspiration scheme ³	Runoff scheme ⁴	Snow scheme	Reference(s)
HTESEL	1 h	R, S, T, W, Q, LW, SW, SP	Yes	Penman-Monteith	Infiltration excess / Darcy	Energy balance	Balsamo et al. (2009)
JULES	1 h	R, S, T, W, Q, LW, SW, SP	Yes	Penman-Monteith	Infiltration excess / Darcy	Energy balance	Cox et al. (1999), Essery et al. (2003)
LPJml	Daily	P, T, LWn, SW	No	Priestley-Taylor	Saturation excess	Degree day	Bondeau et al. (2007), Rost et al. (2008)
MPI-HM	Daily	P, T	No	Thornthwaite	Saturation excess / Beta function	Degree day	Hagemann and Gates (2003), Hagemann and Dümenil (1998)
ORCHIDEE	15 min	R, S, T, W, Q, LW, SW, SP	Yes	Bulk formula	Saturation excess	Energy balance	De Rosnay and Polcher (1998)
VIC	Daily / 3 h	P, Tmax, Tmin, W, Q, LW, SW, SP	Snow season	Penman-Monteith	Saturation excess / Beta function	Energy balance	Liang et al. (1994)

¹ Model names written in bold are classified as LSMs in this paper; the other models are classified as GHMs.

² R: Rainfall rate, S: Snowfall rate, P: Precipitation (rain or snow distinguished in the model), T: Mean daily air temperature, Tmax: Maximum daily air temperature, Tmin: Minimum daily air temperature, W: Wind speed, Q: Specific humidity, LW: Longwave radiation flux (downward), LWn: Longwave radiation flux (net), SW: Shortwave radiation flux (downward), SP: Surface pressure.

³ Bulk formula: Bulk transfer coefficients are used when calculating the turbulent heat fluxes.

⁴ Beta function: Runoff is a nonlinear function of soil moisture.

4.2.2.2 The q06 forcing dataset

The q06 atmospheric forcing dataset, with a resolution of 2.5° longitude by approximately 1.9° latitude, is composed of the following 6-hourly fields of meteorological data combining NCEP/NCAR reanalysis and observational datasets: temperature, precipitation, shortwave downward radiation, pressure, humidity, and wind. This dataset has frequently been used in land hydrology applications, and is considered a reliable atmospheric dataset (Qian et al., 2007; Dai et al., 2009).

4.2.3 Experimental set-up

The simulation period for analysis is 1985-1999, and is preceded by a spin-up run over a period of no less than five years, to ensure negligible initialization drift. The WaterMIP6 models use a common interpolator to adapt the temporal resolution of the WFD to the needs of each individual model. ET and runoff output from these models is aggregated into a multi-model mean for the comparison with the CLM simulations. Three CLM simulations are performed according to the following design:

- “CLMwatch”, using the same set-up and half-degree resolution and WATCH forcing as

the WaterMIP6 models;

- “CLMqian2”, performed at approximately $1.9^\circ \times 2.5^\circ$ resolution and using the q06 forcing with the same original spatial resolution; and
- “CLMqian05”, driven with the the q06 $1.9^\circ \times 2.5^\circ$ resolution forcing at half-degree resolution, with adjacent grid cells sharing the same forcing;

This experimental setup allows the investigation of the individual, separate effects of the different chosen model, model resolution, and atmospheric forcing dataset.

4.3 Results and discussion

4.3.1 Mean ET and runoff

4.3.1.1 Global patterns

Annual mean (1985-1999) ET and runoff for CLMwatch, CLMqian05 and the WaterMIP6 mean are displayed in Fig. 1. Overall, the spatial patterns of ET and Q are consistent among the 3 analysed model datasets, and largely reflect the global distribution of precipitation (Fig. 5). Differences between the CLM simulations and the WaterMIP6 multi-model mean are highlighted in Fig. 2. The largest differences are located in the Eastern U.S., Northern Europe and tropical regions. Since the water cycle is more intense in these humid regions (larger overall fluxes), it is to be expected that the differences are similarly larger. Of these regions, the two extra-tropical humid regions (Eastern U.S., Northern Europe) display lower ET and higher runoff values in CLM 3.5 compared to the WaterMIP6 simulations, while the tropics show the opposite pattern. The differences of the two CLM simulations to the WaterMIP6 simulations are of same sign, and these features are thus not affected by the choice of forcing dataset. But the magnitude of the differences is substantially larger for the CLMqian05 than the CLMwatch simulation. This is also understandable, since CLMwatch shares the same forcing as the WaterMIP6 ensemble and it is thus expected that differences between them would be smaller. It may be noted that the magnitude of these differences is generally larger than 10% of the mean for both ET and runoff for these regions, even for CLMwatch vs WaterMIP6.

4.3.1.2 Regional analysis

We focus here on regional analyses based on the Köppen-Geiger climate zones (Fig. 3). These analyses also include the CLMqian2 simulations in addition to the WaterMIP6 multi-model mean and the

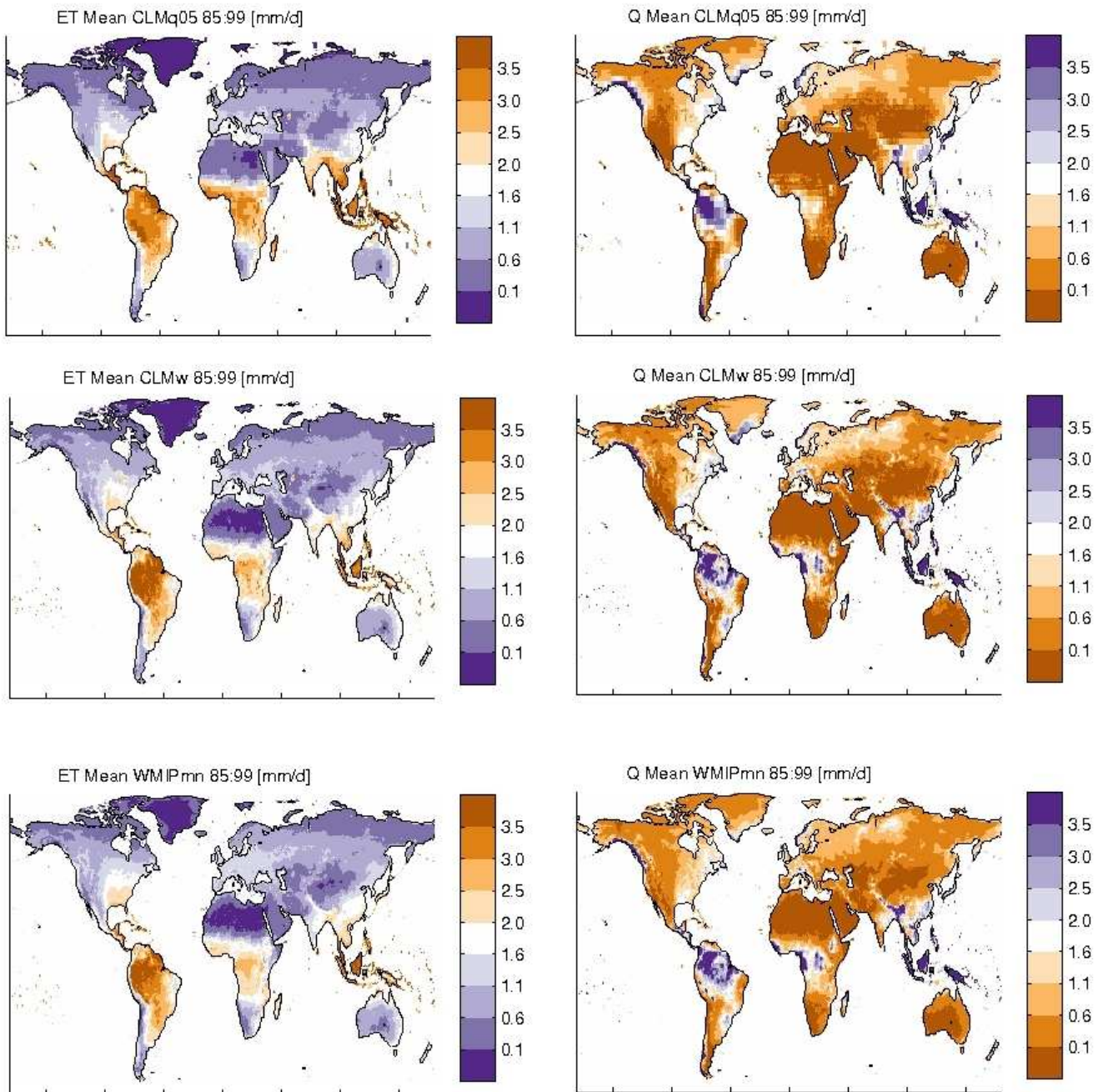


Fig. 1: Global maps of simulated mean 1985-1999 evapotranspiration ("ET", left panels) and runoff ("Q", right), from the CLMqian05 ("CLMq05", top), CLMwatch ("CLMw", middle), and mean of the WaterMIP6 models ("WMIPmn", bottom) simulations, in milimeters/day.

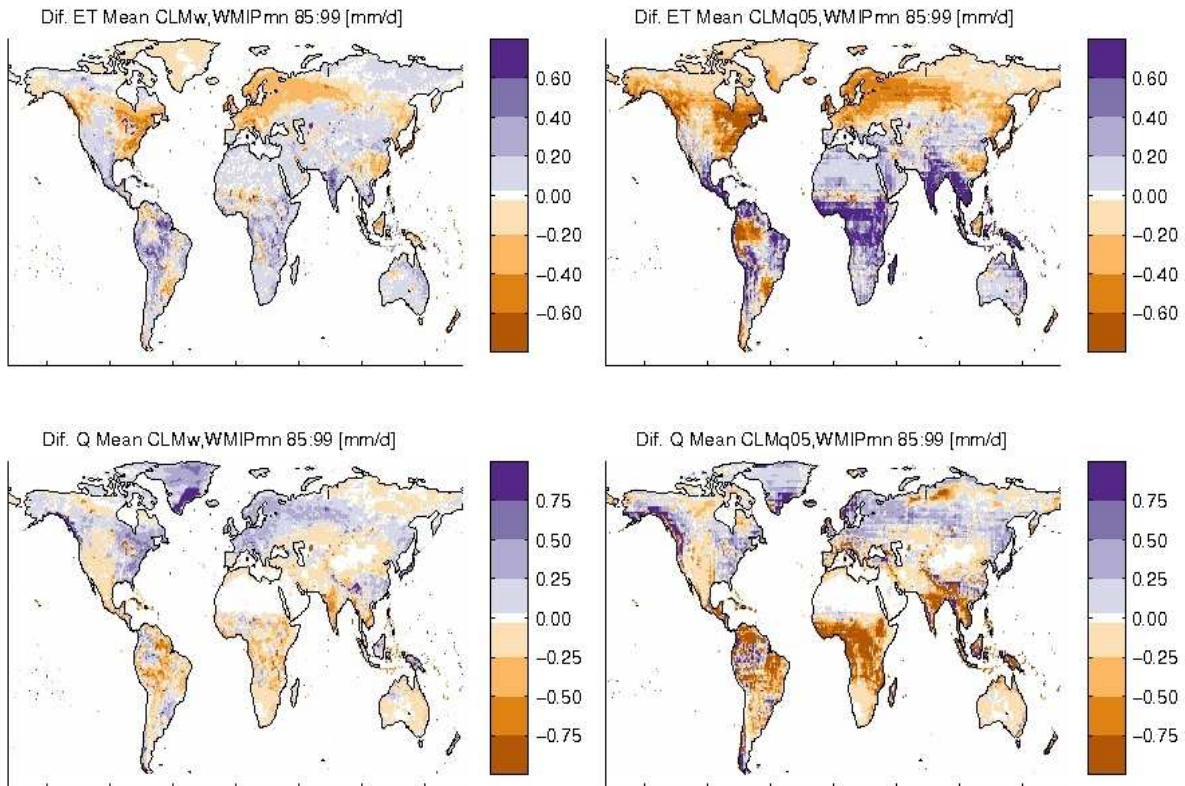


Fig. 2: Global maps of difference in simulated mean 1985-1999 evapotranspiration ("Dif ET", top panels) and runoff ("Dif Q", bottom), between the CLMwatch and the WaterMIP6 model mean ("CLMw,WMIPmn", left panels) and between the CLMq05 and the WaterMIP6 model mean ("CLMqian05,WMIPmn", right) simulations, in milimeters/day.

CLMwatch and CLMqian05 simulations already analysed in Section 3.1.1. The regional mean ET and runoff of the four model datasets are displayed in Fig. 4. For the WaterMIP6 multi-model mean, the spread (standard deviation) between the 6 models is also indicated. Overall, there is reasonably good agreement among the different simulations, with the CLM simulations generally falling within the range of the WaterMIP6 simulations. Nonetheless, substantial differences are noted across tropical humid regions (in South America, Africa, and South/Southeast Asia), where the WFD-driven simulations show mean runoff values that are significantly higher than those forced by q06. This is consistent with the discussion in Section 3.1.1, and is also visible in Fig. 2 where the difference between CLMqian05 and the WaterMIP6 mean reaches negative values consistently in excess of 0.75 mm/d, with corresponding increase in ET. This suggests that the largest uncertainties lie in tropical regions, although other

differences mostly in ET, but of opposite sign, can be observed in temperate humid regions such as maritime western Europe – again consistent with our discussion of the global analyses (Section 3.1.1). In semi-arid regions of central Asia, the western U.S., Australia and the Mediterranean, however, runoff from CLMqian simulations (and also CLMwatch with the exception of the Mediterranean) appear to be slightly below the lower range of the WaterMIP6 models. This is consistent with one of the major findings in Fig. 1 of the study by Haddeland *et al.* (2011), which pinpoints the dry regions as those with the greatest level of runoff discrepancy among models. Conversely, for runoff in the tropical regions, the CLMwatch simulation seems closer to the WaterMIP6 mean, while it more strongly differs from the CLMqian05 and CLMqian2 simulations. These results suggest that the simulated hydrology is affected by both the forcing and model uncertainties in dry regions, while differences in the forcing dataset appear to play a more important role in humid tropical areas. Nonetheless, even in these tropical regions, the respective spread of the WaterMIP6 simulations suggests that model discrepancies can also lead to larger variations in simulated runoff, although the CLMwatch simulations is close to the WaterMIP6 mean. Overall, for the analysed regions, the CLMwatch simulation is generally found to lie within the

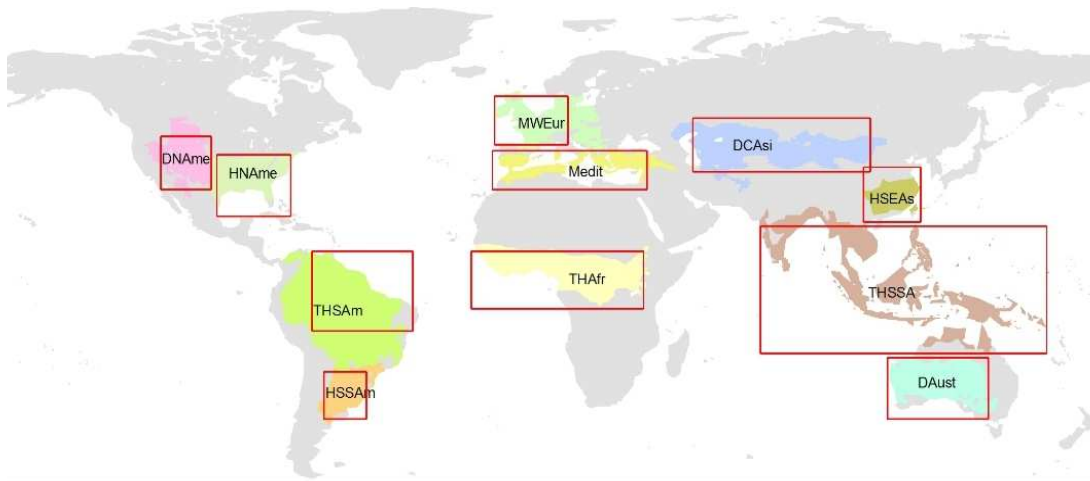


Fig. 3: Map of analysed Köppen-Geiger climate regions and location of model regional subsets: THSA = Tropical Humid South America; THAfr = Tropical Humid Africa; THSSA = Tropical Humid South/Southeast Asia; DNAm = Dry North America; DCAsi = Dry Central Asia; DAust = Dry Australia; HNAm = Humid North America; HSSAm = Humid Subtropical South America; HSEAs = Humid Subtropical East Asia; Medit = Mediterranean; MWEur = Maritime West Europe.

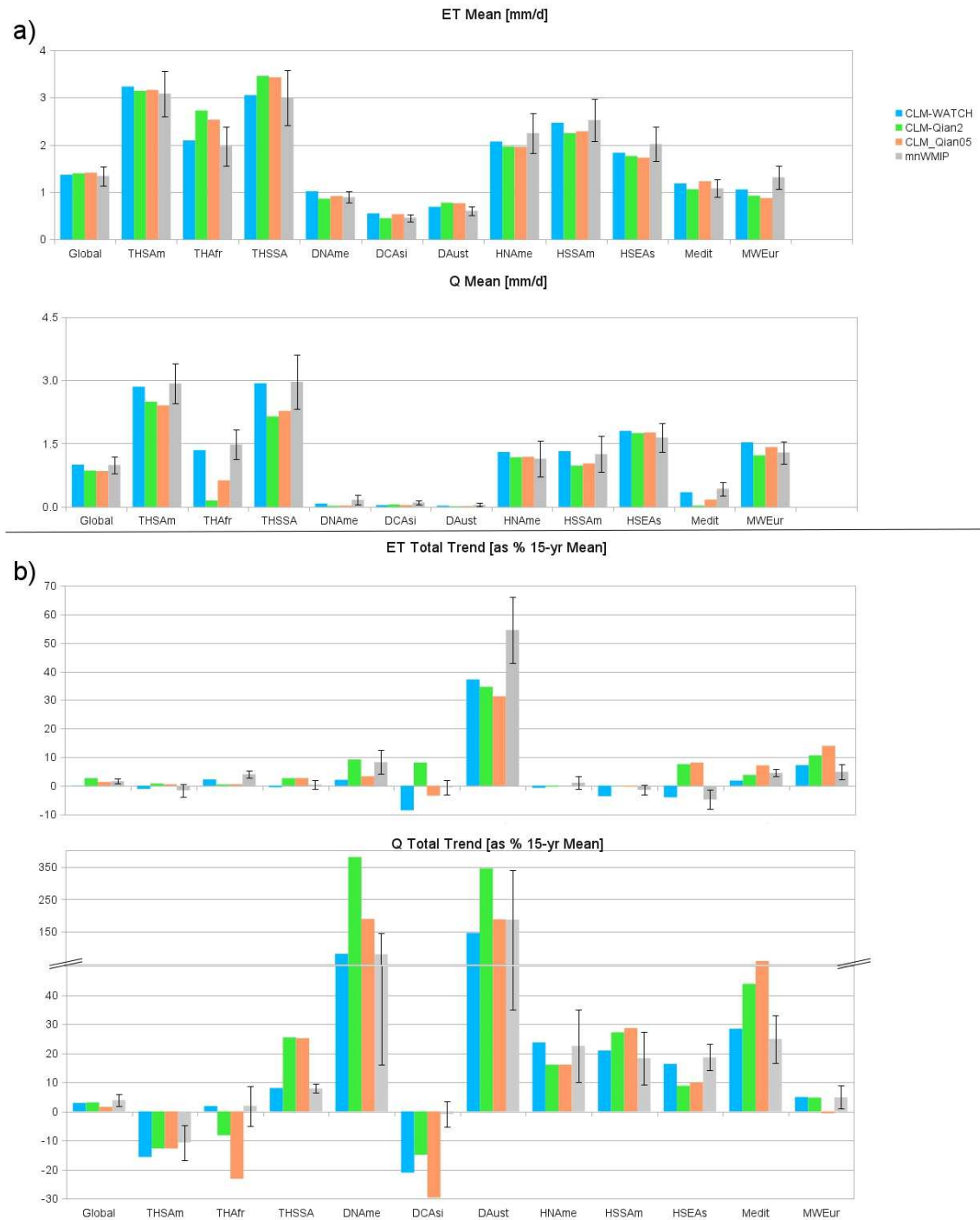


Fig. 4: Model intercomparison of global and regional total 1985-1999: a) means; and b) cumulative linear trends (as % of mean) in evapotranspiration ("ET") and runoff ("Q") simulated by CLMwatch, CLMqian2, CLMqian05, and the mean of the WaterMIP6 models ("mnWMIP", including +/- 1 standard deviation to indicate multi-model spread) simulations. See Fig. 6 for region locations and abbreviations.

spread of the WaterMIP6 models, which indicates that CLM3.5 has a similar performance to other state-of-the-art land surface and hydrological models.

4.3.2 Trends and inter-annual variability

4.3.2.1 Global patterns

Trends in ET and runoff for the period 1985-1999 are shown in Fig. 5. Overall, CLMwatch exhibits patterns of trends very similar to the WaterMIP6 models, suggesting that trends in ET and Q are mainly related to the applied atmospheric forcing. CLMqian05 has a trend pattern that differs from the CLMwatch simulation (especially over Europe and East Asia where ET from CLMqian05 tends to be more positive or even of the opposite sign). These results suggest that simulated decadal trends in land hydrology may be more dependent on the forcing than model choice.

Inter-annual variability for the 1985-1999 period, shown in Fig. 6 for the global domain, is subject to the combined effects of the different forcings and models used, with the mean of the WaterMIP6 models having the highest values for ET followed by CLMwatch, with those from CLMqian05 lying substantially lower. Contrasts among inter-annual variability in runoff are less evident.

Means and trends for three fields of the WFD (precipitation, shortwave downward radiation, and temperature) are displayed in Figure 7, showing a patchy shortwave downward radiation pattern that appears to correlate with the WaterMIP6 trends in runoff and ET. However, analyses of the WFD (not shown) hint at a radiation “dimming” signal for the 1985-1999 period for most of the global domain (except for a small region in central Europe) that is contrary to the “brightening” expected from observation records (Wild *et al.*, 2005). Coincidentally, corresponding analyses of the q06 forcing reveal similar patterns of strongly decreasing radiation for west and central Europe between 1990 and 2004, where a cumulative drop of almost 3% of the mean is also at odds with observations (Oliveira *et al.*, 2011). Changes to global radiation have been shown to potentially impact runoff indirectly through a vegetation-mediated effect on plant transpiration (e.g. Gedney *et al.*, 2006; Piao *et al.*, 2007; Oliveira *et al.*, 2011). The availability of improved gridded atmospheric forcing products for shortwave downward radiation could greatly improve our understanding of physical processes occurring in land hydrology at the Earth surface.

On the other hand, trends in precipitation and temperature appear to be in line with recent studies on climate change (IPCC, 2007). In particular, we note that positive precipitation trends in most dry regions

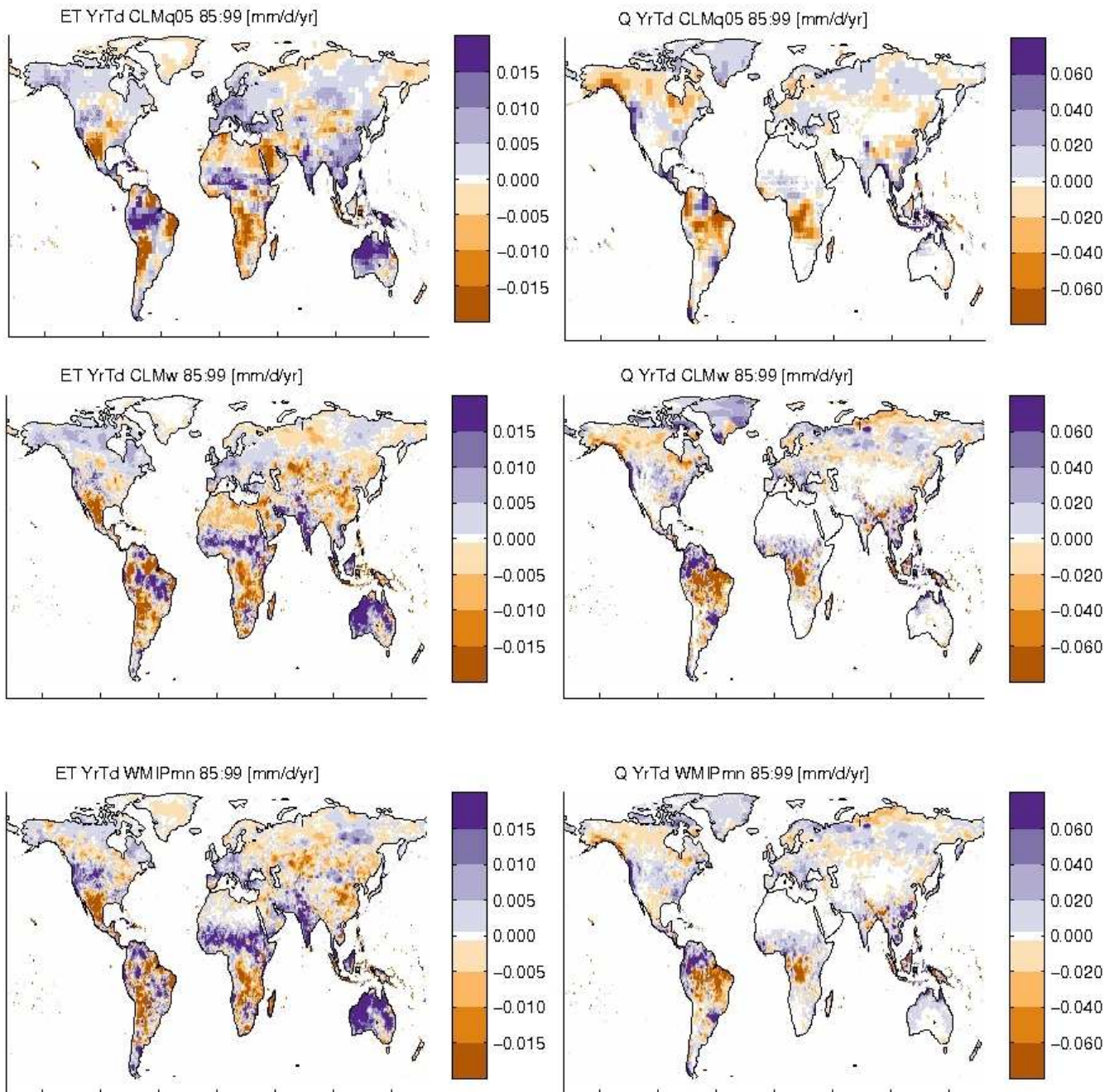


Fig. 5: Global maps of simulated 1985-1999 annual linear trends in evapotranspiration ("ET", left panels) and runoff ("Q", right), from the CLMqian05 ("CLMq05", top), CLMwatch ("CLMw", middle), and the mean of the WaterMIP6 model ("WMIPmn", bottom) simulations, in millimeters/day per year.

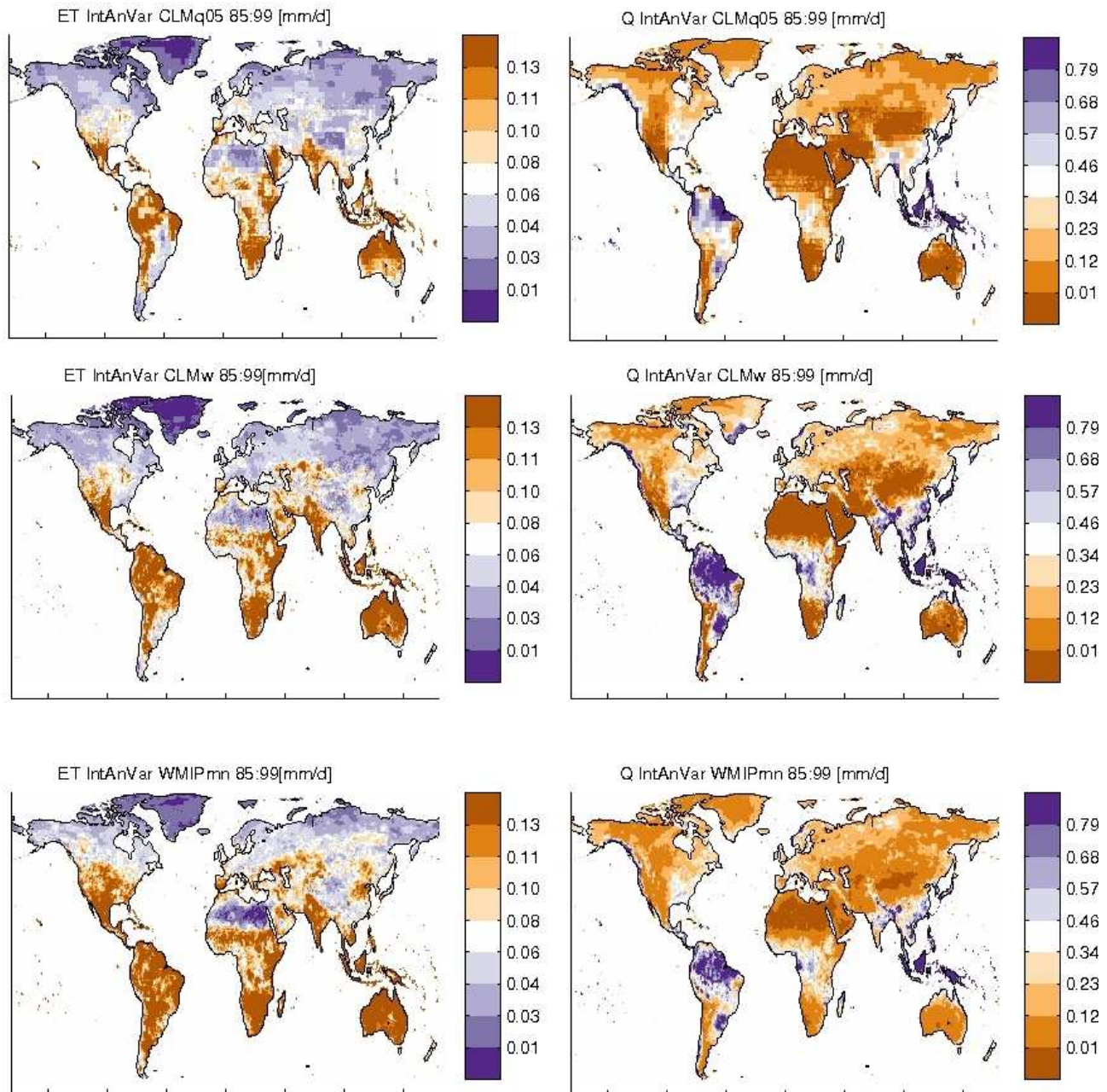


Fig. 6: Global maps of simulated 1985-1999 inter-annual variability of evapotranspiration ("ET", left panels) and runoff ("Q", right), from the CLMqian05 ("CLMq05", top), CLMwatch ("CLMw", middle), and the mean of the WaterMIP6 models ("WMIPmn", bottom) simulations, in millimeters/day.

across the globe including Australia, the Mediterranean, the Sahel, and western U.S. are substantial, unlike in the two large equatorial basins that see a large reduction during the 15-year period.

4.3.2.2 Regional analysis

Some large discrepancies in simulated ET and Q trends can be seen in some regions (Fig. 4). Most notably, dry regions across the globe show large differences among, and within, simulated datasets, as well as the highest rates of runoff change. We note that for ease of comparability across biomes these values are presented in relative terms, as percent of the 15-year mean. Therefore, despite concurring positive trends in precipitation also noted for these regions (see Section 3.2.1), their typical runoff mean values are very low, and the observed two- and threefold increase amount to only a small fraction of mm/d in absolute values. The Mediterranean exhibits also the highest runoff trend discrepancy between WFD- and q06-driven simulations, but this is probably an artifact related to forcing resolution, as this predominantly coastal region contains many grid cells with only a fraction of their area covered by land. This also affects the CLMqian05 simulation, whose 0.5° forcing is based on the original $1.9^\circ \times 2.5^\circ$ grid. For the dry regions and the global domain, trends in ET are substantially higher in the WaterMIP6 models than in CLMwatch simulations, typically ranging between a cumulative 1 and 2% of the 15-year mean. Such differences seem small on a short time scale, but may be non-negligible when performing simulations of future climate at the centennial scale. Possible differences in model design or parameterization may be responsible for the higher allocation of water to runoff relative to ET on the part of CLM.

Coastal regions notwithstanding, and after discarding the runoff trends in dry regions for the reasons stated above, model resolution seems to play a smaller role in this assessment of simulation uncertainties, with nearly negligible effects of differences in means between the CLMqian2 and CLMqian05 simulations. The only noticeable difference occurs in tropical humid Africa, where the finer resolution yields a negative ET trend triple that of the coarse run, for which we fail to find a plausible explanation.

4.4 Conclusions and outlook

We analyse the impacts of model resolution, atmospheric forcing, and the choice of land-surface model on the means, inter-annual variability, and trends in total ET and surface runoff, for the global and 11

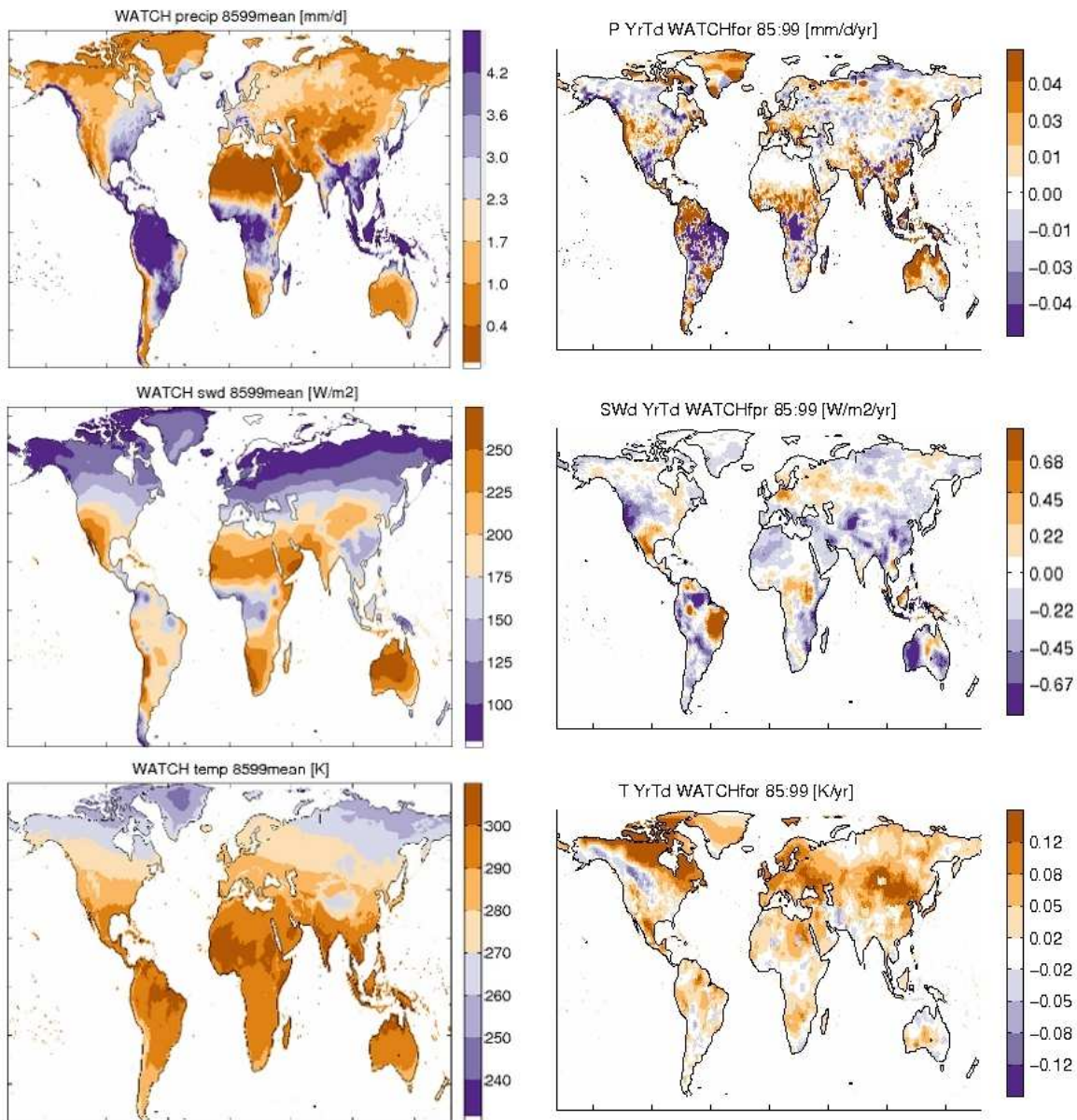


Fig. 7: Global maps of 1985-1999 means (left panels) and annual linear trends (right) in the WFD precipitation (top panels), shortwave downward radiation (middle), and temperature (bottom) fields.

regional domains including most large climate regions. We perform offline simulations with CLM at two different resolutions and driven with two different forcing datasets, and compare the results to six land-surface and global hydrologic models from the WATCH project. We find that CLM-simulated mean runoff in semi-arid regions is mostly lower than the WaterMIP6 average, consistent with previous

results suggesting that mean differences between models are a major source of uncertainty, especially in dry lands (Haddeland *et al.*, 2011). Nonetheless, the regional analysis reveals that the CLMwatch simulation generally lies within the WaterMIP6 model spread.

WFD-driven simulations exhibit similar trend patterns and magnitude, suggesting that the decadal variability of the components of the water cycle is more sensitive to forcing than model choice. Inter-annual variability is subject to the combined effects of the different forcing datasets and models used, with WaterMIP6 being highest in ET followed by CLMwatch, and CLMqian05 displaying lower values. Means and trends in radiation forcing are well correlated with the respective fields in the WaterMIP6 model mean runoff, suggesting a relevance of radiation forcing for the land hydrological trends. However, since neither of the forcing datasets incorporate observed radiation brightening trends, this is likely a source of errors in the simulations. Hence, further investigations considering improved gridded radiation products are needed to assess the impact of such forcing biases.

There is good regional agreement in trends and means among simulations, but in tropical humid regions WFD-driven simulations have higher mean runoff than those forced by q06, reaching 20% of the mean between CLMqian05 and the WaterMIP6 model mean, suggesting an uncertainty that may impact feedbacks to the climate system by affecting energy partitioning between sensible and latent heat fluxes. In dry regions and for the global average trends in ET are higher in the WaterMIP6 mean than in CLMwatch by a cumulative 1 to 2% of the 15-year mean, which may be non-negligible for simulations at the centennial scale. This is possibly due to differences in model parameterization making CLM allocate more water to runoff relative to ET. Lastly, the conducted simulations suggest that model resolution plays a comparably smaller role in simulation uncertainty, at least in the absence of corresponding increase in forcing resolution.

4.5 Acknowledgements

The authors thank the creators of WATCH Forcing Data and the hydrological multi-model dataset from the European Union EC-FP6 funded Integrated Project WATCH (No. 036946, <http://www.eu-watch.org>), in collaboration with the Global Water System Project (GWSP). We acknowledge partial financial support from the EU FP7 CARBO-Extreme (FP7-ENV-2008-1-226701), and CCES MAIOLICA projects.

Chapter 5

Conclusions and outlook

Conclusions and outlook

5.1 Conclusions

In this thesis, the land hydrological cycle and its changes over the last decades have been studied. We use the Community Land Model version 3.5, along with observations and other modelling results, to assess the impacts of changes to radiation and other atmospheric variables on land hydrology. In chapter 2, the sensitivity of the simulated land hydrology to changes in global radiation, and its partitioning into direct and diffuse fractions is investigated. Chapter 3 analyses trends and variability in observed runoff from small, undisturbed European catchments, and compares it to runoff from other observations and model simulations at the continental basin level, to study the effects of elevation, solar radiation, and other atmospheric drivers. Chapter 4 examines the sources of uncertainty affecting the simulated terrestrial water cycle globally and regionally (due to model structure, model resolution and atmospheric forcing). For this purpose simulations at different resolutions, driven with different forcings, and performed by different models are compared. The following overall conclusions can be drawn:

- **Response of simulated hydrology to trends in radiation forcing:** Land surface processes and their impacts on land hydrology are substantially affected by atmospheric forcing trends, in particular solar radiation impacts on evapotranspiration and runoff are significant. The modeled hydrologic cycle response to the imposed radiation changes is globally strong, but weak in regions with a soil moisture-limited evapotranspiration regime. In mid-latitude humid regions an imposed realistic solar dimming signal leads to an evapotranspiration reduction of 5% of the mean, and an enhancement of runoff by equal percentage, with the imposed realistic brightening eliciting a proportional response. The runoff trend resulting from the imposed radiation/aerosols effect is of the same sign and approximate relative magnitude as those from other studies for other potential drivers of runoff change such as climate, CO₂, and land use.

- **Impact of higher diffuse fraction of radiation on water cycle:** Similarly to the terrestrial carbon cycle, also the terrestrial water cycle responds to the simulated impact of higher diffuse radiation fraction. The simulations suggest an increase of evapotranspiration in the tropics of ca. 3% of the mean due to increased photosynthesis from shaded leaves, but smaller opposite effects elsewhere due to the lower values in ground evaporation. The overall effect on hydrology is of approximately one-third the magnitude of that from the solar dimming, and of opposite sign.
- **European runoff from large basins, small near-natural catchments, and simulations:** Runoff from integrated near-natural catchments can be valuable for the validation of model-simulated runoff, as it is a good proxy for continental-scale basin behaviour, and is sensitive to radiation forcing trends, especially in Western and East-central European river basins. The CLM simulations agree reasonably well with observations in terms of inter-annual runoff variability, although regional discrepancies exist mostly in Southwestern European basins, which are subject to a drier climate. However, simulated runoff from a multi-model mean matches observations better than that from single-model CLM simulations. The poorer performance of the simulations driven with one of the forcing datasets highlights the importance of atmospheric forcing to accurately simulate terrestrial hydrology. Despite the differences in scale and the large uncertainty expressed by an overall poor statistical significance level, near-natural streamflow trend behaviour and changes mostly show good agreement with GRDC observations and simulated data.
- **Effect of uncertainties in model and forcing on terrestrial hydrology:** The adequate simulation of land-surface hydrology depends on the choice of atmospheric forcing and land-surface model, which may bias the means, variability, and trends at the global and regional levels. Simulated CLM mean runoff in dry regions is mostly lower than the multi-model average, and overall mean patterns in runoff and evapotranspiration reflect the distribution of precipitation from the forcing. Simulations driven with the same forcing exhibit similar trend patterns and magnitude, suggesting that the decadal variability of the water cycle components is more sensitive to differences in the forcing datasets than to differences in model parameterizations. For the inter-annual variability

of the simulated processes, both the applied forcings and model parameterizations appear relevant. Some of the model and forcing agreement may be erroneously due to the lack of the observed radiation brightening trend in any of the forcing datasets. Differences in forcing datasets lead to substantial simulated differences in mean evapotranspiration and runoff in tropical humid regions, which highlights the importance of forcing data.

5.2 Outlook

The study of land hydrology using land surface models can inform the discussion on the biophysical processes occurring at the surface and help understand how forcing trends can affect the components of the water cycle. Throughout this thesis, model experiments and comparisons with observations contribute to the advancement of the characterisation of the land-climate system, additionally offering further insight into the limitations of the models, datasets and simulation methodology. In doing so, however, other issues have been arisen that merit attention and should be the subject of future investigation. These are briefly addressed here:

- Land-surface models mostly simulate conceptual natural systems excluding the impacts of human water withdrawal or irrigation, but in such hydrologic variables as river runoff anthropogenic disturbances can be large. Observation data from unimpacted catchments can be valuable as a tool to validate simulated natural hydrology, but the temporal and spatial limitations of available datasets is small. The field of land-climate interactions, and the study of land hydrology in particular, would greatly benefit from the expansion of this network to a truly global data collection system similar e.g. to the Fluxnet network (Baldocchi *et al.*, 2001).
- None of the forcing datasets used in this thesis incorporates trends in shortwave downward radiation that are consistent with observations for recent decades. Chapters 2 and 3 of this thesis show that radiation forcing trends can affect the components of the water cycle significantly, so possibly some of the understanding derived from simulations using these data may be erroneous. Global datasets with reliable 2D

CHAPTER 5: CONCLUSIONS AND OUTLOOK

radiation forcing would greatly enhance our understanding of the processes occurring at the land surface including those pertaining to the water and carbon cycles, helping to better constrain forecasts of future climate.

Bibliography

- Abakumova, G. M., E. M. Feigelson, V. Bussak, and V. V. Stadnik (1996) Evaluation of long term changes in radiation, cloudiness and surface temperature on the territory of the former Soviet Union. *J. Clim.*, 9, 1319-1327.
- Alkama, R., M. Kageyama, and G. Ramstein (2010) Relative contributions of climate change, stomatal closure, and leaf area index changes to 20th and 21st century runoff change: A modelling approach using the Organizing Carbon and Hydrology in Dynamic Ecosystems (ORCHIDEE) land surface model, *J. Geophys. Res.*, 115, D17112, doi:10.1029/2009JD013408.
- Allan, R. P., and B. J. Soden (2008) Atmospheric warming and the amplification of precipitation extremes. *Science*, 321, 1481-1484.
- Allen, M. R., and W. J. Ingram (2002) Constraints on future changes in climate and the hydrologic cycle. *Nature*, 429, 224-232.
- Alpert, P., and P. Kishcha (2008) Quantification of the effect of urbanization on solar dimming. *Geophys. Res. Lett.*, 35, L08801, doi:10.1029/2007GL033012.
- Baldocchi, D., E. Falge, L. Gu, R. Olson, D. Hollinger, S. Running, P. Anthoni, C. Bernhofer, K. Davis, J. D. Fuentes, A. Goldstein, G. Katul, B. Law, X. Lee, Y. Malhi, T. Meyers, W. Munger, W. Oechel, K. T. Paw U, K. Pilgaard, H. P. Schmid, R. Valentini, S. Verma, T. Vessala, K. Wilson, and S. Wofsy (2001) Fluxnet: A new tool to study the temporal and spatial variability of ecosystem-scale carbon dioxide, water vapor, and energy flux densities. *Bull. Am. Meteorol. Soc.*, 82, 2415-2434.
- Ball, J. T., I. E. Woodrow, J. A. Berry (1987) A model predicting stomatal conductance and its contribution to the control of photosynthesis under different environmental conditions. In: Biggins,

BIBLIOGRAPHY

- J. (Ed.), Progress in Photosynthesis Research. Nihjoff, Dordrecht, pp. 221-224.
- Balsamo, G., P. Viterbo, A. Beljaars, B. van den Hurk, A. K. Betts, and K. Scipal (2009) A revised hydrology for the ECMWF model: Verification from field site to terrestrial water storage and impact in the Integrated Forecast System. *J. Hydrometeorol.*, 10, 623-643.
- Beniston, M., F. Keller, B. Koffi, and S. Goyette (2003) Estimates of snow accumulation and volume in the Swiss Alps under changing climatic conditions. *Theor. Appl. Climatol.*, 76, 125-140.
- Betts, R. A., O. Boucher, M. Collins, P. M. Cox, P. D. Falloon, N. Gedney, D. L. Hemming, C. Huntingford, C. D. Jones, D. M. H. Sexton, and M. J. Webb (2007) Projected increase in continental runoff due to plant responses to increasing carbon dioxide. *Nature*, 448, 1037-1041, doi:10.1038/nature06045.
- Bondeau, A., P. Smith, S. Zaehle, S. Schaphoff, W. Lucht, W. Cramer, D. Gerten, H. Lotze-Campen, C. Müller, M. Reichstein, and B. Smith, (2007) Modelling the role of agriculture for the 20th century global terrestrial carbon balance. *Glob. Chang. Biol.*, 13, 679-706.
- Brown, R. D. (2000) Northern Hemisphere Snow Cover Variability and Change, 1915-97. *J. Climate*, 13, 2339-2355, doi:10.1175/1520-0442.
- Cao, L., G. Bala, K. Caldeira, R. Nemani, and G. Ban-Weiss (2009) Climate response to physiological forcing of carbon dioxide simulated by the coupled Community Atmosphere Model (CAM3.1) and Community Land Model (CLM3.0). *Geophys Res. Lett.*, 36, L10402, doi:10.1029/2009GL037724.
- Che, H. Z., G. Y. Shi, X. Y. Zhang, R. Arimoto, J. Q. Zhao, L. Xu, B. Wang, and Z. H. Chen (2005) Analysis of 40 years of solar radiation data from China, 1961-2000. *Geophys. Res. Lett.*, 32, L06803, doi:10.1029/2004GL022322.
- Chen, Z., and S. E. Grasby (2009) Impact of decadal and century-scale oscillations on hydroclimate trend analyses. *J. Hydrol.*, 365, 122-133.
- Collatz, G. J., M. Ribas-Carbo, and J. A. Berry (1992) Coupled photosynthesis-stomatal conductance model for leaves of C plants. *Aust. J. Plant Physiol.*, 19, 519-538.

BIBLIOGRAPHY

- Collatz, G. J., J. T. Ball, C. Grivet, and J. A. Berry (1991) Physiological and environmental regulation of stomatal conductance, photosynthesis, and transpiration: A model that includes a laminar boundary layer. *Agric. For. Meteorol.*, 54, 107-136.
- Cox, P. M., R. A. Betts, C. B. Bunton, R. L. H. Essery, P. R. Rowntree, and J. Smith (1999) The impact of new land surface physics on the GCM simulation of climate and climate sensitivity. *Climate Dyn.*, 15, 183-203.
- Crutzen, P.J. (2006) Albedo enhancement by stratospheric sulfur injections: A contribution to resolve a policy dilemma? *Clim. Change*, 77, 211-220, doi:10.1007/s10584-006-9101-y.
- Dai, A., T. Qian, K. E. Trenberth, and J. D. Milliman (2009) Changes in continental freshwater discharge from 1949-2004. *J. Clim.*, 22, 2773-2792, doi: 10.1175/2008JCLI2592.1.
- Davin, E. L., and S. I. Seneviratne (2012) Role of land surface processes and diffuse/direct radiation partitioning in simulating the European climate. *Biogeosciences Discuss.*, 8, 11601-11630, doi:10.5194/bgd-8-11601-2011.
- Davin, E. L., R. Stöckli, E. B. Jaeger, S. Levis and S. I. Seneviratne (2011) COSMO-CLM2: A new version of the COSMO-CLM model coupled to the Community Land Model. *Clim. Dyn.*, 37, 9, 1889-1907, doi:10.1007/s00382-011-1019-z.
- De Rosnay, P., and J. Polcher (1998) Modeling root water uptake in a complex land surface scheme coupled to a GCM. *Hydrol. Earth Syst. Sci.*, 2, 239-256.
- Dickinson, R. E., A. Henderson-Sellers, P. J. Kennedy, and M. F. Wilson (1986) Biosphere-Atmosphere Transfer Scheme (BATS) for the NCAR Community Climate Model. NCAR Tech. Note, TN-275+STR, p. 72.
- Dirmeyer, P. A., X. Gao, M. Zhao, Z. Guo, T. Oki, and N. Hanasaki (2006) GSWP-2: Multi-model analysis and implications for our perception of the land surface. *Bull. Am. Meteorol. Soc.*, 87, 1381-1397, doi:10.1175/bams-87-10-1381.
- Dougherty, R. L., J. A. Bradford, P. I. Coyne, and P. L. Sims (1994) Applying an empirical model of

BIBLIOGRAPHY

- stomatal conductance to three C-4 grasses. *Agric. For. Meteor.*, 67, 269-290.
- Döll, P., K. Fiedler, and J. Zhang (2009) Global scale analysis of river - flow alterations due to water withdrawals and reservoirs. *Hydrol. Earth Syst. Sci.*, 13, 2413-2432, doi:10.5194/hess-13-2413-2009.
- Essery, R. L. H., M. J. Best, R. A. Betts, P. M. Cox, and C. M. Taylor (2003) Explicit representation of subgrid heterogeneity in a GCM land surface scheme. *J. Hydrometeorol.*, 4, 530-543.
- Farquhar, G. D., S. von Caemmerer, and J. A. Berry (1980) A biochemical model of photosynthetic CO₂ assimilation in leaves of C species. *Planta*, 149, 78-90.
- Fasullo, J. T., and K. E. Trenberth (2008) The annual cycle of the energy budget. Part I: Global mean and land-ocean exchanges. *J. Clim.*, 21, 2297-2313.
- Gedney, N., P. M. Cox, R. A. Betts, O. Boucher, C. Huntingford, and P. A. Stott (2006) Detection of a direct carbon dioxide effect in continental river runoff records. *Nature*, 439, 835-838.
- Gerten, D., S. Rost, W. von Bloh, and W. Lucht (2008) Causes of change in 20th century global river discharge. *Geophys Res. Lett.*, 35, L20405.
- Gillett, N. P., A. J. Weaver, F. W. Zwiers, and M. F. Wehner (2004) Detection of volcanic influence on global precipitation. *Geophys. Res. Lett.*, 31, L12217, doi:10.1029/2004GL020044.
- Grabs, W. (1997) Report on the third meeting of the GRDC Steering Committee, Tech. Rep. 15, Global Runoff Data Cent., Koblenz, Germany.
- Gu, L. H., D. D. Baldocchi, S. C. Wofsy, J. W. Munger, J. J. Michalsky, S. P. Urbanski, and T. A. Boden (2003) Response of a deciduous forest to the Mount Pinatubo eruption: Enhanced photosynthesis. *Science*, 299, 2035-2038.
- Gudmundsson, L., L. M. Tallaksen, K. Stahl, E. Dumont, D. B. Clark, S. Hagemann, N. Bertrand, D. Gerten, N. Hanasaki, J. Heinke, F. Voß, and S. Koirala (in press) Comparing Large-scale Hydrological Models to Observed Runoff Percentiles in Europe. *J. Hydrometeorol.*,

BIBLIOGRAPHY

doi:<http://dx.doi.org/10.1175/JHMD-11-083.1>.

- Guo, Z., P.A. Dirmeyer, X. Gao, and M. Zhao (2007) Improving the quality of simulated soil moisture with a multi-model ensemble approach. *Quart. J. Royal Meteorol. Soc.*, 133, 731-747.
- Haddeland, I., J. Heinke, F. Voß, S. Eisner, C. Chen, S. Hagemann, and F. Ludwig (2012) Effects of climate model radiation, humidity and wind estimates on hydrological simulations. *Hydrol. Earth Syst. Sci.*, 16, 305-318.
- Haddeland, I., D. B. Clark, W. Franssen, F. Ludwig, F. Voß, N. W. Arnell, N. Bertrand, M. Best, S. Folwell, D. Gerten, S. Gomes, S. N. Gosling, S. Hagemann, N. Hanasaki, R. Harding, J. Heinke, P. Kabat, S. Koirala, T. Oki, J. Polcher, T. Stacke, P. Viterbo, G. P. Weedon, and P. Yeh (2011) Multi-Model Estimate of the Global Terrestrial Water Balance: Setup and First Results. *J. Hydrometeorol.*, Water and Global Change special collection., doi:10.1175/2011JHM1324.1.
- Hagemann, S., and L. D. Gates (2003) Improving a subgrid runoff parameterization scheme for climate models by the use of high resolution data derived from satellite observations. *Climate Dyn.*, 21, 349-359.
- Hagemann, S., and L. Dümenil (1998) A parameterization of the lateral waterflow for the global scale. *Climate Dyn.*, 14, 17-31.
- Hannah, D. M., S. Demuth, H. A. J. van Lanen, U. Looser, C. Prudhomme, G. Rees, K. Stahl, and L. M. Tallaksen (2010) Large-scale river flow archives: importance, current status and future needs. *Hydrol. Process.*, 25, 1191-1200.
- Haylock, M. R., N. Hofstra, A. M. G. Klein Tank, E. J. Klok, P. D. Jones and M. New (2008) A European daily high-resolution gridded dataset of surface temperature and precipitation. *J. Geophys. Res. (Atmospheres)*, 113, D20119, doi:10.1029/2008JD10201.
- Henderson-Sellers, A., Z.-L. Yang, and R. Dickinson (1993) The Project for Intercomparison of Land-Surface Parameterization Schemes. *Bull. Amer. Meteor. Soc.*, 74, 1335-1349.
- Hirabayashi Y., S. Kanae, S. Emori, T. Oki, and M. Kimoto (2008) Global projections of changing

BIBLIOGRAPHY

risks of floods and droughts in a changing climate. *Hydrol. Sci. J.*, 53, 754-772.

Hofstra, N., M. Haylock, M. New, and P. D. Jones (2009) Testing E-OBS European high-resolution gridded data set of daily precipitation and surface temperature. *J. Geophys. Res.*, 114, D21101, doi:10.1029/2009JD011799.

IPCC (2012) Summary for Policymakers. In: *Managing the Risks of Extreme Events and Disasters to Advance Climate Change Adaptation* [Field, C.B., V. Barros, T.F. Stocker, D. Qin, D.J. Dokken, K.L. Ebi, M.D. Mastrandrea, K.J. Mach, G.-K. Plattner, S.K. Allen, M. Tignor, and P.M. Midgley (Eds.)]. A Special Report of Working Groups I and II of the Intergovernmental Panel on Climate Change. Cambridge University Press, Cambridge, UK, and New York, NY, USA, pp. 1-19.

IPCC (2007) *Climate Change 2007: The Physical Science Basis*. In: *Contribution of Working Group I to the Fourth Assessment Report of the Intergovernmental Panel on Climate Change*. (Eds. S. Solomon, D. Qin, M. Manning, *et al.*). Cambridge University Press, Cambridge, UK, and New York, NY.

Jarvis, P. (1976) The interpretation of the variations in leaf water potential and stomatal conductance found in canopies in the field. *Philos. Trans. R. Soc. B*, 273, 593-610.

Jung, M., M. Reichstein, P. Ciais, S.I. Seneviratne, J. Sheffield, M. L. Goulden, G. Bonan, A. Cescatti, J. Chen, R. de Jeu, A. J. Dolman, W. Eugster, D. Gerten, D. Gianelle, N. Gobron, J. Heinke, J. Kimball, B. E. Law, L. Montagnani, Q. Mu, B. Mueller, K. Oleson, D. Papale, A. D. Richardson, O. Roupsard, S. Running, E. Tomelleri, N. Viovy, U. Weber, C. Williams, E. Wood, S. Zaehle and K. Zhang (2010) Recent decline in the global land evapotranspiration trend due to limited moisture supply. *Nature*, 467, 951-954.

Kiehl, J. T., and K. E. Trenberth (1997) Earth's annual global mean energy budget. *Bull. Amer. Meteor. Soc.*, 78, 197-208.

Krakauer, N. Y. and I. Fung (2008) Mapping and attribution of change in streamflow in the coterminous United States. *Hydrol. Earth Syst. Sci.*, 12, 1111-1120.

BIBLIOGRAPHY

- Labat, D, Y. Godderis, J. L. Probst, and J. L. Guyot (2004) Evidence for global runoff increase related to climate warming. *Adv. Water Res.*, 27, 631-642.
- Laudon H, V. Sjöblom, I. Buffam, J. Seibert, and C. M. Mörth (2007) The role of catchment scale and landscape characteristics for runoff generation of boreal streams. *J. Hydrol.*, 344, 198-209.
- Lawrence, P. J., and T. N. Chase (2007) Representing a new MODIS consistent land surface in the Community Land Model (CLM 3.0). *J. Geophys. Res.*, 112, G01023, doi:10.1029/2006JG000168.
- Legates, D. R., H. F. Lins, and G. J. McCabe (2005) Comments on 'Evidence for global runoff increase related to climate warming' by Labat *et al.* *Adv. Water Res.*, 28, 1310-1315.
- Li, X. W., W. L. Li, and X. J. Zhou (1998) Analysis of the solar radiation variation of the China in recent 30 years (Chinese with English abstract). *Q. J. Appl. Meteorol.*, 9, 24-31.
- Liang, X. (2005) Land Surface Modeling. *Water Encyclopedia*, 533-538.
- Liang, X., D. P. Lettenmaier, E. F. Wood, and S. J. Burges (1994) A simple hydrologically based model of land surface water and energy fluxes for general circulation models. *J. Geophys. Res.*, 99 (D7), 14, 415- 14, 428.
- Liepert, B. G., J. Feichter, U. Lohmann, and E. Roeckner (2004) Aerosols dampen the water cycle in a warmer and moister world. *Geophys. Res. Lett.*, 31, L06207, doi:10.1029/2003GL019060.
- Liepert, B. G. (2002) Observed reductions of surface solar radiation at sites in the United States and worldwide from 1961 to 1990. *Geophys. Res. Lett.*, 29, 1421, doi:10.1029/2002GL014910.
- Liepert, B. G., and I. Tegen (2002) Multidecadal solar radiation trends in the United States and Germany and direct tropospheric aerosol forcing. *J. Geophys. Res.*, 107, 4153, doi:10.1029/2001JD000760.
- Lohmann, U., and J. Feichter (2005) Global indirect aerosol effects: A review. *Atmos. Chem. Phys.*, 5, 715-737.
- López-Moreno, J. I., S. M. Vicente-Serrano, E. Morán-Tejeda, J. Zabalza, J. Lorenzo-Lacruz, and J. M.

BIBLIOGRAPHY

- García-Ruiz (2011) Impact of climate evolution and land use changes on water yield in the Ebro basin. *Hydrol. Earth Syst. Sci.*, 15, 311-322.
- Lorenzo-Lacruz, J., S. M. Vicente-Serrano, J. J. Lopez-Moreno, E. Moran-Tejeda, and J. Zabalza (2011) Recent trends in Iberian streamflows, 1945-2005. *J. Hydrol.*, 414-415, 463-475, doi:10.1016/j.jhydrol.2011.11.023, 2012.
- Manabe, S. (1969) Climate and the ocean circulation: The atmospheric circulation and the hydrology of the Earth's surface. *Monthly Weather Rev.*, 97, 739-805.
- McCabe, G. J., and D. M. Wolock (2002) A step increase in streamflow in the conterminous United States. *Geophys. Res. Lett.*, 29, 38.1-38.4.
- McMahon, T. A., R. M. Vogel, M. C. Peel, and G. G. Pegram (2007) Global streamflows – Part 1: Characteristics of annual streamflows. *J. Hydrol.*, 347, 243-259, doi:10.1016/j.jhydrol.2007.09.002.
- Mercado, L. M., N. Bellouin, S. Sitch, O. Boucher, C. Huntingford, M. Wild, and P. M. Cox (2009) Impact of changes in diffuse radiation on the global land carbon sink. *Nature*, 458, 1014-1017, doi:10.1038/nature07949.
- Milliman, J. D., K. L. Farnsworth, P. D. Jones, K. H. Xu, and L. C. Smith (2008) Climatic and anthropogenic factors affecting river discharge to the global ocean, 1951–2000. *Global Planet. Change*, 62, 187-194.
- Milly, P. C. D., K. A. Dunne, and A. V. Vecchia (2005) Global pattern of trends in streamflow and water availability in a changing climate. *Nature*, 438, 347-350.
- Milly, P. C. D., and K. A. Dunne (2002) Macroscale water fluxes 2. Water and energy supply control of their interannual variability. *Water Resour. Res.*, 38, 1206, doi:10.1029/2001WR000760.
- Mitchell, J. F. B. (1989) The "greenhouse" effect and climate change. *Rev. Geophys.*, 2, 115-139.
- Morgan, J. A., D. R. LeCain, E. Pendall, D. M. Blumenthal, B. A. Kimball, Y. Carrillo, D. G. Williams, J. Heisler-White, F. A. Dijkstra, and M. West (2011) C4 grasses prosper as carbon

BIBLIOGRAPHY

dioxide eliminates desiccation in warmed semi-arid grassland. *Nature*, 476, 202-205.

Mueller, B., M. Hirschi, and S. I. Seneviratne (2011a) New diagnostic estimates of variations in terrestrial water storage based on ERA-Interim data. *Hydrol. Proc.*, 25, 996-1008, doi:10.1002/hyp.7652.

Mueller, B., S.I. Seneviratne, C. Jimenez, T. Corti, M. Hirschi, G. Balsamo, P. Ciais, P. Dirmeyer, J. B. Fisher, Z. Guo, M. Jung, F. Maignan, M. F. McCabe, R. Reichle, M. Reichstein, M. Rodell, J. Sheffield, A. J. Teuling, K. Wang, E. F. Wood, and Y. Zhang (2011b) Evaluation of global observations-based evapotranspiration datasets and IPCC AR4 simulations. *Geophys. Res. Lett.*, 38, L06402, doi:10.1029/2010GL046230.

Oki, T., and S. Kanae (2006) Global hydrological cycles and world water resources. *Science*, 313, 1068-1072.

Oleson, K. W., G.-Y. Niu, Z.-L. Yang, D. M. Lawrence, P. E. Thornton, P. J. Lawrence, R. Stöckli, R. E. Dickinson, G. B. Bonan, S. Levis, A. Dai, and T. Qian (2008) Improvements to the Community Land Model and their impact on the hydrological cycle. *J. Geophys. Res.*, 113, G01021, doi:10.1029/2007JG000563.

Oleson, K. W., Y. Dai, G. Bonan, R. E. Dickinson, K. W. Oleson, G. Bonan, F. Hoffman, P. Thornton, M. Vertenstein, Z.-L. Yang, and X. Zeng (2004) Technical Description of the Community Land Model (CLM). NCAR Technical Note NCAR/TN-461+STR. National Center for Atmospheric Research, Boulder, Colorado 80307, 173 pp.

Oliveira, P. J. C., E. L. Davin, S. Levis and S. I. Seneviratne (2011) Vegetation-mediated impacts of trends in global radiation on land hydrology: a global sensitivity study. *Glob. Chang. Biol.*, doi:10.1111/j.1365-2486.2011.02506.x.

Padma Kumari, B., and B. N. Goswami (2010) Seminal role of clouds on solar dimming over the Indian monsoon region. *Geophys. Res. Lett.*, 37, L06703, doi:10.1029/2009GL042133.

Palissy, B. (1580) Discours admirable de la nature des eaux et fontaines tant naturelles qu'artificielles,

BIBLIOGRAPHY

des metaux, des sels & salines, des pierres, des terres, du feu & des emaux. M. Le Jeune, Paris, 361 pp.

Peterson, B. J., R.M. Holmes, J.W. McClelland, C.J. Vörösmarty, R.B. Lammers, A.I. Shiklomanov, I.A. Shiklomanov and S. Rahmstorf (2002) Increasing river discharge to the Arctic Ocean. *Science*, 298, 2171-2173.

Piao, S., P. Friedlingstein, P. Ciais, N. de Noblet-Ducoudre, D. Labat, and S. Zaehle (2007) Changes in climate and land use have a larger direct impact than rising CO₂ on global river runoff trends. *Proc. Natl. Acad. Sci.*, 104,15242-15247.

Pieruschka, R., G. Huber, and J. A. Berry (2010) Control of transpiration by radiation. *Proc. Natl. Acad. Sci.*, 107, 13372-13377.

Pinker, R. T., B. Zhang, and E. G. Dutton (2005) Do satellites detect trends in surface solar radiation? *Science*, 308, 850-854.

Pitman, A. J., N. de Noblet-Ducoudré, F. T. Cruz, E. L. Davin, G. B. Bonan, V. Brovkin, M. Claussen, C. Delire, L. Ganzeveld, V. Gayler, B. J. J. M. van den Hurk, P. J. Lawrence, M. K. van der Molen, C. Müller, C. H. Reick, S. I. Seneviratne, B. J. Strengers, and A. Voltaire (2009) Uncertainties in climate responses to past land cover change: First results from the LUCID intercomparison study. *Geophys. Res. Lett.*, 36, L14814, doi:10.1029/2009GL039076.

Pitman, A. J. (2003) The evolution of, and revolution in, land surface schemes designed for climate models. *Int. J. Climatol.*, 23, 479-510.

Probst, J. L., and Y. Tardy (1987) Long range streamflow and world continental runoff fluctuations since the beginning of this century. *J. Hydrol.*, 94, 289-311.

Qian, T., A. Dai, and K. E. Trenberth (2007) Hydroclimatic trends in the Mississippi River basin from 1948 to 2004. *J. Clim.*, 20, 4599-4614.

Qian, T., A. Dai, K. E. Trenberth, and K. W. Oleson (2006) Simulation of global land surface conditions from 1948 to 2004 Part I: Forcing data and evaluations. *J. Hydrometeorol.*, 7, 953-975.

BIBLIOGRAPHY

- Ramanathan, V., P. J. Crutzen, J. T. Kiehl, and D. Rosenfeld (2001) Aerosols, climate, and the hydrological cycle. *Science*, 294, 2119-2124.
- Randerson, J. T., F. M. Hoffman, P. E. Thornton, N. M. Mahowald, K. Lindsay, Y. H. Lee, C. D. Nevison, S. C. Doney, G. Bonan, R. Stockli, C. Covey, S. W. Running, and I. Y. Fung (2009) Systematic assessment of terrestrial biogeochemistry in coupled climate–carbon models. *Global Change Biol.*, 15, 2462-2484.
- Richter, I., and S.-P. Xie (2008) Muted precipitation increase in global warming simulations: a surface evaporation perspective. *J. Geophys. Res.*, 113, D24118, doi:10.1029/2008JD010561.
- Robock, A., and H. Li (2006) Solar dimming and CO₂ effects on soil moisture trends. *Geophys. Res. Lett.*, 33, L20708, doi:10.1029/2006GL027585.
- Roderick, M. L., G. D. Farquhar, S. L. Berry, and I. R. Noble (2001) On the direct effect of clouds and atmospheric particles on the productivity and structure of vegetation. *Oecologia*, 129, 21-30.
- Roderick, M. L., and G. D. Farquhar (2002) The cause of decreased pan evaporation over the past 50 years. *Science*, 298, 1410-1411.
- Rost, S., D. Gerten, A. Bondeau, W. Lucht, J. Rohwer, and S. Schaphoff (2008) Agricultural green and blue water consumption and its influence on the global water system. *Water Resour. Res.*, 44, W09405, doi:10.1029/2007WR006331.
- Sellers, P. J., J. A. Berry, G. J. Collatz, C. B. Field, and F. G. Hall (1992) Canopy reflectance, photosynthesis and transpiration. III. A reanalysis using improved leaf models and a new canopy integration scheme. *Remote Sens. Environ.*, 42, 187-216.
- Sellers, P. J., Y. Mintz, Y. C. Sud, and A. Dalcher (1986) A simple biosphere model (SiB) for use within general circulation models. *J. Atmos. Sci.*, 43, 505-531.
- Seneviratne, S. I., T. Corti, E. L. Davin, M. Hirschi, E. B. Jaeger, I. Lehner, B. Orlowsky, and A. J. Teuling (2010) Investigating soil moisture-climate interactions in a changing climate: A review.

BIBLIOGRAPHY

Earth-Sci. Rev., 99, 125-161, doi:10.1016/j.earscirev.2010.02.004.

Seneviratne, S. I., D. Lüthi, M. Litschi, and C. Schär (2006) Land-atmosphere coupling and climate change in Europe. *Nature*, 443, 205-209.

Serreze, M. C., D. H. Bromwich, M. P. Clark, A. J. Etringer, T. Zhang, and R. Lammers (2002) Large-scale hydro-climatology of the terrestrial Arctic drainage system. *J. Geophys. Res.*, 108, 8160, doi:10.1029/2001JD000919.

Stahl, K., L. M. Tallaksen, J. Hannaford, and H. A. J. van Lanen (2012) Filling the white space on maps of European runoff trends: Estimates from a multi-model ensemble. *Hydrol. Earth Syst. Sci. Disc.*, 9, 2005-2032, doi:10.5194/hessd-9-2005-2012.

Stahl, K., L. M. Tallaksen, L. Gudmundsson, and J. H. Christensen (2011) Streamflow data from smallbasins: a challenging test to high resolution regional climate modeling. *J. Hydrometeorol.*, doi:10.1175/2011JHM1356.1.

Stahl, K., H. Hisdal, J. Hannaford, L. M. Tallaksen, H. A. J. van Lanen, E. Sauquet, S. Demuth, M. Fendekova, and J. Jódar (2010) Streamflow trends in Europe: evidence from a dataset of near-natural catchments. *Hydrol. Earth Syst. Sci.*, 14, 2367-2382.

Stanhill, G., and S. Cohen (2001) Global dimming: a review of the evidence for a widespread and significant reduction in global radiation with discussion of its probable causes and possible agricultural consequences. *Agric. For. Meteorol.*, 107, 255-278.

Stanhill, G., and S. Moreshet (1992) Global radiation climate changes: The world network. *Clim. Change*, 21, 57-75.

Stewart, I. T. (2009) Changes in snowpack and snowmelt runoff for key mountain regions. *Hydrol. Process.*, 23, 78-94.

Stöckli, R., D. M. Lawrence, G.-Y. Niu, K. W. Oleson, P. E. Thornton, Z.-L. Yang, G. B. Bonan, A. S. Denning, and S. W. Running (2008) Use of FLUXNET in the Community Land Model development. *J. Geophys. Res.*, 113, G01025, doi:10.1029/2007JG000562.

BIBLIOGRAPHY

- Streets, D. G., Y. Wu, and M. Chin (2006) Two-decadal aerosol trends as a likely explanation of the global dimming/brightening transition. *Geophys. Res. Lett.*, 33, L15806, doi:10.1029/2006GL026471.
- Tang, G., and P. J. Bartlein (2008) Simulating the climatic effects on vegetation: approaches, issues and challenges. *Progress in Physical Geography*, 32, 543-556.
- Teuling, A. J. M. Hirschi, A. Ohmura, M. Wild, M. Reichstein, P. Ciais, N. Buchmann, C. Ammann, L. Montagnani, A. D. Richardson, G. Wohlfahrt, and S. I. Seneviratne (2009) A regional perspective on trends in continental evaporation. *Geophys. Res. Lett.*, 36, L02404, doi:10.1029/2008GL036584.
- Thornton, P. E., and N. E. Zimmermann (2007) An improved canopy integration scheme for a land surface model with prognostic canopy structure. *J. Clim.*, 20, 3902-3923.
- Trenberth, K. E., J. T. Fasullo, and J. Kiehl (2009) Earth's global energy budget. *Bull. Amer. Meteor. Soc.*, 90, 311-323.
- Trenberth, K. E. and Josey, S. A. (2007) Observations: surface and atmospheric climate change. In, Solomon, S., Qin, D., Manning, M., Chen, Z., Marquis, M., Averyt, K. B., Tignor, M. and Miller, H. L. (eds.) *Climate Change 2007: The Physical Science Basis: Contribution of Working Group I to the Fourth Assessment Report of the Intergovernmental Panel on Climate Change*. Cambridge, UK, Cambridge University Press, 235-336.
- Trenberth, K. E., L. Smith, T. Qian, A. Dai, and J. Fasullo (2007) Estimates of the Global Water Budget and Its Annual Cycle Using Observational and Model Data. *J. Hydrometeorol.*, 8, 758-769. doi:10.1175/JHM600.1.
- Trigo, R. M., D. Pozo-Vázquez, T. J. Osborn, Y. Castro-Díez, S. Gámiz-Fortis, and M. J. Esteban-Parra (2004) North Atlantic oscillation influence on precipitation, river flow and water resources in the Iberian Peninsula. *Int. J. Climatol.*, 24, 925-944, doi:10.1002/joc.1048.
- Troy, T. J., and E. F. Wood (2009) Comparison and evaluation of gridded radiation products across northern Eurasia. *Environ. Res. Lett.*, 4, 045008, doi:10.1088/1748-9326/4/4/045008.

BIBLIOGRAPHY

- Uppala, S. M., Kållberg, P. W., Simmons, U. Andrae, V. Da Costa Bechtold, M. Fiorino, J. K. Gibson, J. Haseler, A. Hernandez, G. A. Kelly, X. Li, K. Onogi, S. Saarinen, N. Sokka, R. P. Allan, E. Andersson, K. Arpe, M. A. Balmaseda, A. C. M. Beljaars, L. Van De Berg, J. Bidlot, N. Bormann, S. Caires, F. Chevallier, A. Dethof, M. Dragosavac, M. Fisher, M. Fuentes, S. Hagemann, E. Hólm, B. J. Hoskins, L. Isaksen, P. A. E. M. Janssen, R. Jenne, A. P. McNally, J.-F. Mahfouf, J.-J. Morcrette, N. A. Rayner, R. W. Saunders, P. Simon, A. Ster, K. E. Trenberth, A. Untch, D. Vasiljevic, P. Viterbo, and J. Woollen (2005) The ERA-40 re-analysis. *Quart. J. Meteo. Soc.*, 131, 2961-3012.
- Viviroli, D., and R. Weingartner (2004) The hydrological significance of mountains: from regional to global scale. *Hydrol. Earth Syst. Sci.*, 8, 1016-1029.
- Vörösmarty, C. J., and D. Sahagian (2000) Anthropogenic disturbance of the terrestrial water cycle. *Bioscience*, 50, 753-765.
- Weedon, G. (2011) Creation of the WATCH 20th Century Ensemble product, WATCH Technical Report 37, (available at www.eu-watch.org).
- Weedon, G., S. Gomes, P. Viterbo, H. Sterle, J. Adam, N. Bellouin, O. Boucher, and M. Best (2010) The WATCH forcing data 1958-2001: a meteorological forcing dataset for land surface and hydrological models, WATCH Technical Report 22, (available at www.eu-watch.org).
- Wild, M., and B. G. Liepert (2010) The radiation balance as driver of the global hydrological cycle. *Environ. Res. Lett.*, 5, 025003, doi:10.1088/1748-9326/5/2/025003.
- Wild, M. (2009) Global dimming and brightening: A review. *J. Geophys. Res.*, 114, D00D16, doi:10.1029/2008JD011470.
- Wild, M., J. Grieser, and C. Schär (2008) Combined surface solar brightening and increasing greenhouse effect support recent intensification of the global land-based hydrological cycle. *Geophys. Res. Lett.*, 35, L17706, doi:10.1029/2008GL034842.
- Wild, M., H. Gilgen, A. Roesch, A. Ohmura, C. N. Long, E. G. Dutton, B. Forgan, A. Kallis, V.

BIBLIOGRAPHY

Russak, and A. Tsvetkov (2005) From dimming to brightening: Decadal changes in solar radiation at Earth's surface. *Science*, 308, 847-850.

Zhang, X., F. W. Zwiers, G. C. Hegerl, F. H. Lambert, N. P. Gillett, S. Solomon, P. A. Stott, and T. Nozawa (2007) Detection of human influence on twentieth-century precipitation trends. *Nature*, 448, 461-465.

Acknowledgements

This doctoral thesis would not have been possible without the knowledge and guidance of my main doctoral supervisor, Sonia Seneviratne.

I am also thankful to my doctoral co-supervisor, Edouard Davin, for his patience, wise advice and constant support and encouragement.

It is a pleasure to thank other fellow researchers who helped me in my work, including Christian Reick, Kerstin Stahl, Sam Levis, and Lena Tallaksen.

I owe my deepest gratitude to Benoît, Boris, Brigitte, Heidi, Irene, and all other colleagues at the land-climate interactions group, whose constant good disposition and willingness to engage in both interesting discussions at work, and extra-curricular fun activities off it, helped make this a more pleasurable experience. I am also particularly thankful to my office colleagues Nathalie and Sarah, and to the IT and administrative staff.

I am greatly indebted to my flatmates Ryan, Bettina and Christiane, and to my friends and family, including Ana, João Luís, Jorge, Laura, Maria, Quentin, Roland, among many others, for their support. Lastly, I would like to thank my parents, Noémia and José, for their love and support throughout all my life. This thesis is for you!

Curriculum Vitae

Paulo José da Silva Costa de Oliveira

Brahmsstrasse 141, 8003 Zürich

ecoluso@gmail.com

citizen of Portugal

Relevant education

- Ph.D. (Dr. sc.) ETH Zurich (defense October 12, 2011), Zürich, Switzerland
- M.Sc., University of San Francisco, San Francisco, CA, USA, 2007
- B.A., University of California, Santa Cruz, CA, USA, 2002

Work experience in research

- 2008- - ETH Zurich, Inst. Atmospheric and Climate Science, Zürich, Switzerland
- 2004-2008 - Carnegie Institution, Dept. Global Ecology, Stanford Univ., Stanford, CA, USA
- 2002-2004 - Stanford Univ., Dept. Biological Sciences, Stanford, CA, USA

Teaching Assistant

- Land-Climate Interactions M.Sc. course (ETH Zurich):
Land-surface modeling exercises - Fall Semesters 2008/2009/2010

Journal Reviewing

- Journal of Hydrology

Peer-reviewed publications

- Oliveira, P.J.C., E.L. Davin, B. Orlowsky, K. Stahl, L.M. Tallaksen, and S.I. Seneviratne (2012) Simulated and observed decadal variability and trends in European runoff. *Submitted to Journal of Hydrology*.
- Oliveira, P.J.C., E.L. Davin, S. Levis, and S.I. Seneviratne, 2011: Vegetation-mediated impacts of trends in global radiation on land hydrology: A global sensitivity study. *Global Change Biology*, doi: 10.1111/j.1365-2486.2011.02506.x.
- Broadbent, E.N., G.P. Asner, M. Keller, D.E. Knapp, P.J.C. Oliveira, and J.N.M. Silva, 2008: Forest fragmentation and edge effects from deforestation and selective logging in the Brazilian Amazon. *Biological Conservation*, 141, 1745-1757.
- Oliveira, P.J.C, G.P. Asner, D.E. Knapp, A. Almeyda, R. Galvan-Gildemeister, S. Keene, R.F. Raybin, and R.C. Smith, 2007: Land-use allocation protects the Peruvian Amazon. *Science*, 317, 1233-1236.
- Asner, G.P., E.N. Broadbent, P.J.C. Oliveira, M. Keller, D.E. Knapp, and J.N.M. Silva, 2006: Condition and fate of logged forests in the Brazilian Amazon. *Proceedings of the National Academy of Sciences*, 103, 12947-12950.
- Asner, G.P., D.E. Knapp, E.N. Broadbent, P.J.C. Oliveira, M. Keller, and J.N. Silva, 2005: Selective logging in the Brazilian Amazon. *Science*, 310, 480-482.

Published abstracts (1st–author)

- Oliveira, P.J.C., E.L. Davin, and S.I. Seneviratne, 2010: Modeling the effects of increased diffuse radiation on plant productivity and the water cycle. 6th Ginkgo Network Meeting, September 30 2010, Frankfurt am Main, Germany
- Oliveira, P.J.C., E.L. Davin, and S.I. Seneviratne, 2010: Vegetation-mediated impacts of trends in global radiation on land hydrology: A global sensitivity study. CARBO-Extreme 1st Annual Meeting, September 13 2010, Roskilde, Denmark [Best Poster Award]
- Oliveira, P.J.C., E.L. Davin, and S.I. Seneviratne, 2010: Modeling the impacts of solar radiation partitioning into direct and diffuse fractions for the global water cycle. European Geosciences Union General Assembly, May 6 2010, Vienna, Austria

CURRICULUM VITAE

- Oliveira, P.J.C., E.L. Davin, and S.I. Seneviratne, 2010: The role of decadal changes in incident radiation for trends in global evapotranspiration and runoff. European Geosciences Union General Assembly, May 3 2010, Vienna, Austria
- Oliveira, P.J.C., E.L. Davin, and S.I. Seneviratne, 2009: Investigating the influence of global radiation on trends in water cycle using CLM. 8th International N.C.C.R. Climate Summer School, August 31 2009, Grindelwald, Switzerland
- Oliveira, P.J.C., E.L. Davin, and S.I. Seneviratne, 2009: Dimming, brightening, and runoff: Studying the impacts of radiative forcing on the water cycle during the second half of the 20th century using CLM. European Geosciences Union General Assembly, April 23 2009, Vienna, Austria
- Oliveira, P.J.C., E.L. Davin, and S.I. Seneviratne, 2008: Investigating the influence of land surface processes in global trends in water cycle using CLM3.5. 13th Annual Climate Community System Modeling Workshop, June 17 2008, Breckenridge, CO, USA
- Oliveira, P.J.C., G.P. Asner, D.E. Knapp, and R.F. Raybin, 2007: Remote sensing and tropical forest damage: Using CLAS-II for the detection of forest disturbances and deforestation in the Peruvian Amazon. Ecological Society of America Annual Meeting, August 7 2007, San Jose, CA, USA
- Oliveira, P., S.S. Anderson, and A.E. Launer, 2004: Recreational trails and the dispersal of exotic invasive plants in Bay Area open space: conservation and restoration implications. Bay Area Conservation Biology Symposium, Davis, CA, USA

Miscellaneous

- International Max-Planck School for Earth Systems Modeling Annual Group Retreat, September 22-24, 2010, Reinstorf, Germany [Oral Presentation]
- Fellowship "International Max Planck Research School on Earth System Modelling Guest Program", August 22-September 30, Max Planck Institute for Meteorology, Hamburg, Germany [Oral Presentation Land in the Earth System Meeting September 1 2010. Oliveira, P.J.C., E.L. Davin, and S.I. Seneviratne, 2010: Vegetation-mediated impacts of trends in global radiation on land hydrology: A global sensitivity study.]

CURRICULUM VITAE

- 8th International NCCR Climate Summer School, August 30-September 4 2009, Grindelwald, Switzerland
- Two Week Course in Flux Measurements and Advanced Modeling, July 14-25 2008, Univ. Colorado Mountain Research Station, CO, USA

